

6  
AFWAL-TR-80-3015

AD A091014

DESIGN OF A LATERAL STABILITY AUGMENTATION SYSTEM  
FOR THE F-106 TO IMPROVE LATERAL HANDLING QUALITIES  
DURING TRACKING

Richard D. Holdridge, Captain, USAF

Flight Control ADP Branch  
Flight Control Division

July 1980

TECHNICAL REPORT AFWAL-TR-80-3015

Final Report for Period May 1977 to January 1979

DTIC  
SELECTED  
OCT 30 1980

Approved for public release; distribution unlimited.

DDC FILE COPY


FLIGHT DYNAMICS LABORATORY  
AIR FORCE WRIGHT AERONAUTICAL LABORATORIES  
AIR-FORCE SYSTEMS COMMAND  
WRIGHT-PATTERSON AIR FORCE BASE, OHIO 45433

80 10 29 132

# NOTICE

When Government drawings, specifications, or other data are used for any purpose other than in connection with a definitely related Government procurement operation, the United States Government thereby incurs no responsibility nor any obligation whatsoever, and the fact that the government may have formulated, furnished, or in any way supplied the said drawings, specifications, or other data, is not to be regarded by implication or otherwise as in any manner licensing the holder or any other person or corporation, or conveying any rights or permission to manufacture, use, or sell any patented invention that may in any way be related thereto.

This technical report has been reviewed and is approved for publication.

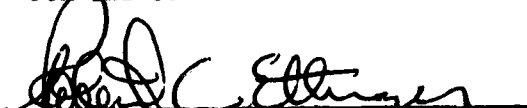


RICHARD D. HOLDRIDGE, Captain, USAF  
Project Engineer  
Flight Control ADP Branch



WILLIAM F. SWARTZ  
Chief, Flight Control ADP Branch

FOR THE COMMANDER:



ROBERT C. ETTINGER, Lt Col, USAF  
Chief, Flight Control Division

"If your address has changed, if you wish to be removed from our mailing list, or if the addressee is no longer employed by your organization please notify AEWAL/FIGX, W-P AFB, OH 45433 to help us maintain a current mailing list".

Copies of this report should not be returned unless return is required by security considerations, contractual obligations, or notice on a specific document.

SECURITY CLASSIFICATION OF THIS PAGE (When Data Entered)

REPORT DOCUMENTATION PAGE		READ INSTRUCTIONS BEFORE COMPLETING FORM
1. REPORT NUMBER AFWAL-TR-80-3015	2. GOVT ACCESSION NO. AD A091014	3. RECIPIENT'S CATALOG NUMBER 9
4. TITLE (and Subtitle) DESIGN OF A LATERAL STABILITY AUGMENTATION SYSTEM FOR THE F-106 TO IMPROVE LATERAL HANDLING QUALITIES DURING TRACKING		5. REPORT TYPE AND DATES COVERED Technical Report, May 77 - Jan 79
7. AUTHOR(s) Richard D. Holdridge, Captain, USAF		6. PERFORMING ORG. REPORT NUMBER
9. PERFORMING ORGANIZATION NAME AND ADDRESS Flight Dynamics Laboratory (AFWAL/FIGX) Air Force Wright Aeronautical Laboratories Wright-Patterson AFB, Ohio 45433		8. CONTRACT OR GRANT NUMBER(s)
11. CONTROLLING OFFICE NAME AND ADDRESS Flight Dynamics Laboratory (AFWAL/FIG) Air Force Wright Aeronautical Laboratories Wright-Patterson AFB, Ohio 45433		10. PROGRAM ELEMENT, PROJECT, TASK AREA & WORK UNIT NUMBERS Program Element 62201F, 2403, Task 240302, Work Unit 24030209
14. MONITORING AGENCY NAME & ADDRESS (if different from Controlling Office)		12. REPORT DATE Jul 80
(12) 165		13. NUMBER OF PAGES 165
16. DISTRIBUTION STATEMENT (of this Report) Approved for public release; distribution unlimited.		15. SECURITY CLASS. (of this report) Unclassified
17. DISTRIBUTION STATEMENT (of the abstract entered in Block 20, if different from Report)		15a. DECLASSIFICATION/DOWNGRADING SCHEDULE
18. SUPPLEMENTARY NOTES		
19. KEY WORDS (Continue on reverse side if necessary and identify by block number) Air-to-Air Gunnery      Man-Machine Dynamics Flight Control      Simulation Handling Qualities      Handling Qualities During Tracking Gunnery      Aircraft Dynamics		
20. ABSTRACT (Continue on reverse side if necessary and identify by block number) An improved lateral stability augmentation system has been developed to improve the handling qualities of the F-106 in the air-to-air tracking task. The existing yaw rate and roll rate feedbacks, as well as the aileron to rudder interconnect, were removed and replaced with calculated sideslip rate and measured sideslip feedbacks. An advanced root locus technique, the root map was used to set the gains on sideslip and sideslip rate. The resulting system was evaluated using a nonpiloted hybrid simulation as well as a digital		

DD FORM 1 JAN 73 1473 EDITION OF 1 NOV 65 IS OBSOLETE

SECURITY CLASSIFICATION OF THIS PAGE (When Data Entered)

392662

DW

20. ABSTRACT (Concluded)

frequency domain analysis program. The system was then evaluated by operational F-106 pilots using the Flight Dynamics Laboratory's LAMARS motion based simulator. Based on simulator results, the system was installed on an F-106 and flight tested at Tyndall AFB, Florida. The results of basic analyses, nonpiloted simulations, piloted simulations, and flight test are presented.

FOREWORD

This report documents an effort to use conventional design methods in the design of an improved stability augmentation system for the F-106.

Acknowledged is the guidance and direction given by Dr. Robert Huber of the Flight Dynamics Laboratory in the application of the design and analysis methods used for this project, the assistance provided in data collection and data analysis methods by Lt Cliff Alston, Capt Mitchell Cary, Mr. Frank George and Mr David Potts, the timely criticisms and assistance provided by Dr. David Quam of the University of Dayton, and the assistance in the preparation of the final draft of this report by Miss Celeste Brown and Mrs. Jayna Haller.

Accession For	
AFWAL-TR-80-3015	<input checked="checked" type="checkbox"/>
AFWAL-TR-80-3015	<input type="checkbox"/>
AFWAL-TR-80-3015	<input type="checkbox"/>
Justification	
By _____	
Distributor/	
Availability Codes	
Availability	
Not Applicable	
A	

## CONTENTS

SECTION	PAGE
I INTRODUCTION	1
II BACKGROUND	2
1. Air-to-Air Tracking	2
2. Factors Affecting Air-to-Air Tracking	4
3. Control Systems for Air-to-Air Tracking	7
4. F-106 Dynamics	9
III SYSTEM DESCRIPTION	16
1. Preliminary Design Model	16
2. Root Map Analysis	16
3. Frequency Response Analysis	33
4. Detailed Design Model	34
IV F-106 LAMARS SIMULATION	58
1. Simulation Description	58
2. Simulation Results	62
V F-106 FLIGHT TEST	73
1. System Configuration and Implementation	73
2. Flight Test Results	82
VI CONCLUSIONS AND RECOMMENDATIONS	96
1. Conclusions	96
2. Recommendations	96
APPENDIX A ASD HYBRID SIMULATION	97
APPENDIX B ROOT MAP DATA FOR THE F-106	99
APPENDIX C EASY DYNAMIC ANALYSIS PROGRAM	109
APPENDIX D DERIVATION OF SIDESLIP RATE	129
APPENDIX E ANALYSIS OF VARIANCE OF TRACKING DATA	132
APPENDIX F ASSEMBLY LISTING OF FLIGHT TEST OPERATIONAL FLIGHT PROGRAM	134
REFERENCES	153

## LIST OF ILLUSTRATIONS

FIGURE		PAGE
1	Reticle Depression Angle and Tracking Error	3
2	Fixed Depressed Reticle	4
3	The Pendulum Effect	6
4	Roll/Sideslip Coupling	7
5	Rolling about Velocity Vector	8
6	Sideslip Control System	10
7a	F-106 Longitudinal SAS	11
7b	F-106 Lateral SAS	12
8	Bare Airframe Response to 60° Bank Angle	13
9	Standard SAS Response to 60° Bank Angle	15
10	Preliminary Design Model	17
11	System Model for Constant $K_\beta$	18
12	System Model for Constant $K_\beta^*$	21
13a.	Root Map at Mach .4, Sea Level	23
13b.	Root Map at Mach .9, Sea Level	24
13c.	Root Map at Mach .7, 10000 Feet	25
13d.	Root Map at Mach .6, 15000 Feet	26
13e.	Root Map at Mach .9, 15000 Feet	27
13f.	Root Map at Mach 1.2, 15000 Feet	28
13g.	Root Map at Mach .6, 30000 Feet	29
13h.	Root Map at Mach .9, 30000 Feet	30
13i.	Root Map at Mach 1.4, 30000 Feet	31
14a.	Bare Airframe Beta/Delta Rudder .8, 10000	35
14b.	Standard SAS Beta/Delta Rudder .8, 10000	36
14c.	Betadot SAS Beta/Delta Rudder .8, 10000	37

## LIST OF ILLUSTRATIONS (CONTINUED)

FIGURE		PAGE
15a	Bare Airframe Beta/Delta Rudder .6, 30000	38
15b	Standard SAS Beta/Delta Rudder .6, 30000	39
15c	Betadot SAS Beta/Delta Rudder .6, 30000	40
16a	Bare Airframe Phi/Delta Rudder .8, 10000	41
16b	Standard SAS Phi/Delta Rudder .8, 10000	42
16c	Betadot SAS Phi/Delta Rudder .8, 10000	43
17a	Bare Airframe Phi/Delta Rudder .6, 30000	44
17b	Standard SAS Phi/Delta Rudder .6, 30000	45
17c	Betadot SAS Phi/Delta Rudder .6, 30000	46
18a	Bare Airframe Beta/Delta Aileron .8, 10000	47
18b	Standard SAS Beta/Delta Aileron .8, 10000	48
18c	Betadot SAS Beta/Delta Aileron .8, 10000	49
19a	Bare Airframe Beta/Delta Aileron .6, 30000	50
19b	Standard SAS Beta/Delta Aileron .6, 30000	51
19c	Betadot SAS Beta/Delta Aileron .6, 30000	52
20	Detailed Design Model	54
21	$\beta$ - $\dot{\beta}$ SAS Response to 60° Bank Angle	56
22	Response to One Degree Sideslip	57
23a	SAS Comparison at Mach .9, 10000 Feet	59
23b	SAS Comparison at Mach .6, 30000 Feet	60
24	Cooper Harper Rating Scale	63
25a	Standard SAS Pipper Trace at Mach .9, 10000 Feet, 3 g	69
25b	$\beta$ - $\dot{\beta}$ SAS Pipper Trace at Mach .9, 10000 Feet, 3 g	70
25c	$\dot{\beta}$ SAS Pipper Trace at Mach .9, 10000 Feet, 3 g	71
26	Tracking Error Reduction with $\dot{\beta}$ SAS	72



## LIST OF ILLUSTRATIONS (CONCLUDED)

FIGURE		PAGE
27	F-106 SAS Conceptual Block Diagram	75
28	$\dot{\beta}$ SAS Implementation	76
29	$\dot{\beta}$ SAS Inputs and Switching Logic	77
30	Roll SAS Implementation	78
31	Roll SAS Inputs and Switching Logic	79
32	Built-in-Test	81
33	Standard SAS, Aileron Reversal, Mach .8, 10000 Feet	84
34	$K_{\dot{\beta}}=1.5$ , $K_p=3.45$ , Aileron Reversal, Mach .8, 10000 Feet	85
35	Standard SAS, 4 g Turn, Mach .8, 10000 Feet	86
36	$K_{\dot{\beta}}=1.5$ , $K_p=3.45$ , 4 g Turn, Mach .8, 10000 Feet	87
37	Standard SAS, 3.5 g, Mach .7, 10000 Feet	89
38	$K_{\dot{\beta}}=1.9$ , $K_p=5$ , 3.7 g, Mach .7, 10000 Feet	90
39	$K_{\dot{\beta}}=1.9$ , $K_p=2.5$ , 4 g, Mach .75, 10000 Feet	91
40	$K_{\dot{\beta}}=1.25$ , $K_p=3.28$ , 4 g, Mach .75, 10000 Feet	92
41	$K_{\dot{\beta}}=1.9$ , $K_p=2.5$ , 4 g, Mach .75, 10000 Feet	93
42	$K_{\dot{\beta}}=1.5$ , $K_p=3.45$ , 4 g, Mach .75, 10000 Feet	94
43	Pilot Workload Comparison, 4 g Tracking Task	95
C-1	EASY Model Generation Data and Resulting Model for $\beta$ - $\dot{\beta}$ SAS	110
C-2	EASY Model Generation Data and Resulting Model for Standard SAS	118
C-3	EASY $\beta$ - $\dot{\beta}$ SAS Analysis Data	125
C-4	EASY Standard SAS Analysis Data	127

## LIST OF TABLES

TABLE		PAGE
1	Root Map Flight Conditions	22
2	F-106 Response at $K_{\beta}=6.5$ and $K_{\beta}=2.5$	32
3	Simulation Results	64
4	Analysis of Variance Results	66
5	Percent Improvements over Standard SAS	67
6	Cooper Harper Ratings (3 g Encounters)	68
7	Homing Point Select Gain Values	80
B-1	Transfer Function Data for Mach .4, Sea Level	100
B-2	Transfer Function Data for Mach .9, Sea Level	101
B-3	Transfer Function Data for Mach .7, 10000 Feet	102
B-4	Transfer Function Data for Mach .6, 15000 Feet	103
B-5	Transfer Function Data for Mach .9, 15000 Feet	104
B-6	Transfer Function Data for Mach 1.2, 15000 Feet	105
B-7	Transfer Function Data for Mach .6, 30000 Feet	106
B-8	Transfer Function Data for Mach .9, 30000 Feet	107
B-9	Transfer Function Data for Mach 1.4, 30000 Feet	108
E-1	Azimuth Error ANOVA	133
E-2	Elevation Error ANOVA	133
E-3	Total Error ANOVA	133

## LIST OF SYMBOLS

$A_y)_{acc}$	Accelerometer measured lateral acceleration (ft/sec <sup>2</sup> )
$b$	Wingspan (ft)
$\bar{c}$	Mean aerodynamic chord (ft)
$C_D$	Non-dimensional drag coefficient
$C_L$	Non-dimensional lift coefficient
$C_l$	Non-dimensional rolling moment coefficient
$C_m$	Non-dimensional pitching moment coefficient
$C_n$	Non-dimensional yawing moment coefficient
$C_y$	Non-dimensional sideforce coefficient
$F_x$	Total force in body x-direction (lb)
$F_y$	Total force in body y-direction (lb)
$F_z$	Total force in body z-direction (lb)
$g$	Gravitational acceleration, 32.174 ft/sec <sup>2</sup>
$I_x$	Moment of inertia about body x-axis (slug ft <sup>2</sup> )
$I_y$	Moment of inertia about body y-axis (slug ft <sup>2</sup> )
$I_z$	Moment of inertia about body z-axis (slug ft <sup>2</sup> )
$I_{xz}$	Moment of inertia xz cross-product (slug ft <sup>2</sup> )
$K$	Transfer function gain for $\beta/\delta r$
$K_I$	Gain on integrator in proportional plus integral compensator
$K_p$	Gain from rudder pedals to control system (rad/in)
$K_\beta$	Gain on sideslip angle feedback (rad/rad)
$K_{\dot{\beta}}$	Gain on sideslip angle rate feedback (rad/rad/sec)
$L$	Total rolling moment (ft-lb)
$M$	Total pitching moment (ft-lb)
$M$	Mach number
$m$	Mass (slugs)

N	Total yawing moment (ft-lb)
n.p.	Neutral Point (ft)
p	Roll rate (rad/sec)
q	Pitch rate (rad/sec)
$\bar{q}$	Dynamic pressure (lb/ft <sup>2</sup> )
r	Yaw rate (rad/sec)
S	Wing area (ft <sup>2</sup> )
u	Velocity in body x-direction (ft/sec)
U	Total velocity (ft/sec)
v	Velocity in body y-direction (ft/sec)
$\bar{v}_b$	Body velocity vector (ft/sec)
$\dot{\bar{v}}_b$	Body acceleration vector (ft/sec <sup>2</sup> )
$\ddot{\bar{v}}_b$	Inertial acceleration vector (ft/sec <sup>2</sup> )
w	Velocity in body z-direction (ft/sec)
$x_{c.g.}$	Center of Gravity (ft)
$\alpha$	Angle of attack (rad)
$\beta$	Sideslip angle (rad)
$\dot{\beta}_a$	Sideslip angle rate (rad/sec)
$\delta'_a$	Aileron deflection (rad)
$\delta_e$	Elevator deflector (rad)
$\delta_r$	Rudder deflection (rad)
$\phi$	Roll angle (rad)
$\theta$	Pitch angle (rad)
$\bar{\omega}$	Body angular rate vector (rad/sec)

## SECTION I

### INTRODUCTION

An improved lateral stability augmentation system (SAS) for the F-106 has been designed and simulated in both piloted and non-piloted real-time simulations and in a frequency domain simulation. The new system emphasizes improvement in lateral handling qualities for the air-to-air (ATA) tracking task.

The present lateral SAS is composed of washed out yaw rate, for stability purposes, and a combination of washed out roll rate and an aileron to rudder interconnect (ARI), for turn coordination. The new system uses sideslip angle ( $\beta$ ) and sideslip angle rate ( $\dot{\beta}$ ) to achieve both improved stability and improved turn coordination. The design also includes a direct electrical signal from the pilot through the rudder pedals to the control system to allow for direct command of sideslip angle or sideslip rate.

The new system eliminates large unintentional sideslip perturbations caused by the pilot's attempts to place the gunsight reticle, or pipper, on the target aircraft. The system also allows the pilot to point more accurately the aircraft when azimuth tracking error is small. An added benefit provided by the system is an improvement in elevation tracking error through a reduction of pilot workload in the lateral task.

A piloted simulation was conducted to evaluate the new lateral SAS. Two Air Defense Command (ADCOM) flight test pilots, both current in the F-106, spent a week flying approximately 150 ATA tracking passes. Several configurations of the improved system were flown and compared with the existing system. The pilots typically achieved reductions of 30% in both elevation and azimuth tracking error using the improved lateral SAS. The system was then installed on an F-106 and flight tested. The performance improvements were similar to those measured during piloted simulations.

## SECTION II

### BACKGROUND

#### 1. AIR-TO-AIR TRACKING

Before continuing with a specific discussion of the F-106, it is perhaps instructive to look at the ATA tracking task and how the difficulty of the task is heavily influenced by the aircraft flight control system. ATA tracking is typically a high-g maneuver which has superimposed on it the extremely difficult task of precise aircraft pointing. The task is further complicated because the aircraft is not being pointed as an end in itself but to enable the pilot to place a gunsight reticle (pipper), either fixed or computed and displayed, on the target aircraft. Since the pipper is a representation of a target for which the gun is presently correctly aimed, it will be depressed some angle from the aircraft body x-axis. This depression is due to target aircraft acceleration, attacker velocity and acceleration, and bullet gravity drop; its magnitude is further dependent on the angle of the gun with respect to the aircraft (gun depression angle). Figure 1 shows this situation and how it is viewed by the pilot in the headup display (HUD). Figure 1 also shows how elevation tracking error is defined. The tracking error is usually measured in angular units of milliradians (mil). In the situation shown in Figure 1, the pilot's task is simple: he pitches the aircraft up until the reticle is superimposed on the target.

Unfortunately, when a large azimuth error also exists, the pilot cannot simply move the reticle onto the target. To zero a large azimuth tracking error, the pilot must first roll the aircraft to approximately null the azimuth error and then pitch the aircraft to null the remaining elevation error. After these large azimuth errors have been nulled, the rudder pedals can be used to zero the remaining error. This sequence of first nulling azimuth error then elevation error is the basis upon which each pilot develops his own technique.

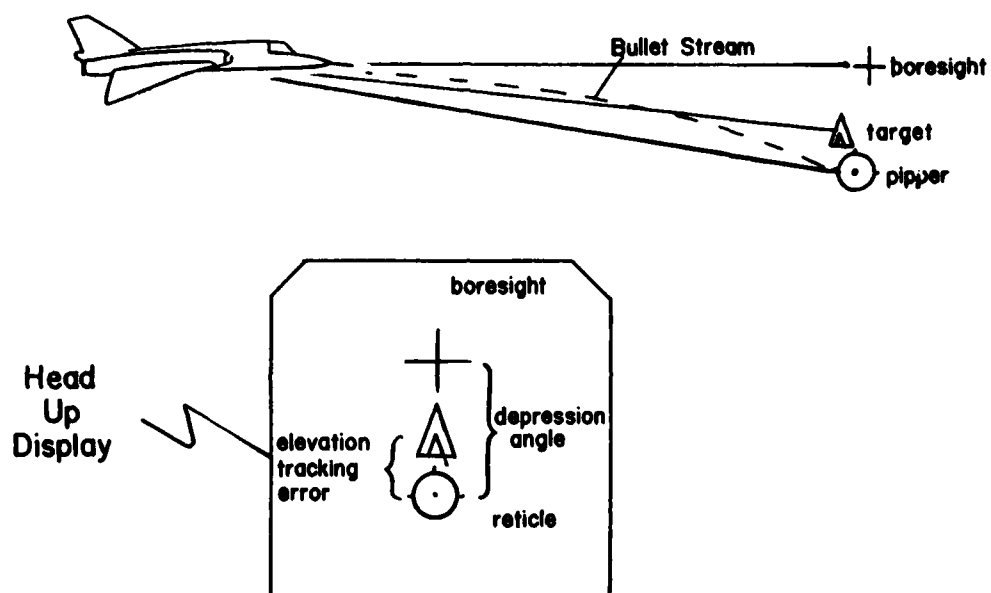


Figure 1. Reticle Depression Angle and Tracking Error

## 2. FACTORS AFFECTING ATA TRACKING

There are many factors which affect the pilot's ability to track a target. Some of these factors are turbulence, evasive target maneuvers, gunsight dynamics, and the attacker's own vehicle dynamics. The first two are factors that cannot be controlled or changed by modifications to the attacking aircraft. The third term can have a significant effect on tracking performance and to a large extent can be controlled or changed by modifications to the fire control system of the attacking aircraft. The study of gunsight dynamics and other associated fire control problems is, however, beyond the scope of this paper. To simplify the effects of gunsight dynamics, a fixed depressed reticle was used for the remainder of this study. A fixed depressed reticle, as the name implies, is a gunsight reticle which is depressed a constant angle from the boresight cross. Figure 2 shows a simple fixed depressed reticle as seen on the HUD. The fourth factor affecting the pilot's ability to track the target is vehicle dynamics. Like gunsight dynamics, vehicle dynamics can be changed by modifications to the attacking aircraft.

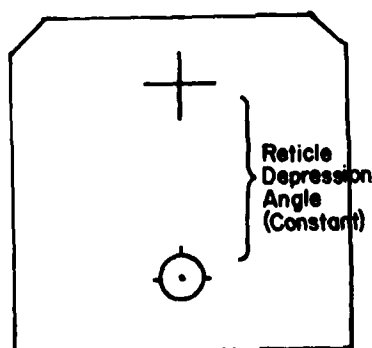


Figure 2. Fixed Depressed Reticle



To see how the vehicle dynamics affect the tracking error, one must compare what the pilot sees through the HUD to what the aircraft is doing within the airmass. Consider the HUD display in Figure 3(a) with a fixed depressed reticle. Since the pipper is left of the target, the pilot must null the azimuth error. Since the pilot cannot move his aircraft laterally, he must first roll the aircraft right and then turn to zero the error. Herein lies the problem. If the aircraft is unaugmented or contains just simple yaw damping, the aileron deflection will cause the aircraft to rotate about its nearest principle axis. For a rolling moment, this principle axis is very near the x-axis of the aircraft or, from the pilot's point of view, the boresight axis. This roll/sideslip coupling is shown in Figure 4. What then happens from the pilot's viewpoint is shown in Figure 3(b). When he rolls the aircraft, he rolls approximately about the boresight cross thus generating a transient sideslip angle which causes the pipper to move in the direction opposite that desired by the pilot. The pilot perceives this as an increased azimuth error, so he rolls the aircraft more to the right (Figure 3(c)), compounding the problem. This phenomenon of the pipper rotating under the boresight cross is known as the pendulum effect and has a destabilizing effect on ATA tracking.

The pendulum effect can be eliminated or greatly reduced by lateral augmentation of the aircraft. Figures 3 and 4 show that the pendulum effect is caused by the aircraft's natural tendency to roll about its own x-axis. This results in the angle-of-attack changing into sideslip as the roll angle goes from 0 to 90 degrees. Of course, this sideslip will die out at the aircraft's dutch roll frequency and damping, but this is too slow for the tracking task.

Another aspect of aircraft dynamics that affects the pilot's ability to track becomes obvious only when large tracking errors have been eliminated and the pilot is using the rudder to point the aircraft. When the pilot is using the rudder for fine control of azimuth error, the dutch roll frequency and damping become critical to the tracking task. To be effective during this precise phase of tracking, the aircraft should respond quickly to the pilot's input with a damping ratio which eliminates large overshoots and at the same time avoids the excessive lag of an

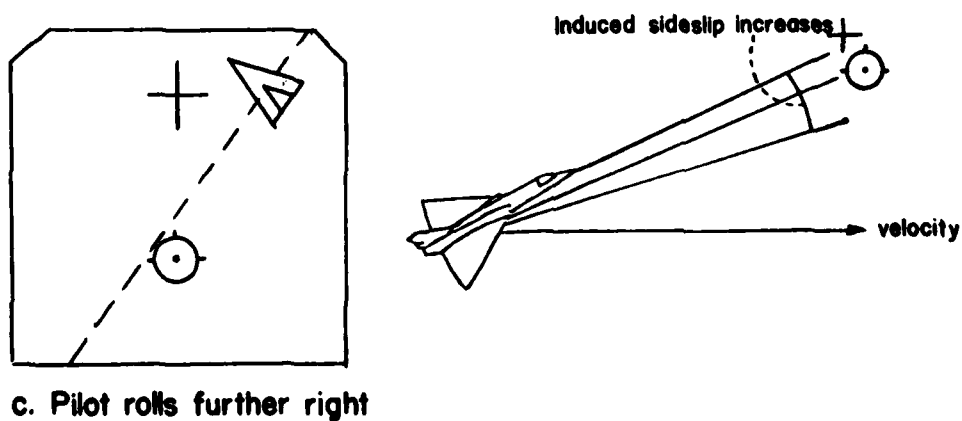
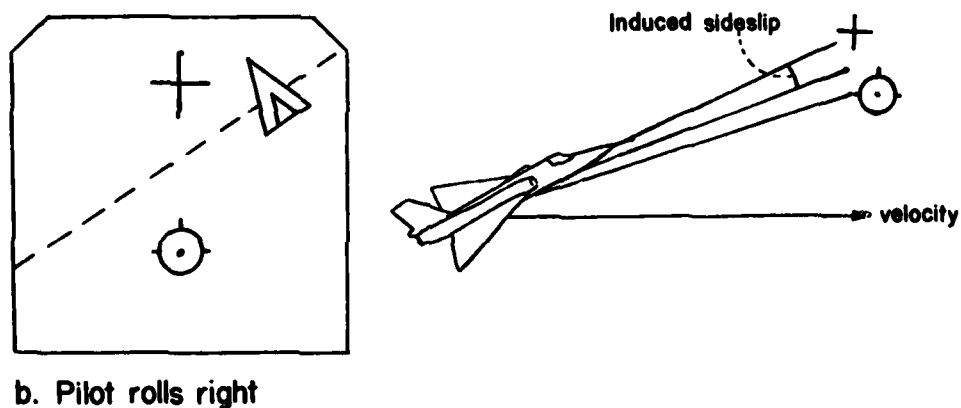
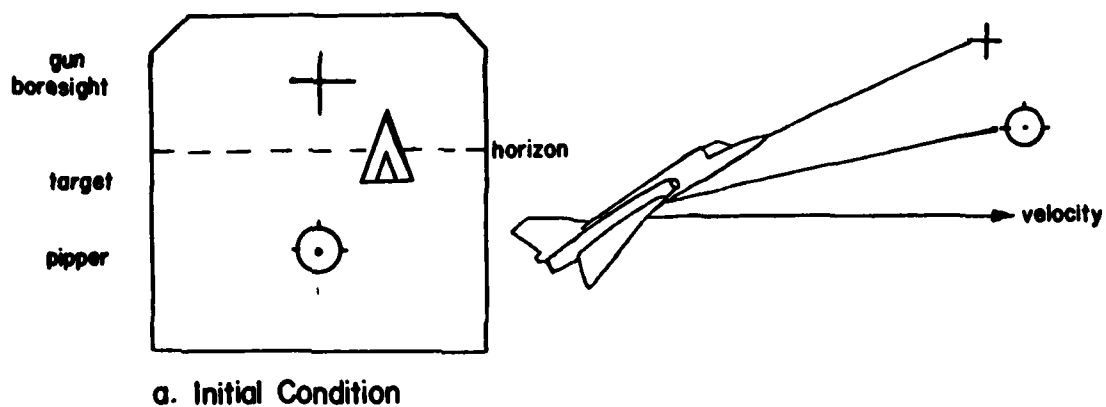


Figure 3. The Pendulum Effect

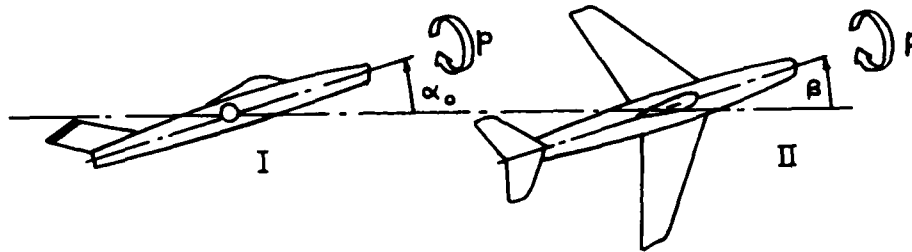


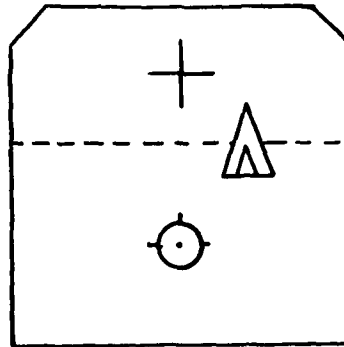
Figure 4. Roll/Sideslip Coupling

overdamped response. An overdamped response could result in the airplane becoming too sluggish as perceived by the pilot. Typically a dutch roll damping ratio of .7 to 1 is adequate. In this precise lateral pointing, the pilot desires to yaw the aircraft without significant roll coupling.

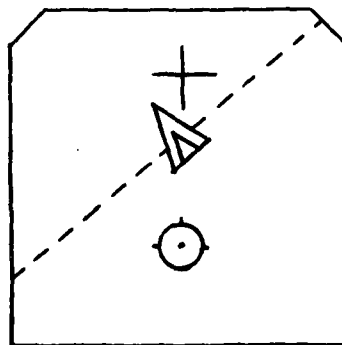
### 3. CONTROL SYSTEMS FOR AIR-TO-AIR TRACKING

After seeing how an unaugmented aircraft behaves when used to track a target, the possibilities of improvement using augmentation are obviously significant. The answer is found by looking again at Figures 3 and 4. If the aircraft were to roll about the velocity vector instead of the x-axis, the pendulum effect could be eliminated or greatly reduced. Figure 5 shows the same initial conditions as Figure 3 but shows how the pilot's task would be simplified if the aircraft was forced to roll about the velocity vector.

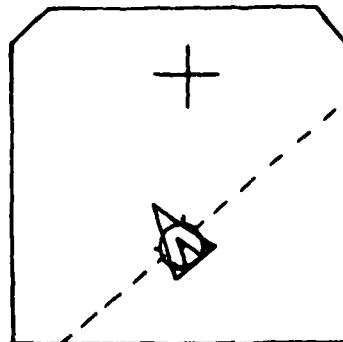
The design of a control system to improve aircraft dynamics for ATA tracking is based on this capability of rolling about the velocity vector. The result of rolling about the x-axis in the case of an unaugmented aircraft, is the increase of sideslip and reduction of angle of attack. This induced sideslip is the basis for the design of the control system. If the sideslip angle is kept at zero during the roll, then the aircraft is rolling about the velocity vector. The desired control system is therefore an accurate and responsive turn coordinator. The feedbacks needed to achieve this turn coordination are sideslip angle and sideslip



a. Initial Condition



b. Roll Right to Zero Azimuth Error



c. Pitch Up to Null Final Elevation Error

Figure 5. Rolling about Velocity Vector

angle rate. A simplified block diagram of this control system is shown in Figure 6. Since sideslip angle and sideslip rate are also the aircraft states which can be controlled by the pilot with the rudder pedals, this control system will also affect the aircraft response to rudder pedal input. This means that the pilot's task of fine lateral pointing can be improved using the system of Figure 6.

#### 4. F-106 DYNAMICS

A hybrid simulation of the F-106 was conducted on the Aeronautical Systems Division Hybrid Computer to study the F-106 in a real-time situation. The simulation was validated by checking angle of attack and elevator deflection at numerous flight conditions throughout the F-106 flight envelope. Dynamic longitudinal and lateral checks were also made at various flight conditions. The model used in the simulation proved to be an accurate representation of the real aircraft. A description of the simulation is included in Appendix A.

The purpose of the hybrid simulation was to look at the aircraft with the present control system and determine if it did demonstrate characteristics detrimental to ATA tracking. The two characteristics most likely to be encountered were the roll/sideslip coupling and the underdamped dutch roll. The standard SAS is shown in Figures 7a and 7b. The yaw rate feedback is present primarily to achieve the needed dutch roll damping. The roll rate feedback and ARI exist primarily to achieve turn coordination or, equivalently, to allow the aircraft to roll approximately about the velocity vector.

The responses of the bare airframe (SAS turned off) to a 60-degree roll input are shown in Figure 8. The roll angles were input using a roll autopilot with a 1-second time constant. These responses show sideslip perturbations of more than 1 degree with very low damping, on the order of .15. Both characteristics would indicate the F-106 with the SAS turned off could have deficient lateral handling qualities during ATA tracking. The 60-degree roll angle command was also input to the F-106 at the same flight conditions but with the standard SAS turned on. The results, shown in Figure 9, are significantly better than the bare airframe.

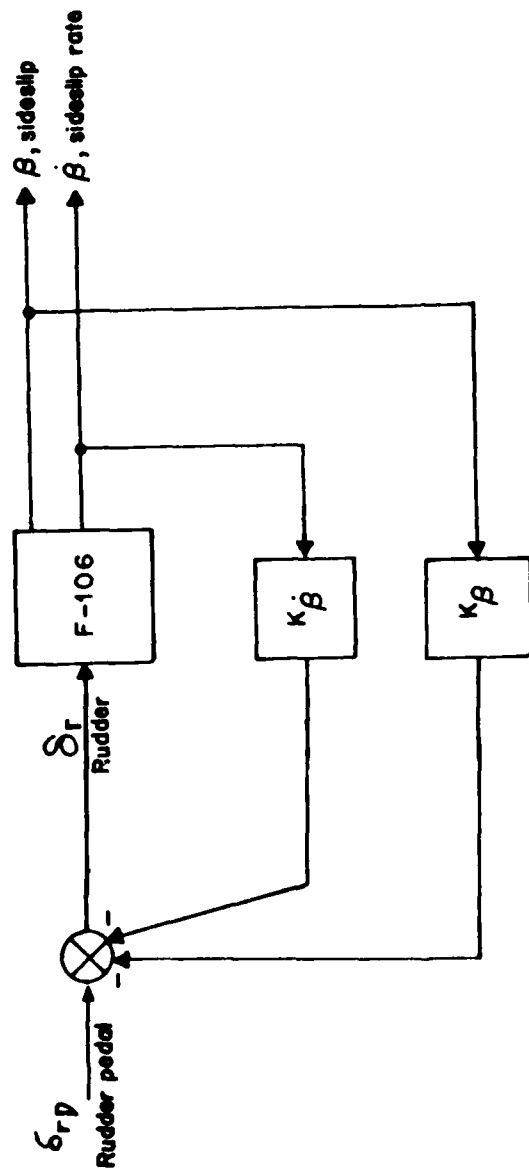
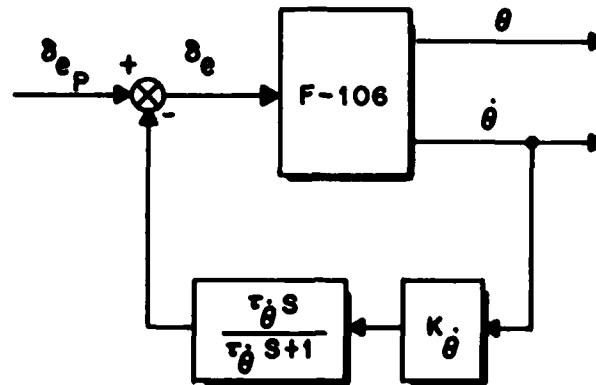


Figure 6. Sideslip Control System



### SCHEDULED GAIN AND TIME CONSTANTS

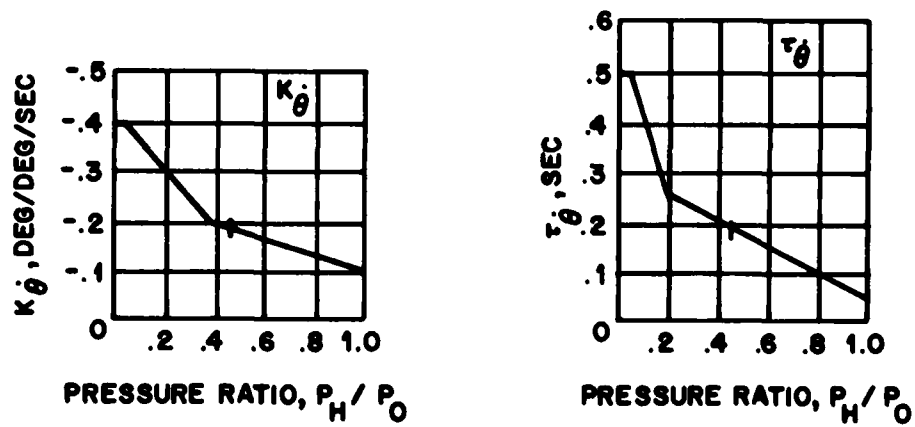
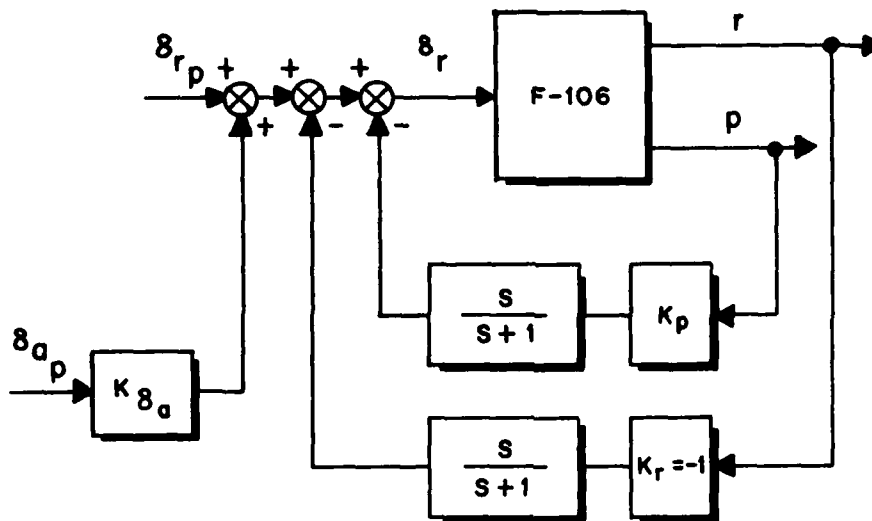


Figure 7a. F-106 Longitudinal SAS



### SCHEDULED GAINS

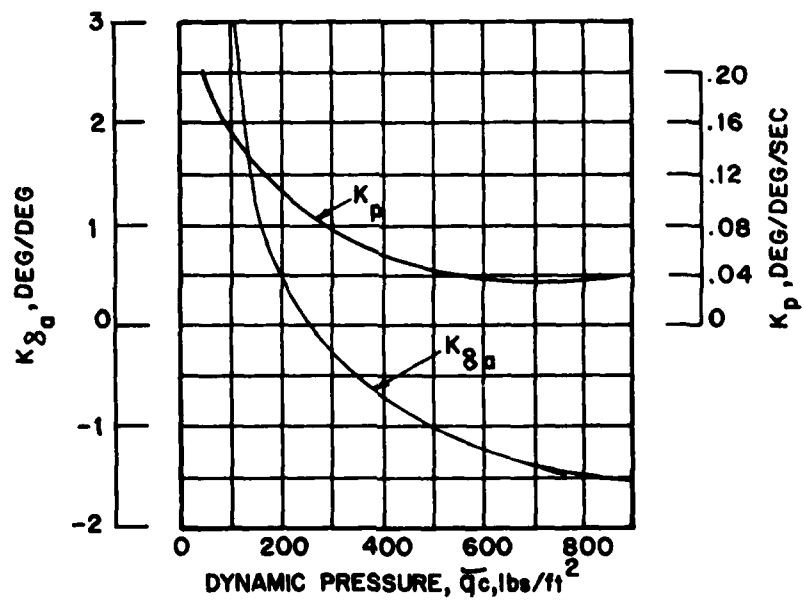


Figure 7b. F-106 Lateral SAS



Mach .8, 10000 feet

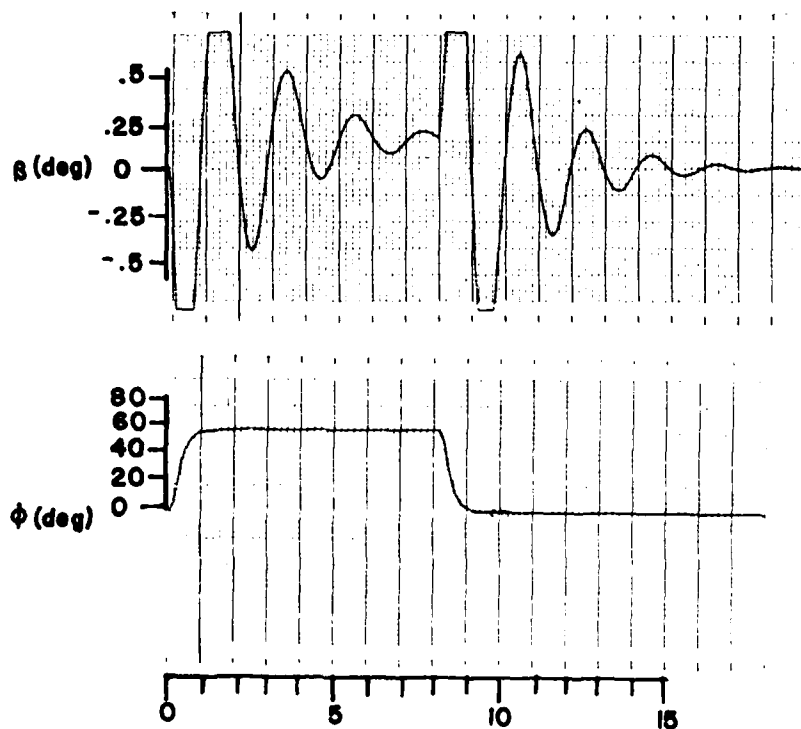
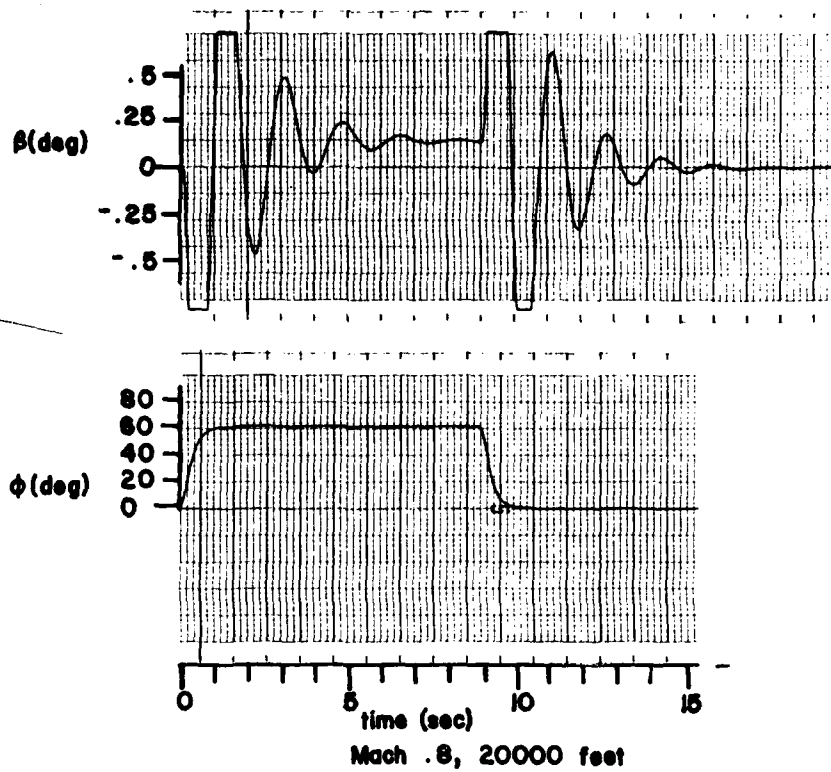


Figure 8. Bare Airframe Response to 60° Band Angle

The damping increases markedly from about .1 to .7. Although the standard SAS improves the underdamped dutch roll characteristic, the large sideslip perturbation, as seen in the bare airframe responses, is also present in the standard SAS. This roll/sideslip coupling indicates a factor which will affect the lateral tracking characteristics of the aircraft.

This preliminary analysis of the F-106 indicates possible areas of improvement in the lateral handling qualities. The bare airframe is obviously undesirable in terms of both dutch roll damping and roll/sideslip coupling. The standard SAS improves dutch roll damping considerably but the roll/sideslip perturbations are still large. Figures 8 and 9 show the dynamic responses for the standard SAS due to roll angle inputs from straight and level, 1 g flight. At higher g loadings, typical for air-to-air tracking, the induced sideslip angle would be larger than those shown in Figures 8 and 9. Based on these significant sideslip perturbations, it therefore seemed appropriate to consider a sideslip angle/sideslip angle rate ( $\beta-\dot{\beta}$ ) control system, as mentioned earlier, for use on the F-106.

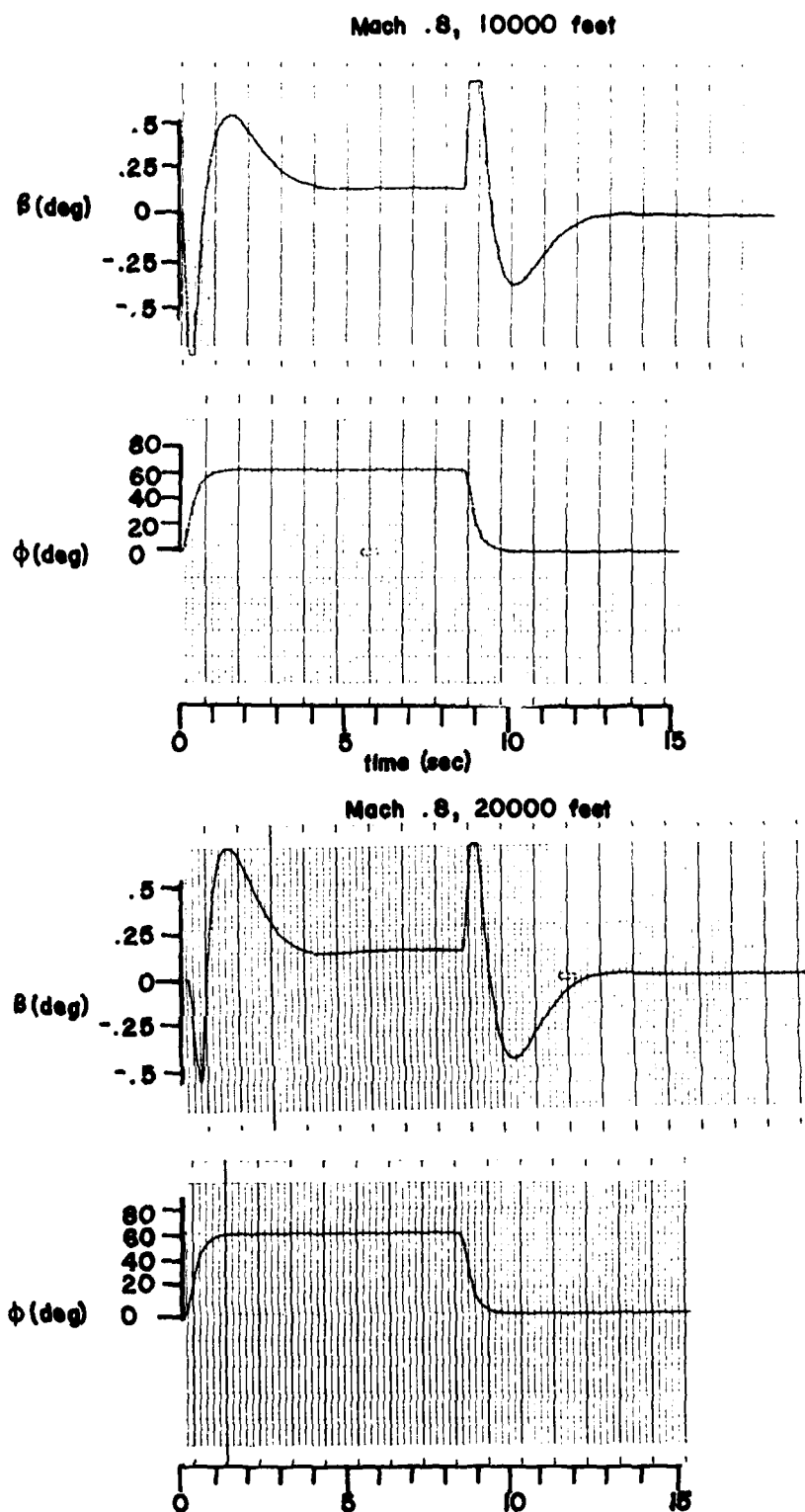


Figure 9. Standard SAS Response to 60° Bank Angle

### SECTION III

#### SYSTEM DESCRIPTION

##### 1. PRELIMINARY DESIGN MODEL

The system shown in Figure 10 is the basis for a preliminary design of a  $\beta$ - $\dot{\beta}$  SAS for the F-106. By design, the system will tend to cause the aircraft to maintain coordinated flight or, equivalently, to roll about the velocity vector; therefore, the task remaining in the preliminary design is to find the gains  $K_\beta$  and  $K_{\dot{\beta}}$  to provide sufficient damping and adequate speed of response. The proportional plus integral compensator is included to remove the steady-state error resulting from the  $\beta$  feedback. The integral gain  $K_I$  is nominally set to .2 for the analysis.

##### 2. ROOT MAP ANALYSIS

The closed-loop dynamic characteristics of the system are analyzed using the root map technique (Reference 3). This technique involves closing one loop at a constant gain, either sideslip or sideslip rate, then plotting the root locus by allowing the other gain to vary from zero to infinity. For generating a root locus at a constant  $K_\beta$ , the system model appears as Figure 11. The simplified transfer function,  $\beta/\delta r$ , is based on McRuer's (Reference 7) fourth order model and is shown below.

$$\beta/\delta r = \frac{K(s + a)}{s^2 + bs + c}$$

$$\begin{aligned} K &= Y_{\delta r}^* & b &= -(Y_v + N_r') \\ a &= -(Y_{\delta r}^* N_r' + N_{\delta r}')/Y_{\delta r}^* & c &= (N_\beta' + Y_v N_r') \end{aligned} \quad (1)$$

The dimensional aerodynamic derivatives making up the transfer function are described in Reference 7 and the resulting transfer functions are displayed in Appendix B.

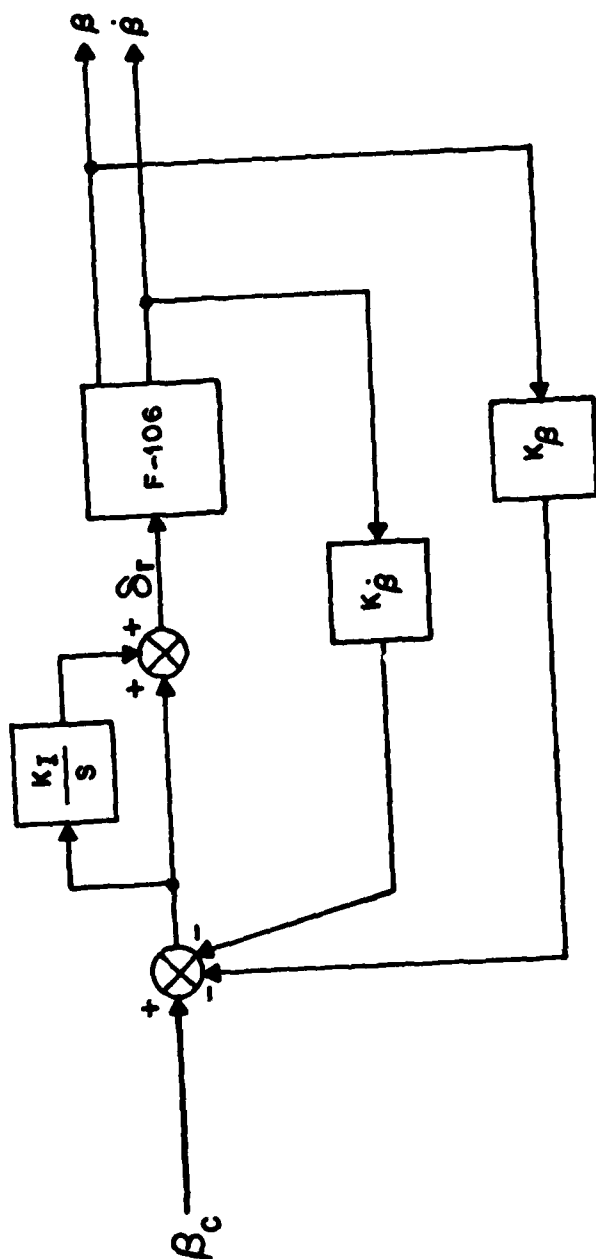


Figure 10. Preliminary Design Model

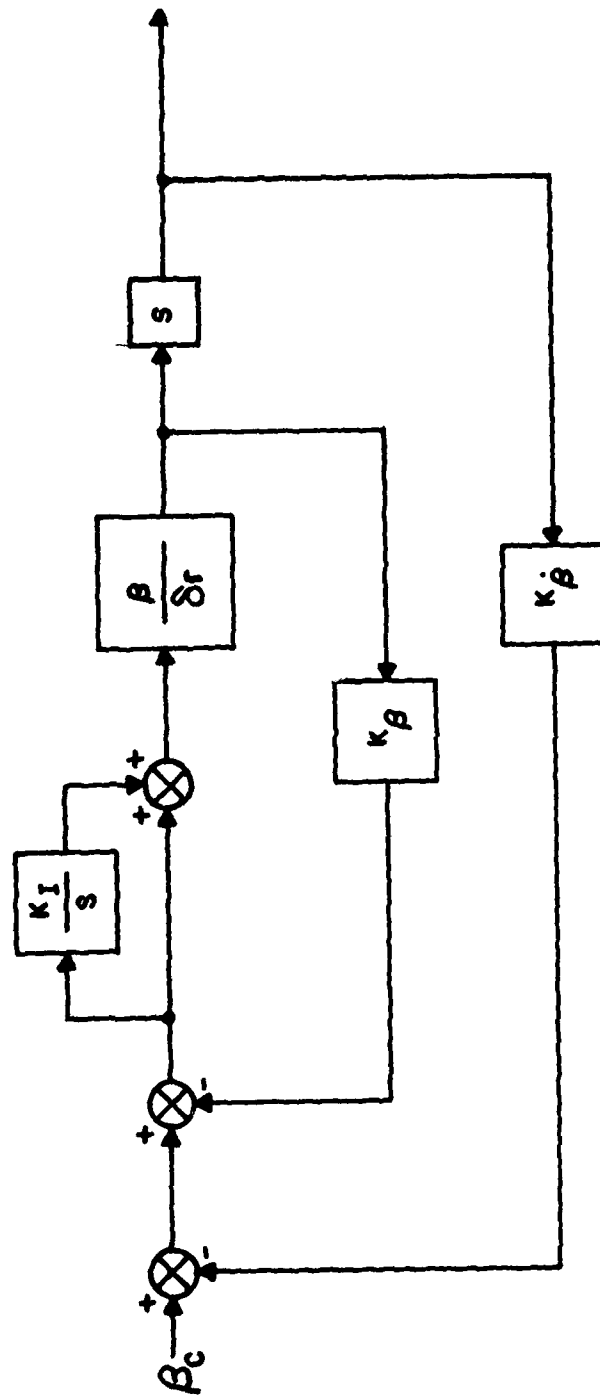


Figure 11. System Model for Constant  $K_g$

To generate a root locus for a varying  $K_\beta$ , the beta inner loop must first be closed at a given value of  $K_\beta$  and the inner loop transfer function calculated.

$$\frac{G}{1 + GH} \text{ Inner Loop } = \frac{K(s + a)(s + K_I)}{s(s^2 + bs + c) + K_\beta K(s + a)(s + K_I)} \quad (2)$$

Simplifying.

$$\frac{G}{1 + GH} \text{ Inner Loop } = \frac{K(s + a)(s + K_I)}{s^3 + (b + KK_\beta)s^2 + [c + KK_\beta(K_I + a)]s + KK_I K_\beta a} \quad (3)$$

The open loop transfer function for the complete system is now obtained by multiplying the inner loop transfer function, Equation 3, by  $sK_\beta$ .

$$\text{GH) Overall } = \frac{K_\beta K s(s + a)(s + K_I)}{s^3 + (b + KK_\beta)s^2 + [c + KK_\beta(K_I + a)]s + KK_I K_\beta a} \quad (4)$$

Using Equation 4, root locus plots are drawn for different values of  $K_\beta$ . These plots show the closed loop poles for a given value of  $K_\beta$  as  $K_\beta$  varies from zero to infinity. Unfortunately, the gain  $K_\beta$  is not explicit on the root locus. The desired closed-loop pole location must be chosen and then compared with the tabular output to find the corresponding value of  $K_\beta$ . This is an extremely time consuming process when responses at given values

of  $K_\beta$  and  $K_\beta^*$  must be compared throughout the flight envelope. To simplify this process of gain selection, root loci were also drawn at constant values of  $K_\beta^*$ .

A procedure similar to the method described above is used to get these root locus plots at constant values of  $K_\beta^*$ . Figure 12 shows the system model used for this procedure. The transfer function  $\dot{\beta}/\delta r$  is just  $s\beta/\delta r$ , as shown below, where  $\beta/\delta r$  is the same as Equation 1.

$$\dot{\beta}/\delta r = \frac{Ks(s+a)}{s^2 + bs + c} \quad (5)$$

Using Figure 12, the betadot inner loop is closed first to obtain the inner-loop transfer function.

$$\frac{G}{1+GH} \text{ Inner Loop } \text{Const } K_\beta^* = \frac{\frac{Ks(s+a)(s+K_I)}{s(s^2+bs+c)}}{1 + \frac{K_\beta^* K(s+a)(s+K_I)s}{s(s^2+bs+c)}} \quad (6)$$

Simplifying.

$$\frac{G}{1+GH} \text{ Inner Loop } \text{Const } K_\beta^* = \frac{\frac{K}{1+K_\beta^* K} s(s+a)(s+K_I)}{s^3 + \frac{b+K_\beta^* K(K_I+a)}{1+K_\beta^* K} s^2 + \frac{c+K_\beta^* K_I Ka}{1+K_\beta^* K} s} \quad (7)$$

The open-loop transfer function for the complete system is obtained by multiplying the inner loop transfer function, Equation 7, by  $K_\beta/s$ .



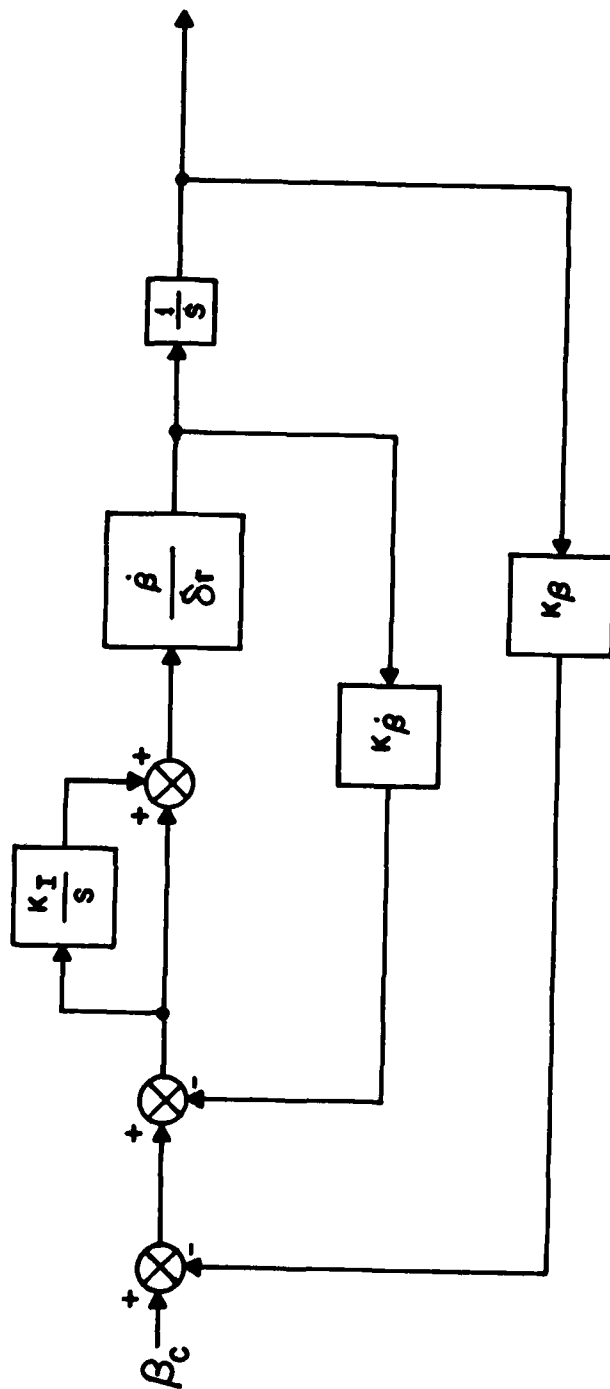


Figure 12. System Model for Constant  $K_\beta$

$$\text{GH) Overall} = \frac{\text{Const } K_{\beta}}{K_{\beta} K} \frac{1 + K_{\beta} K (s + a)(s + K_I)}{s^3 + \frac{b + K_{\beta} K (K_I + a)}{1 + K_{\beta} K} s^2 + \frac{c + K_{\beta} K_I K a}{1 + K_{\beta} K} s} \quad (8)$$

Using Equation 8, root locus plots for different values of  $K_{\beta}$  can be drawn. Poles and zeros of Equations 4 and 8 are tabulated in Appendix B for the flight condition analyzed.

To construct a root map, root loci are calculated, using Equations 4 and 8. Constant  $K_{\beta}$  root locus plots are drawn by setting  $K_{\beta}$  constant in Equation 4 and letting  $K_I$  vary from zero to infinity. Values of  $K_{\beta}$  from 1 to 15 are used. The constant  $K_I$  root locus plots are drawn in the same manner except that  $K_{\beta}$  is fixed and  $K_I$  varies. Values of  $K_I$  from 1 to 7 are used. The root map consists of these 22 root locus plots displayed on the same s-plane.

Root maps were constructed for the flight conditions shown in Table 1 to insure that the gains chosen for  $K_{\beta}$  and  $K_I$  are adequate for the entire flight envelope. Figures 13a through 13i show these root maps. Also displayed on the maps is the boundary for a good response, a response acceptable for ATA tracking. The boundary represents specifications of the damping ratio from .65 to .75 and the natural frequency from 3.5 to 6 rad/sec. The specified damping ratio would provide good lateral damping while the specified natural frequency provides adequate speed of response.

TABLE 1  
ROOT MAP FLIGHT CONDITIONS

Map	Mach	Altitude
1	.4	S.L.
2	.9	S.L.
3	.7	10000
4	.6	15000
5	.9	15000
6	1.2	15000
7	.6	30000
8	.9	30000
9	1.4	30000

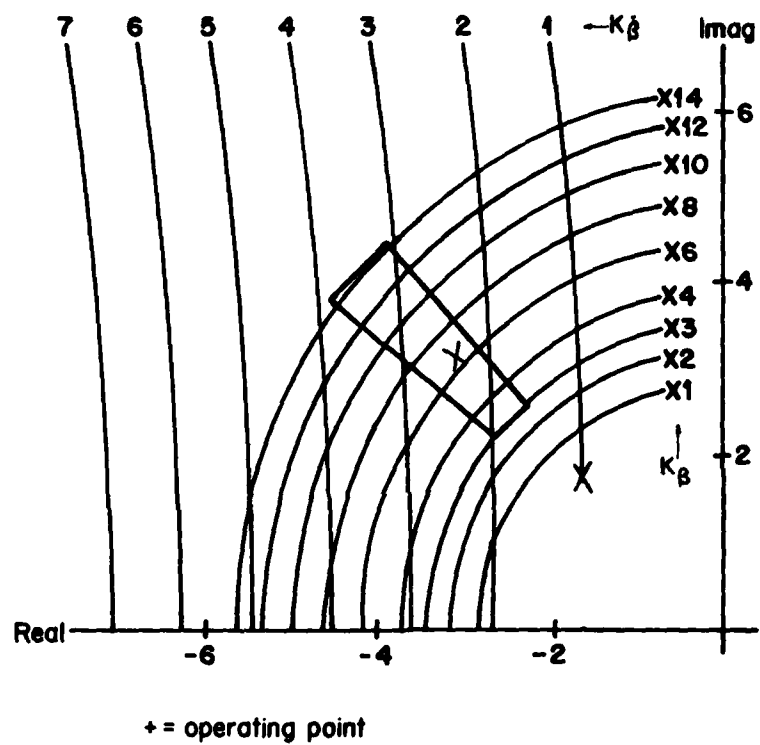


Figure 13a. Root Map at Mach .4, Sea Level

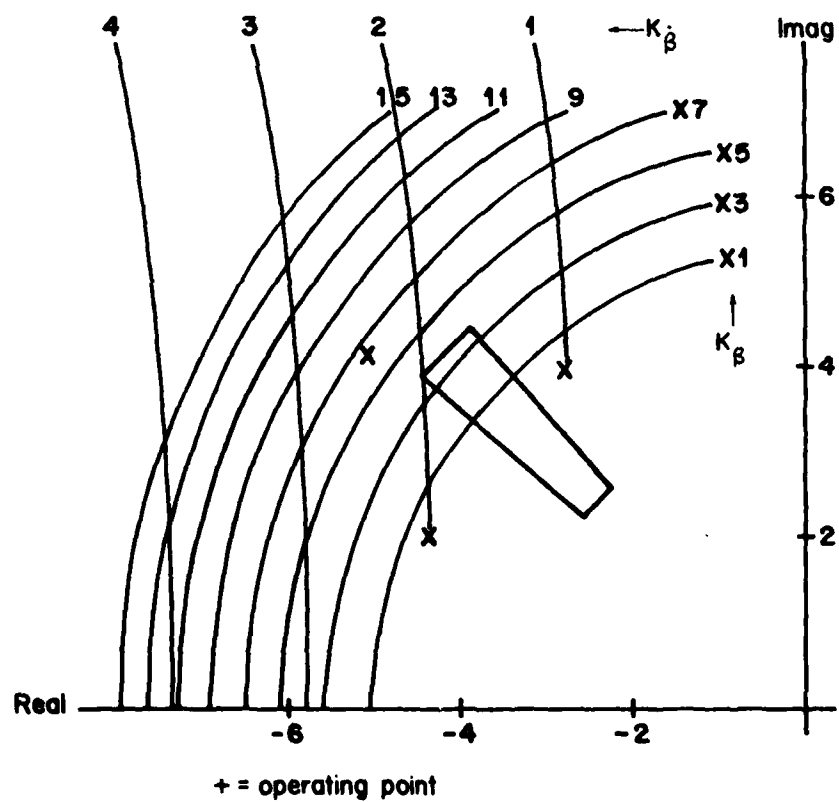


Figure 13b. Root Map at Mach .9, Sea Level

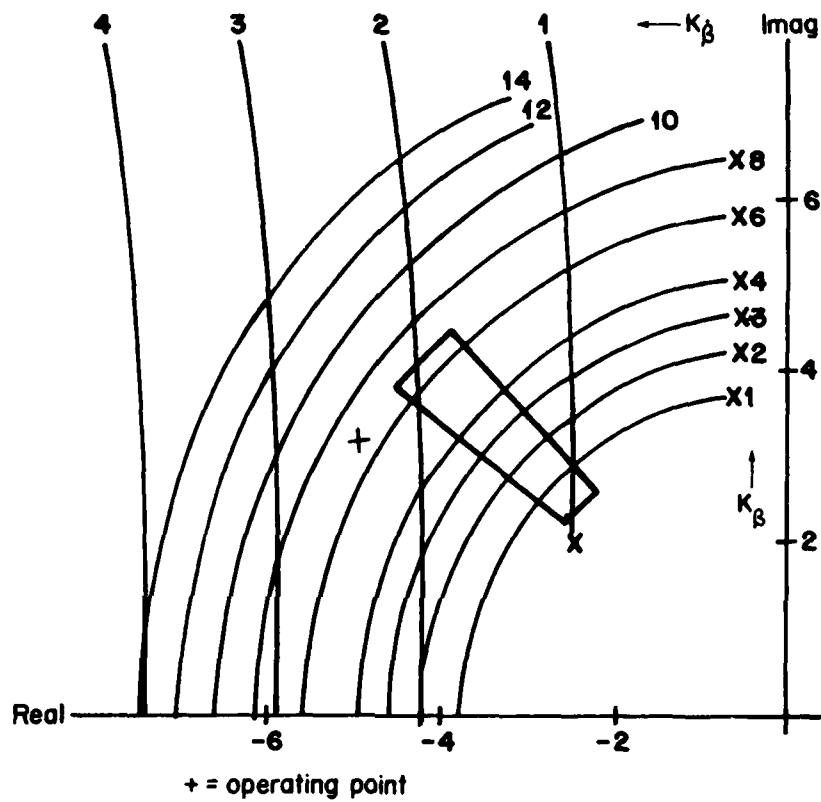


Figure 13c. Root Map at Mach .7, 10000 Feet

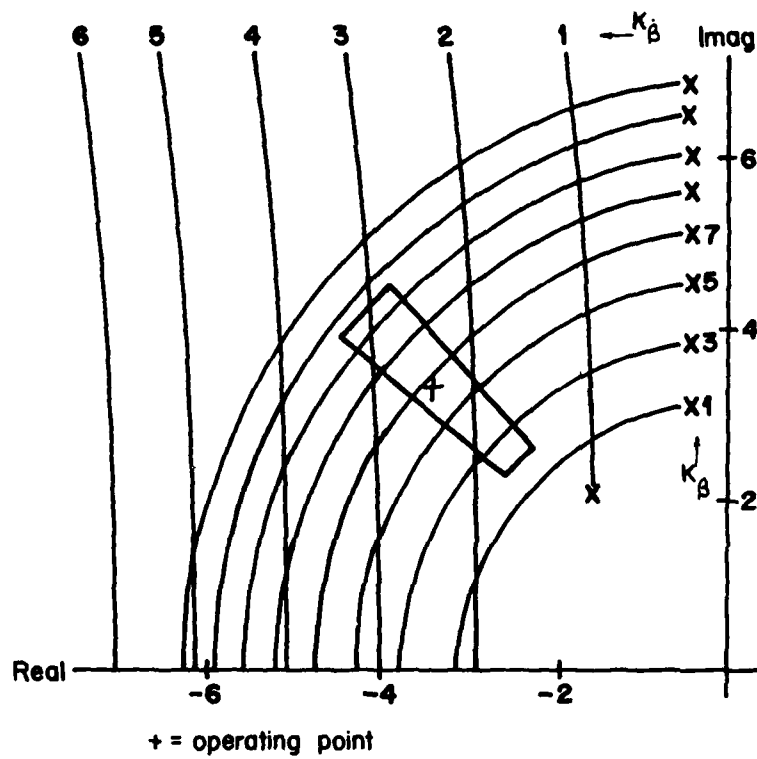


Figure 13d. Root Map at Mach .6, 15000 Feet

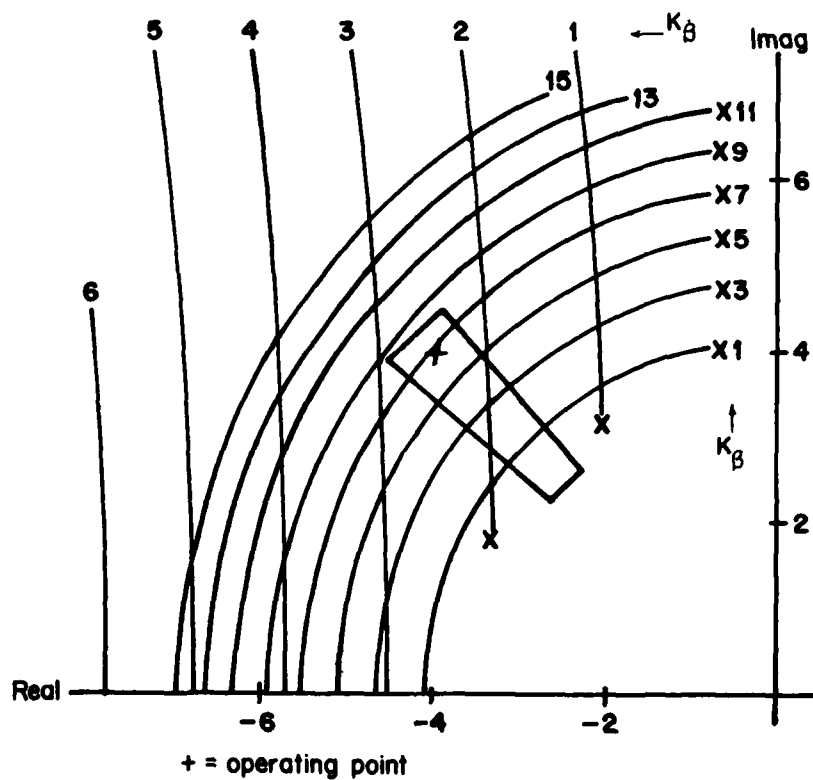


Figure 13e. Root Map at Mach .9, 15000 Feet

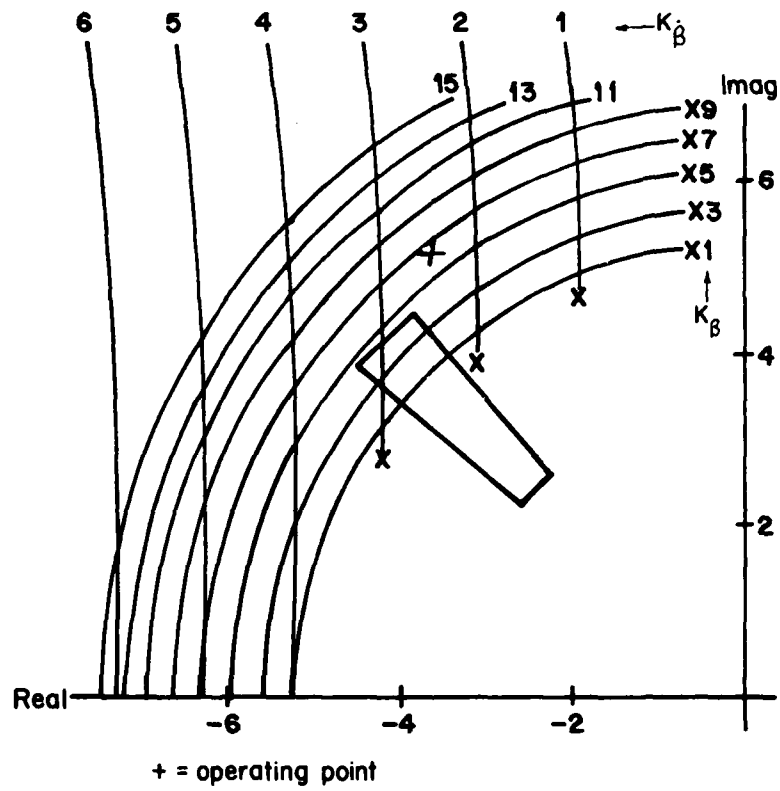


Figure 13f. Root Map at Mach 1.2, 15000 Feet



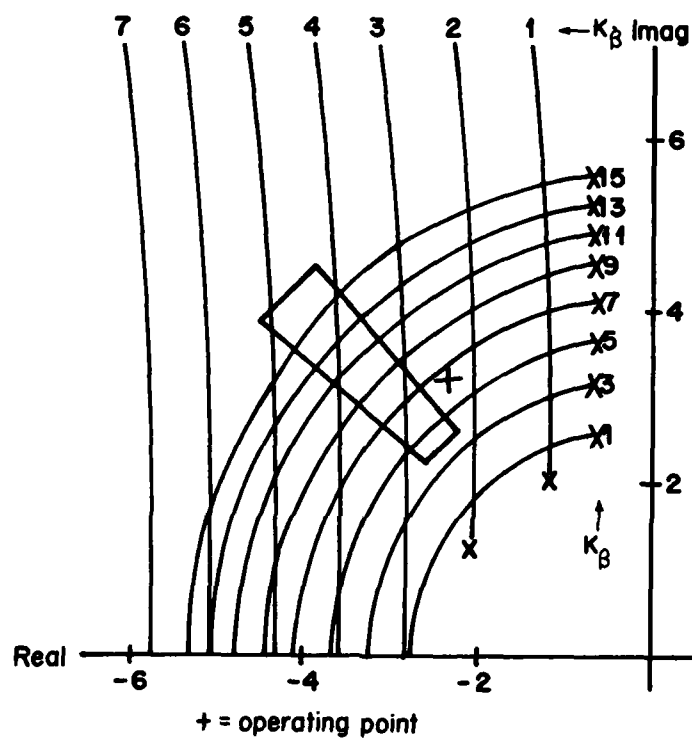


Figure 13g. Root Map at Mach .6, 30000 Feet

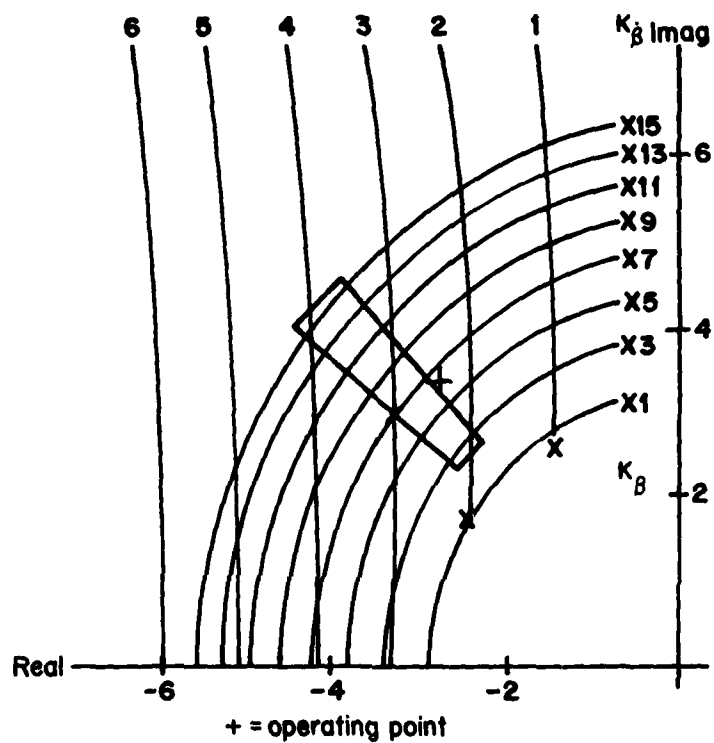


Figure 13h. Root Map at Mach .9, 30000 Feet

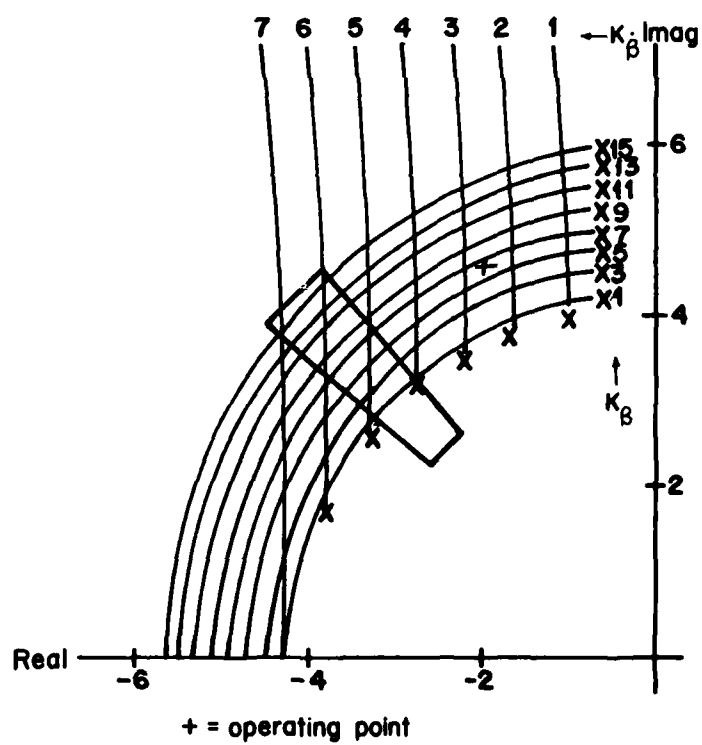


Figure 13i. Root Map at Mach 1.4, 30000 Feet

To simplify the design, the option of gain scheduling  $K_\beta$  and  $K_\beta^*$  is eliminated. This means that the values of  $K_\beta$  and  $K_\beta^*$  should be set to obtain an adequate response throughout the envelope but, if possible, a good response at flight conditions typical for ATA tracking. ATA tracking typically occurs at high subsonic Mach numbers at low and middle altitudes. Using this somewhat subjective criterion, values of  $K_\beta$  and  $K_\beta^*$  were chosen as 6.5 and 2.5, respectively. These values are shown on the root maps as the operating gains. Table 2 shows the response of the aircraft in terms of damping and natural frequency at these operating gains.

TABLE 2  
F-106 RESPONSE AT  $K_\beta = 6.5$  AND  $K_\beta^* = 2.5$

<u>Map</u>	<u>Mach, Altitude</u>	<u>Damping Ratio</u>	<u>Natural Frequency (rad/sec)</u>
Figure 13a	.4, S.L.	.71	4.5
Figure 13b	.9, S.L.	.79	6.6
Figure 13c	.7, 10000	.86	5.8
Figure 13d	.6, 15000	.67	4.8
Figure 13e	.9, 15000	.71	5.6
Figure 13f	1.2, 15000	.6	6.4
Figure 13g	.6, 30000	.6	4.0
Figure 13h	.9, 30000	.68	4.4
Figure 13i	1.4, 30000	.4	5.0

Table 2 shows that the chosen gains for  $K_\beta$  and  $K_\beta^*$  of 6.5 and 2.5 do provide a good response at the lower altitude, subsonic flight conditions. At the two supersonic conditions, however, the response is somewhat underdamped. This tendency of an underdamped response at supersonic Mach numbers should not be important since almost no tracking is done supersonically.

### 3. FREQUENCY RESPONSE ANALYSIS

The preliminary design of the  $\beta-\dot{\beta}$  system using the model from Figure 10 shows that acceptable responses can be achieved using gains of 6.5 and 2.5 for  $K_{\beta}$  and  $K_{\dot{\beta}}$ . This acceptability criteria is based subjectively on the values of dutch roll damping and natural frequency. Since these gains come from the root map analysis, which assumes a second-order-linear aircraft model, it is appropriate to look at these gains in a more sophisticated model. The EASY Dynamic Analysis Program (Reference 2) is used to achieve this more elaborate model. Appendix C contains a short description of the EASY program and contains the input data for the frequency analyses.

The EASY program was used to obtain closed-loop frequency plots for the following transfer functions:  $\beta/\delta r$ ,  $\phi/\delta r$ ,  $\beta/\delta a$ . These plots are shown for flight conditions of Mach .8 at 10000 feet and Mach .6 at 30000 feet. The first condition is somewhat typical of an ATA engagement and the second is representative of a low dynamic pressure situation for the aircraft. The three transfer functions above are chosen specifically because each shows information significant to the ATA tracking task. The frequencies of greatest importance for ATA tracking are those around the dutch roll frequency. These frequencies are important because the dutch roll mode is continually being excited during tracking. The frequencies range from about two to seven rad/sec depending on control system and flight condition.  $\beta/\delta r$  gives an indication of the ease with which the pilot can point the aircraft using the rudder.  $\phi/\delta r$  shows the coupling effect of rudder into roll angle and it can also give an indication of the ease with which the pilot can point the aircraft. An aircraft with a control system designed to facilitate ATA tracking should have a large magnitude for  $\beta/\delta r$  (near 0 db) to provide adequate pointing capability while maintaining a low magnitude for  $\phi/\delta r$ , or low roll/sideslip coupling. The effect of a large  $\phi/\delta r$  would be an increase in pilot workload due to the inadvertent roll angles.  $\beta/\delta a$  is an indicator of how well the aircraft is maintaining coordinated flight, or equivalently, how precisely the aircraft is rolling about the velocity vector. A low magnitude for  $\beta/\delta a$  is most advantageous for ATA tracking.

The closed-loop frequency plots for the two flight conditions are shown for the bare airframe, standard SAS, and  $\beta-\dot{\beta}$  SAS. Figures 14a - 14c and Figures 15a - 15c show the frequency response for  $\beta/\delta r$  for both flight conditions. The plots show that the desirable quality of a relatively large  $\beta/\delta r$  is achieved by both the bare airframe and the  $\beta-\dot{\beta}$  SAS at both flight conditions. Figures 16a - 16c and Figures 17a - 17c show  $\phi/\delta r$  at the two flight conditions. The bare airframe  $\phi/\delta r$  is unacceptably large, but the standard SAS and the  $\beta-\dot{\beta}$  SAS both have much lower magnitudes and are therefore more desirable. This same desirable quality of low coupling magnitude is also shown by the standard and  $\beta-\dot{\beta}$  SAS's in their  $\beta/\delta a$  frequency plots. These frequency plots are shown in Figures 18a - 18c and Figures 19a - 19c.

Based on these frequency plots, the bare airframe is obviously least desirable for ATA tracking due to its large  $\phi/\delta r$  and  $\beta/\delta a$  ratios. On the other hand the standard SAS and the  $\beta-\dot{\beta}$  SAS have much smaller magnitudes for  $\beta/\delta a$  and  $\phi/\delta r$  and therefore are probably more applicable to ATA tracking. The  $\beta-\dot{\beta}$  SAS shows a larger magnitude  $\beta/\delta r$  than the standard SAS, possibly making it easier for the pilot to point the aircraft, but the standard SAS has smaller  $\phi/\delta r$  and  $\beta/\delta a$  coupling magnitudes, possibly decreasing pilot workload. In summary, the bare airframe is probably not adequate for the tracking task while both the standard and  $\beta-\dot{\beta}$  SAS's appear to be about equal in their capabilities.

#### 4. DETAILED DESIGN MODEL

The preliminary design model from Figure 12 provided a basis for the engineering analysis of the  $\beta-\dot{\beta}$  control. A more detailed model is now presented which includes "real world" criteria in its design. The very first question asked on seeing the preliminary design model is, "Can  $\beta$  and  $\dot{\beta}$  be measured?" The answer is yes for the sideslip angle. Beta vanes provide adequate, though somewhat noisy, measurements of  $\beta$ . Sideslip angle rate, on the other hand, is not so easily measured. The beta signal is too noisy to differentiate; hence, some other source for  $\dot{\beta}$  must be found.

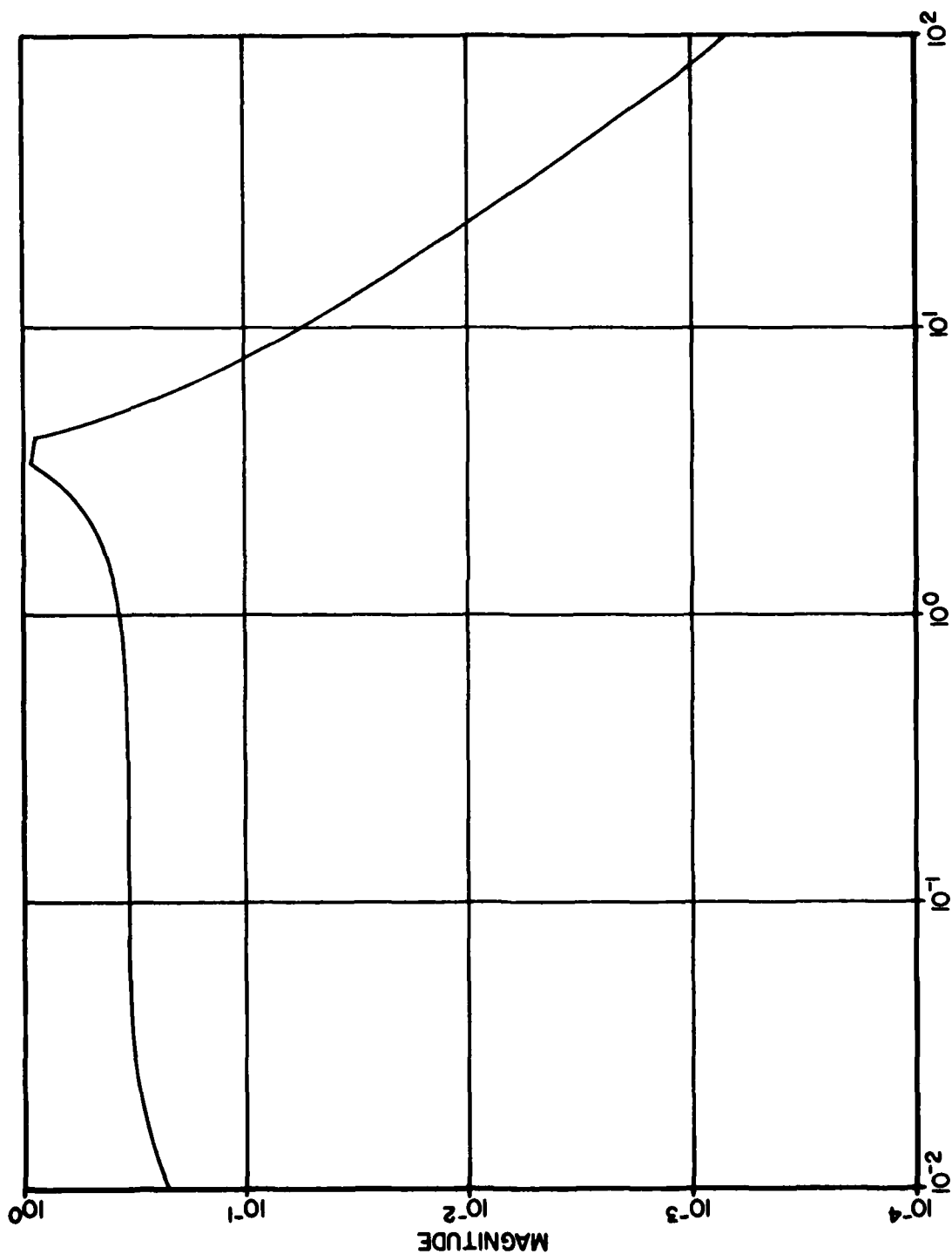


Figure 14a. Bare Airframe Beta/Delta Rudder .8, 10000

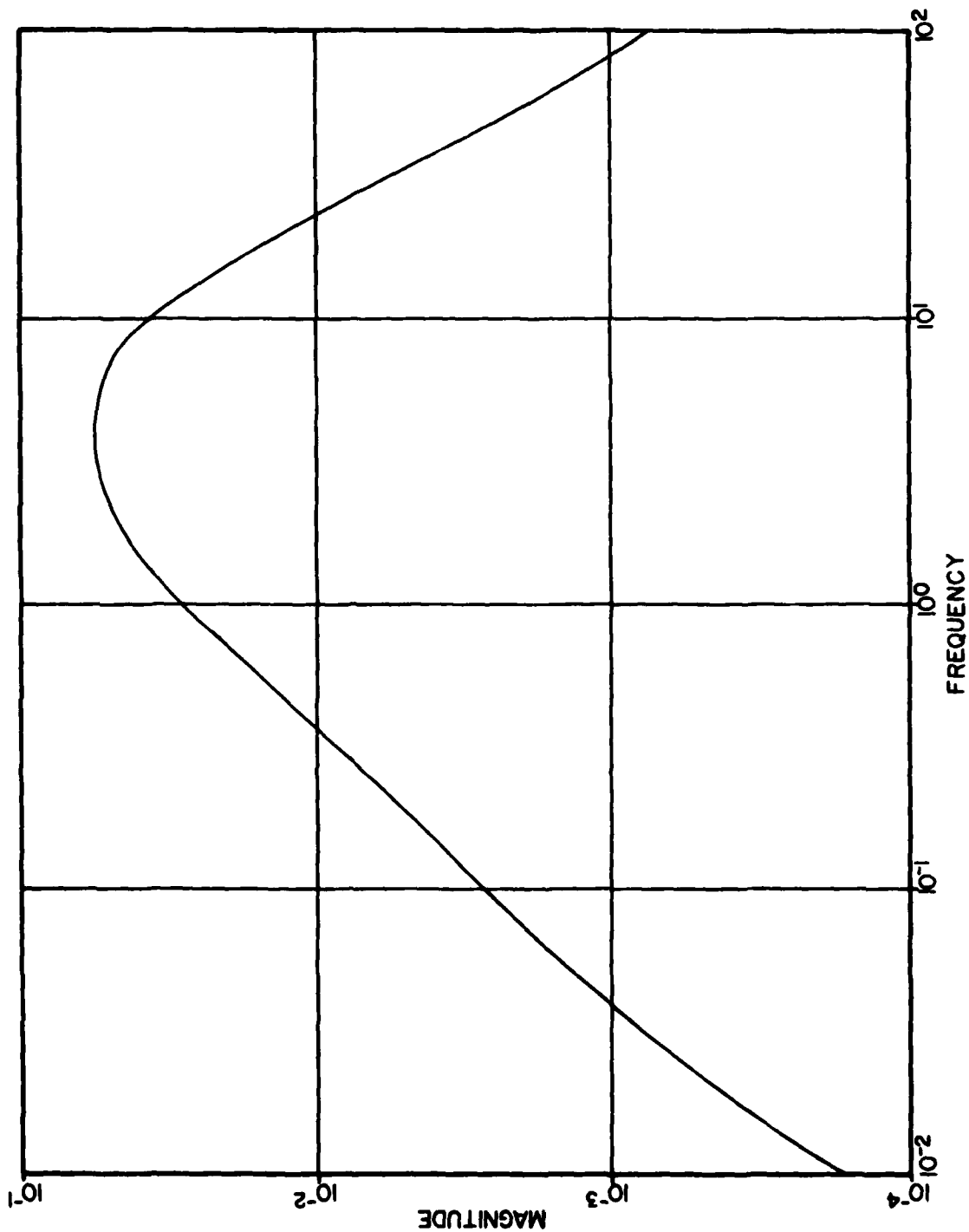


Figure 14b. Standard SAS Beta/Delta Rudder .8, 10000



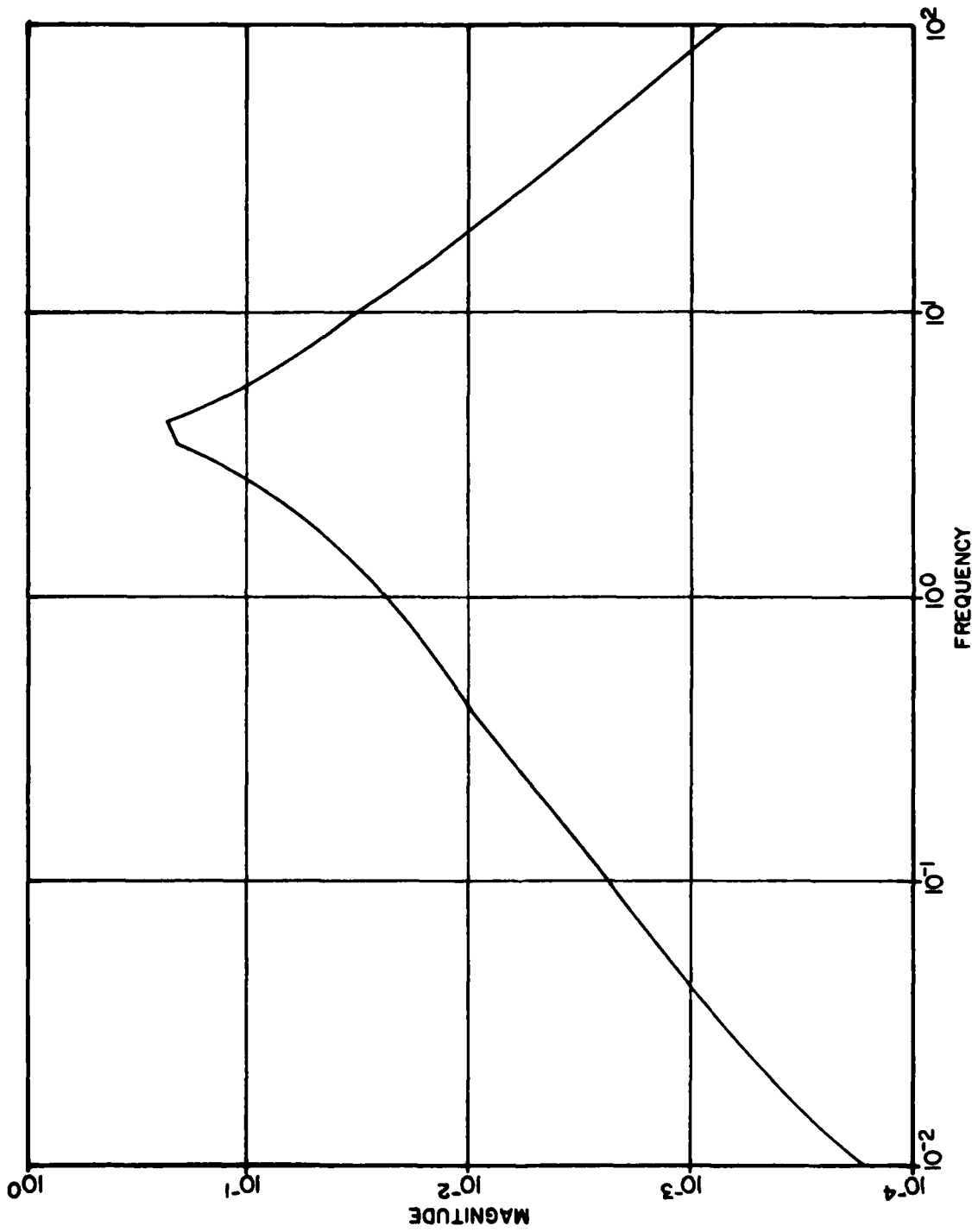


Figure 14c. Betadot SAS Beta/Delta Rudder .8, 10000

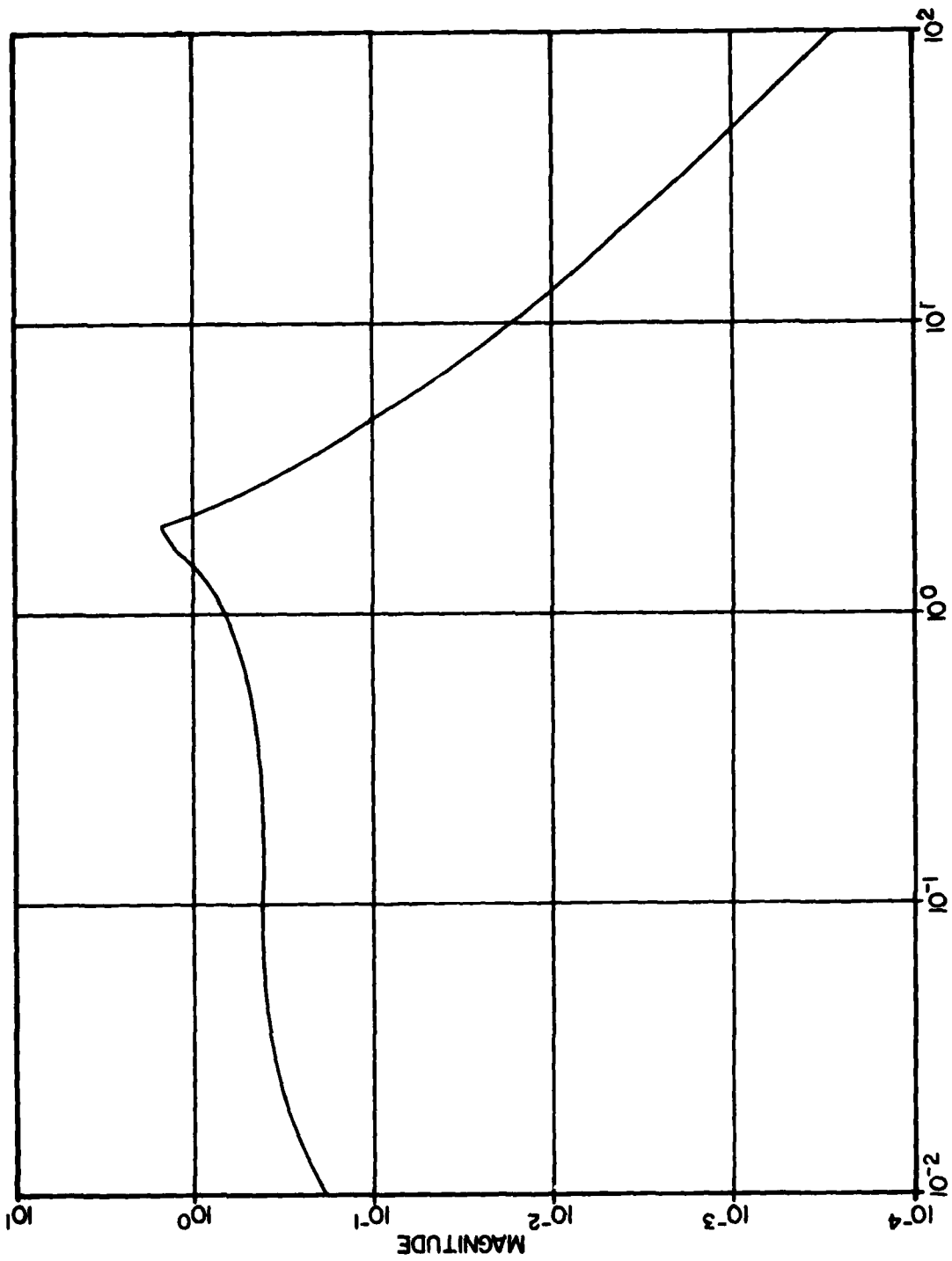


Figure 15a. Bare Airframe Beta/Delta Rudder .6, 30000

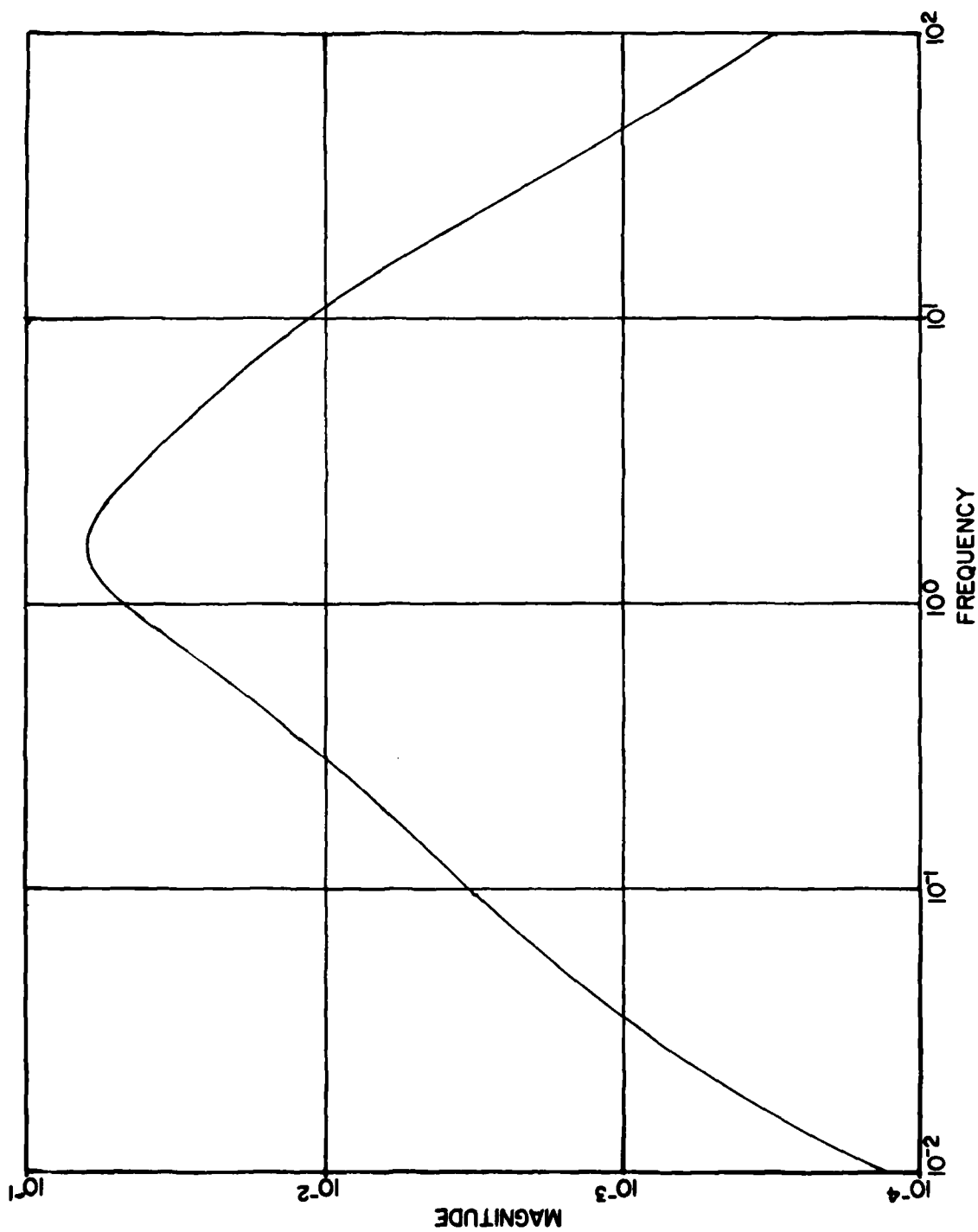


Figure 15b. Standard SAS Beta/Delta Rudder .6, 30000

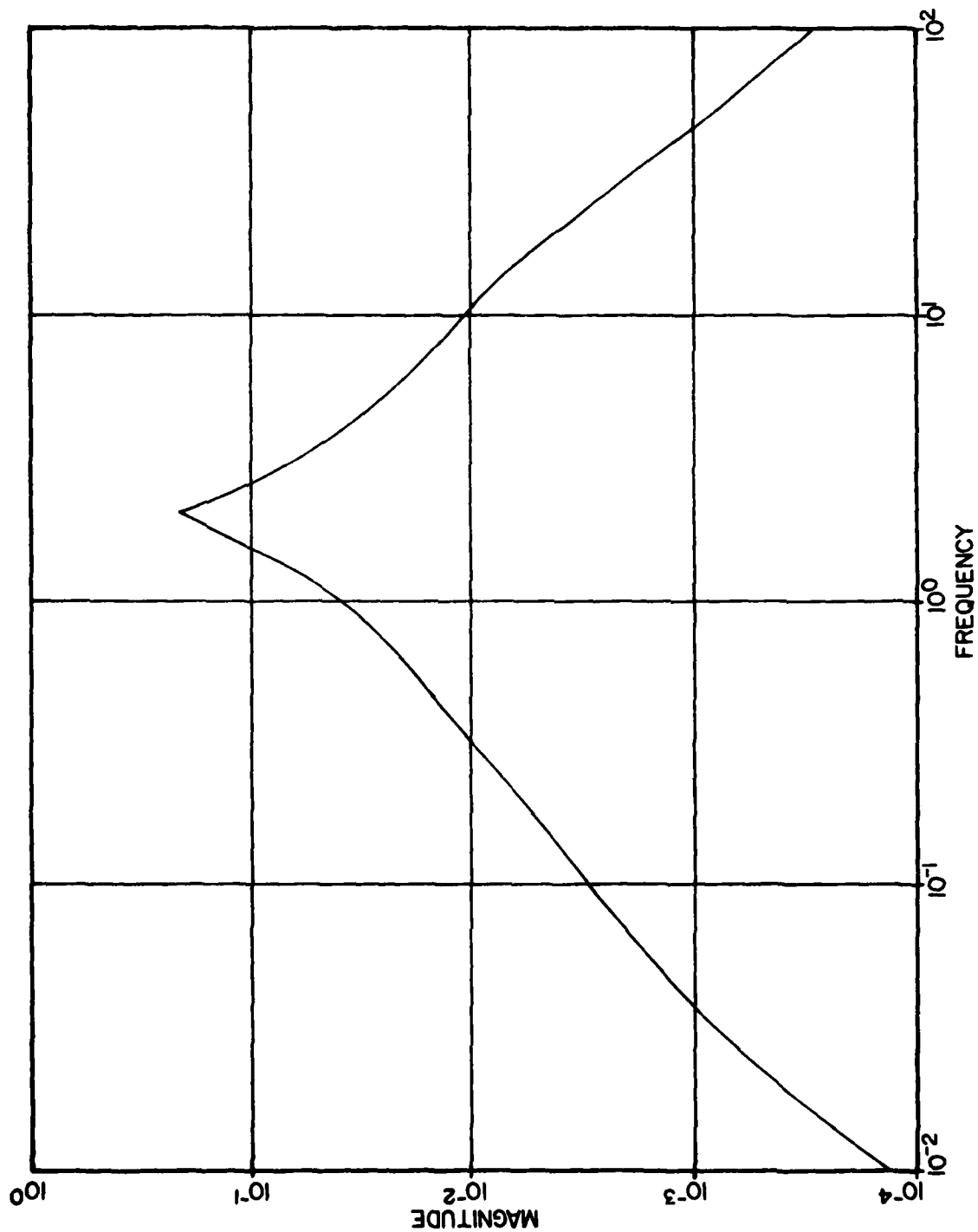


Figure 15c. Betadot SAS Beta/Delta Rudder .6, 30000

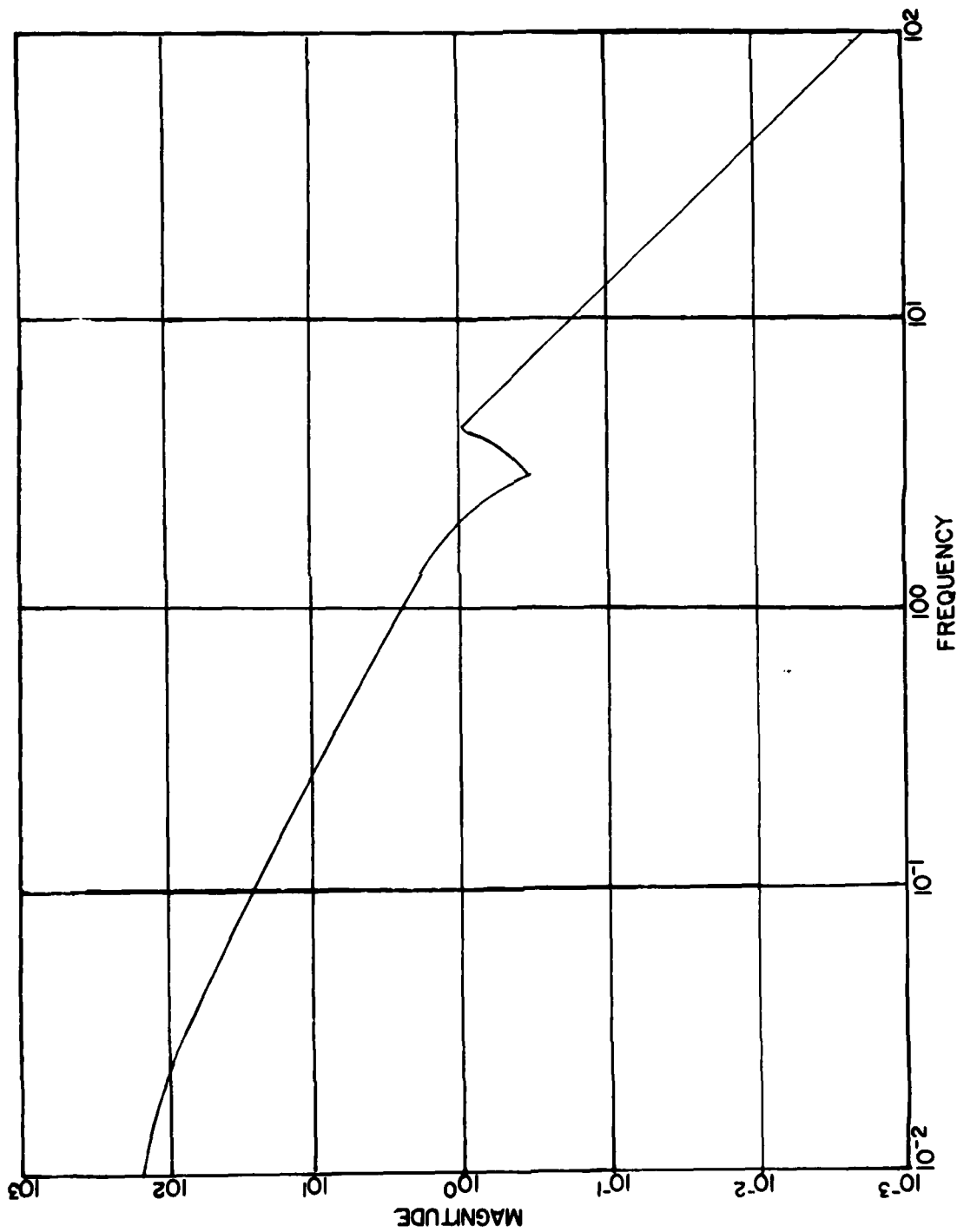


Figure 16a. Bare Airframe Phi/Delta Rudder .8, 10000

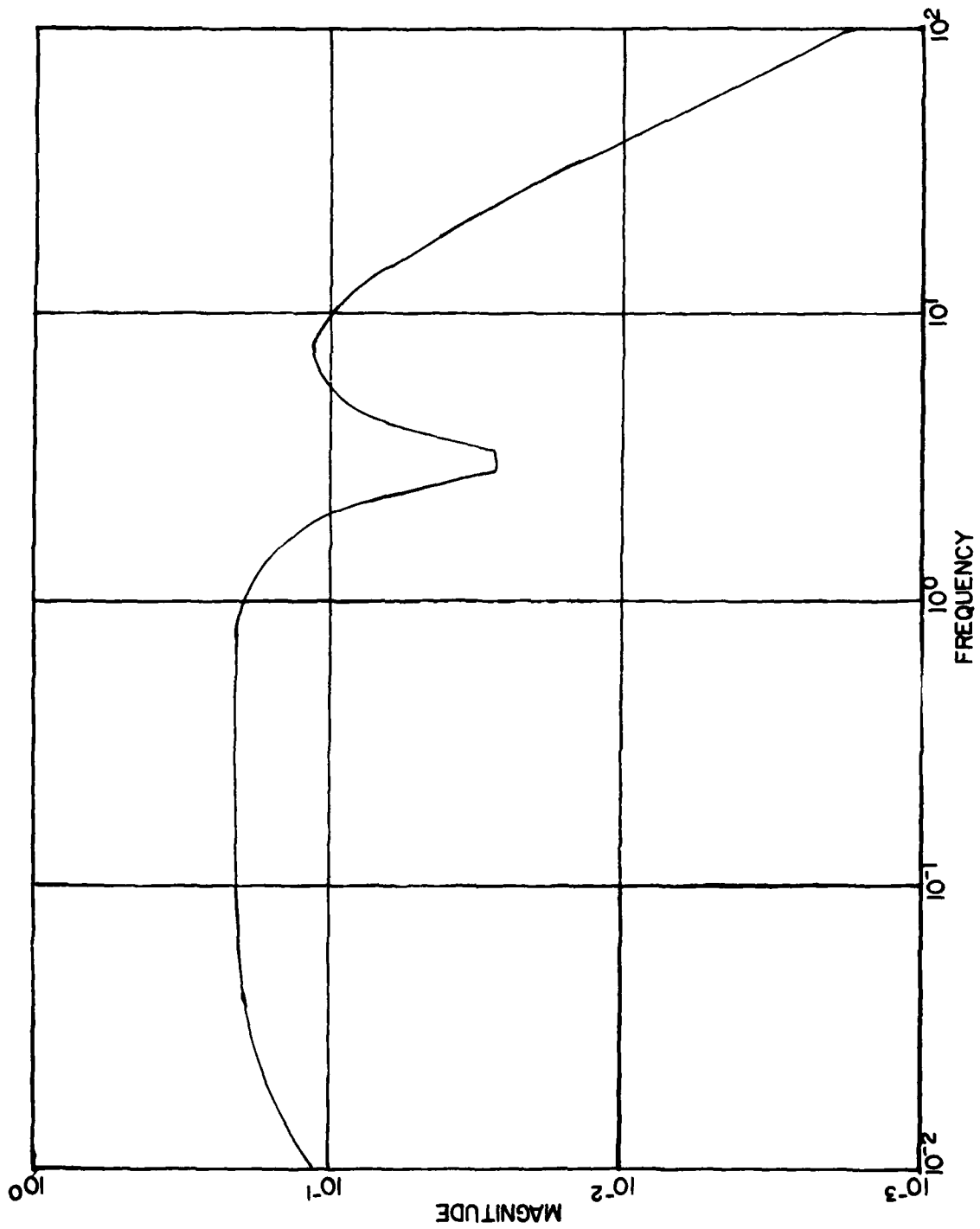


Figure 16b. Standard SAS Phi/Delta Rudder .8, 10000

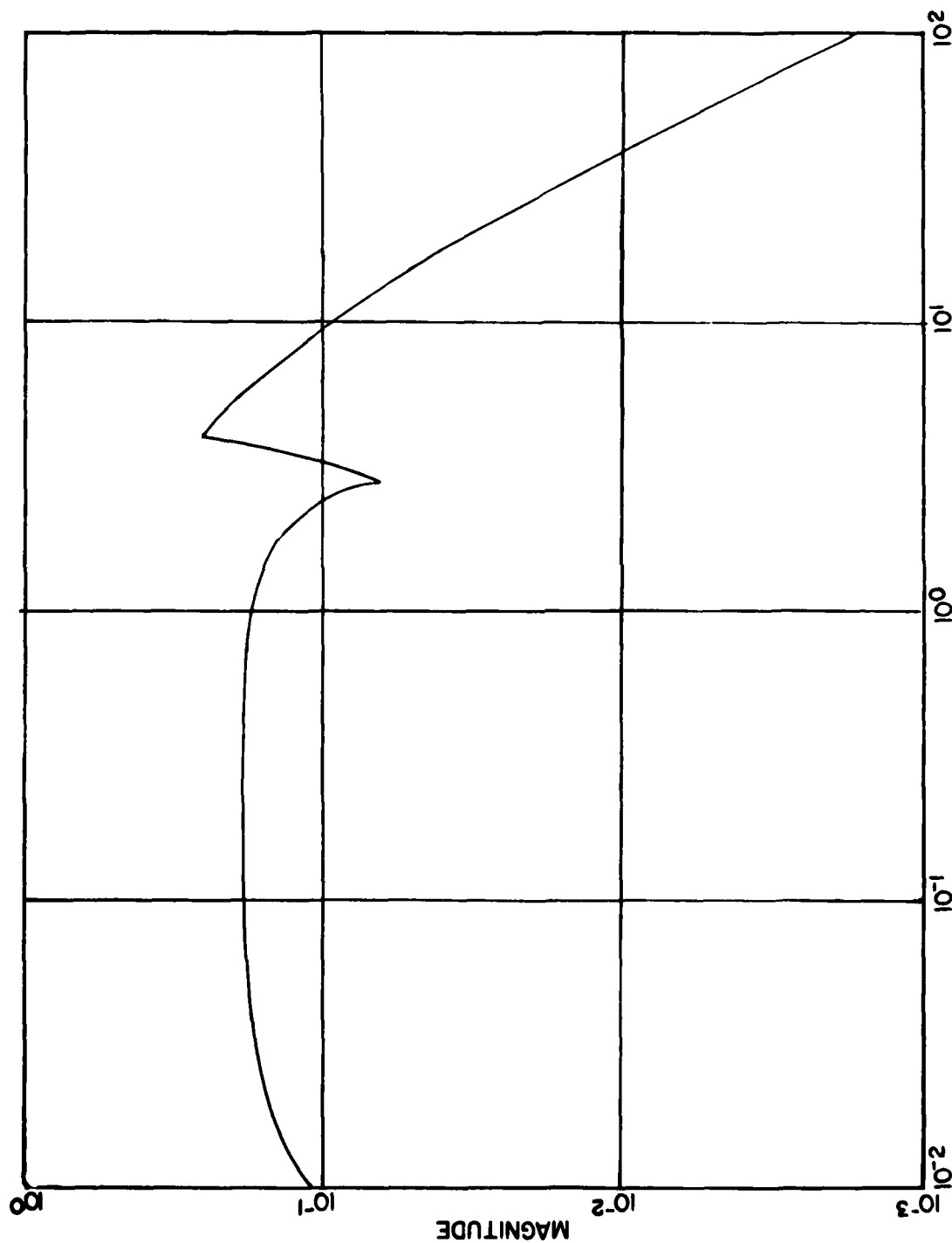


Figure 16c. Betadot SAS Phi/Delta Rudder .8, 10000

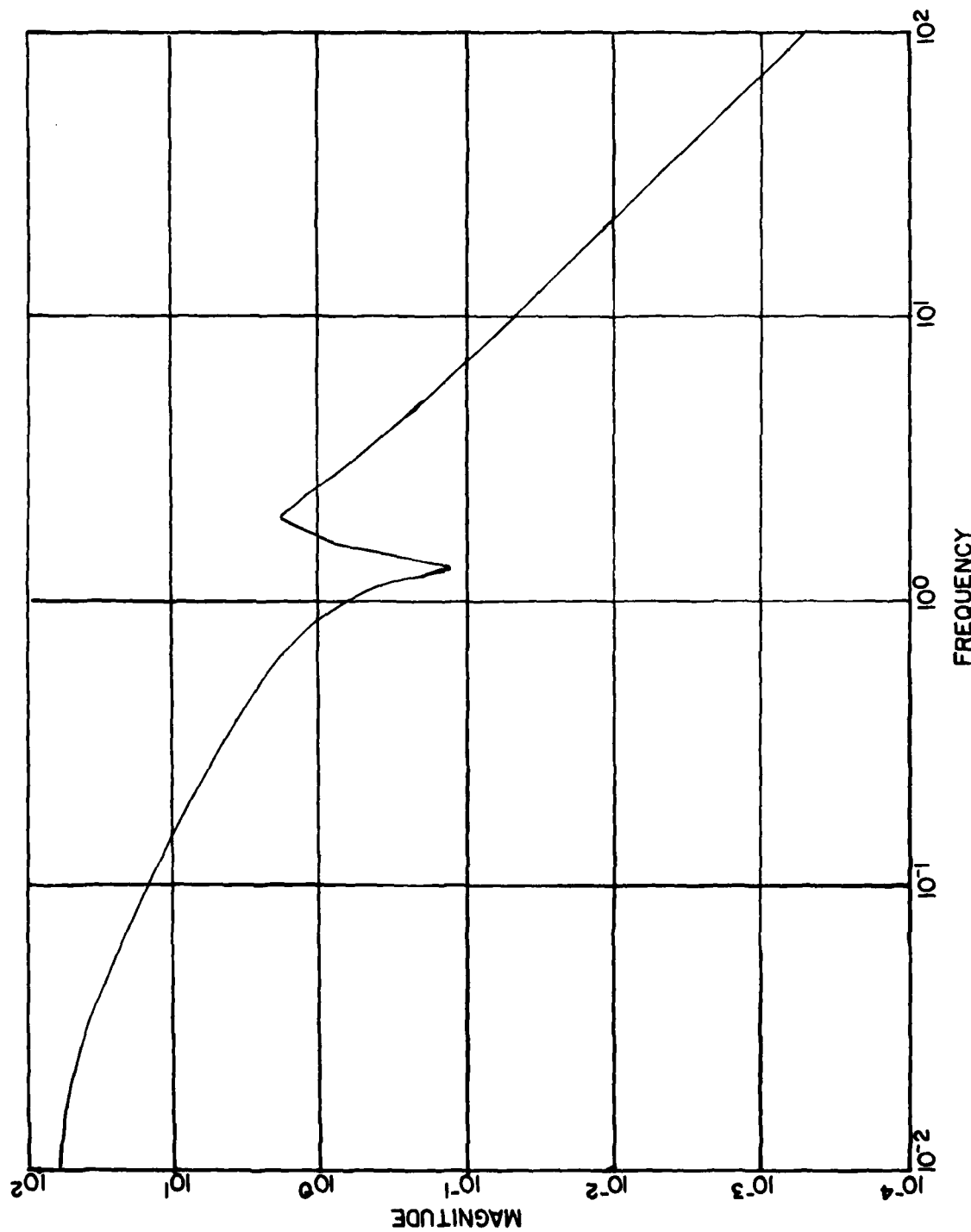


Figure 17a. Bare Airframe Phi/Delta Rudder .6, 30000



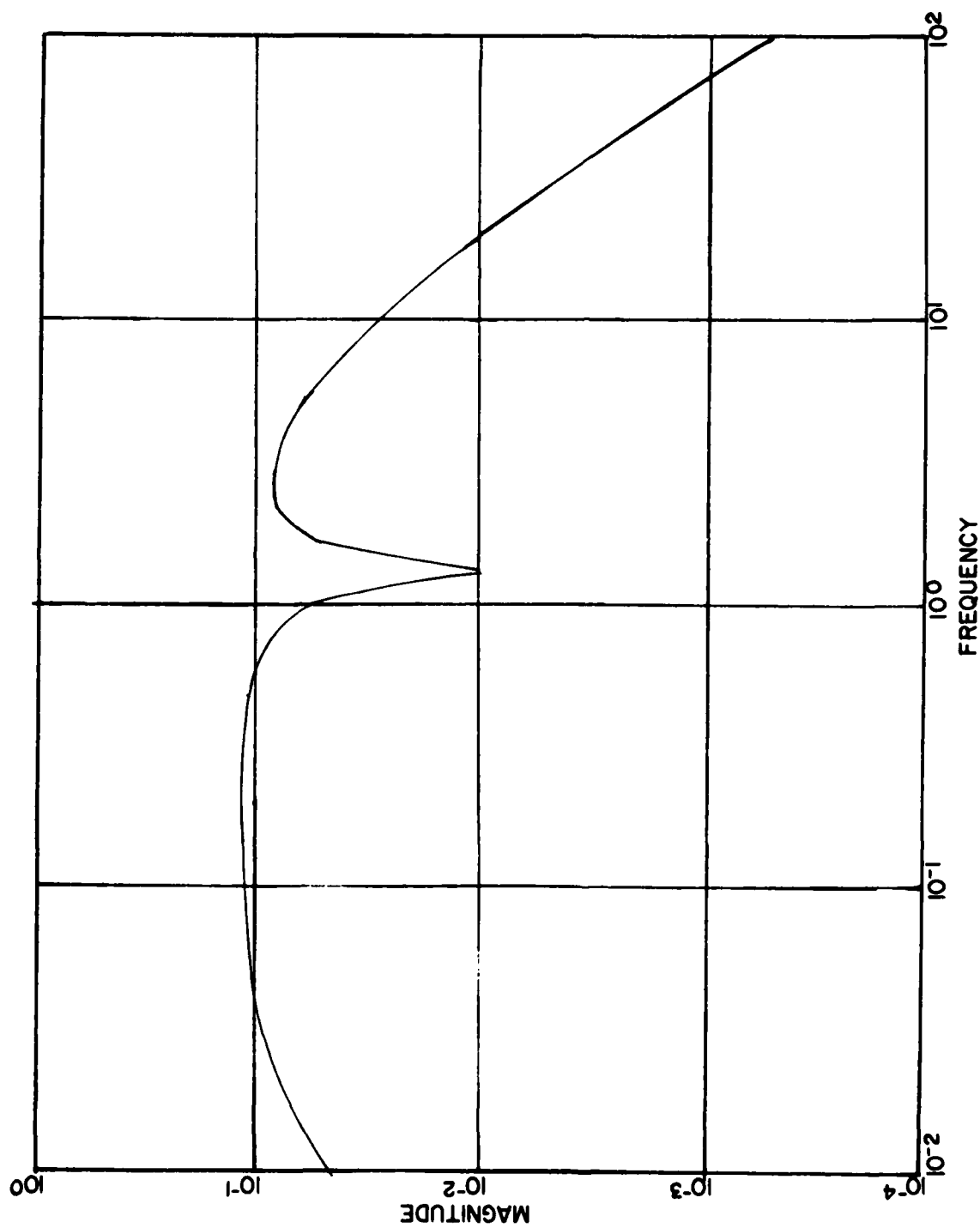


Figure 17b. Standard SAS Phi/Delta Rudder .6, 30000

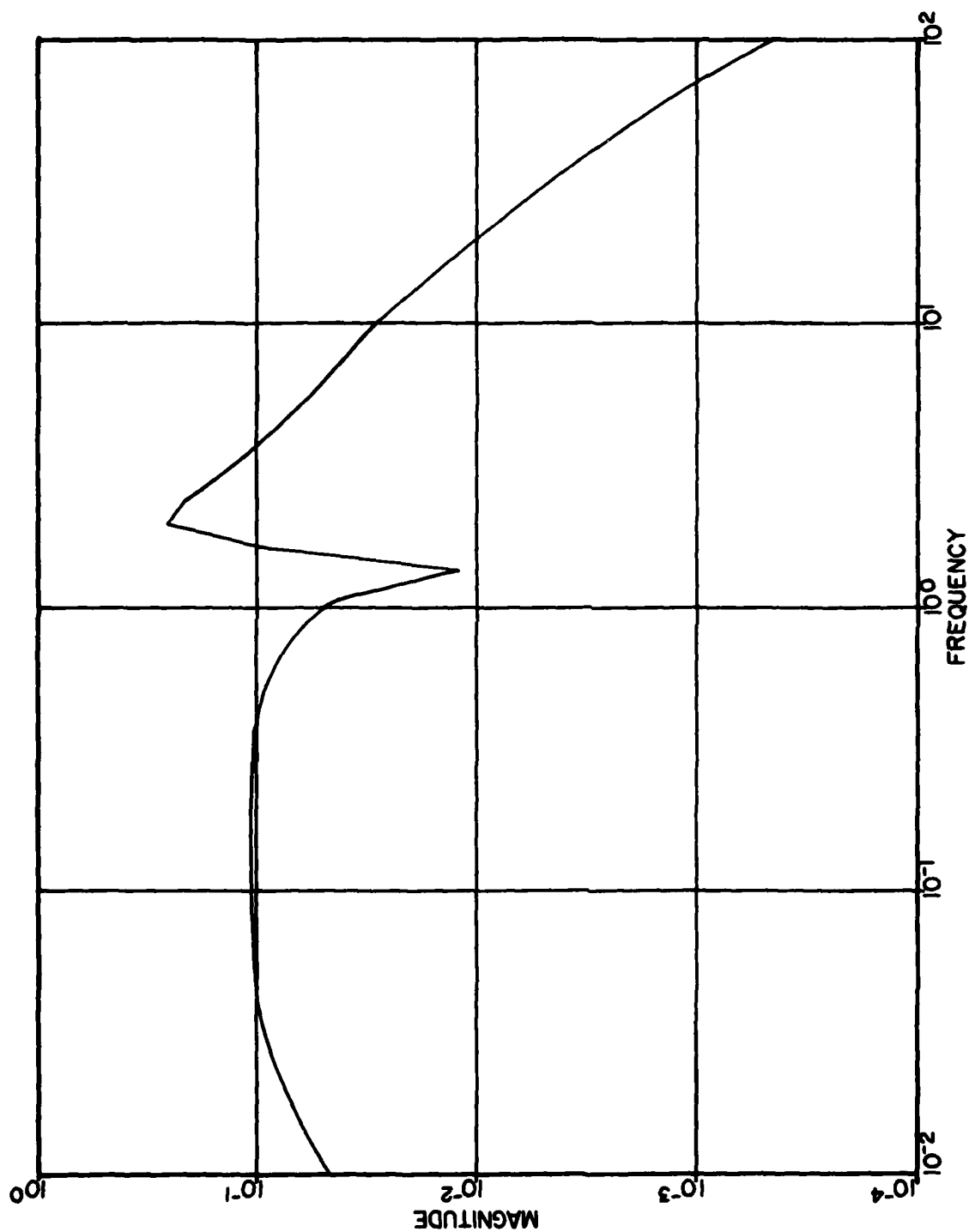


Figure 17c. Betadot SAS Phi/Delta Rudder .6, 30000

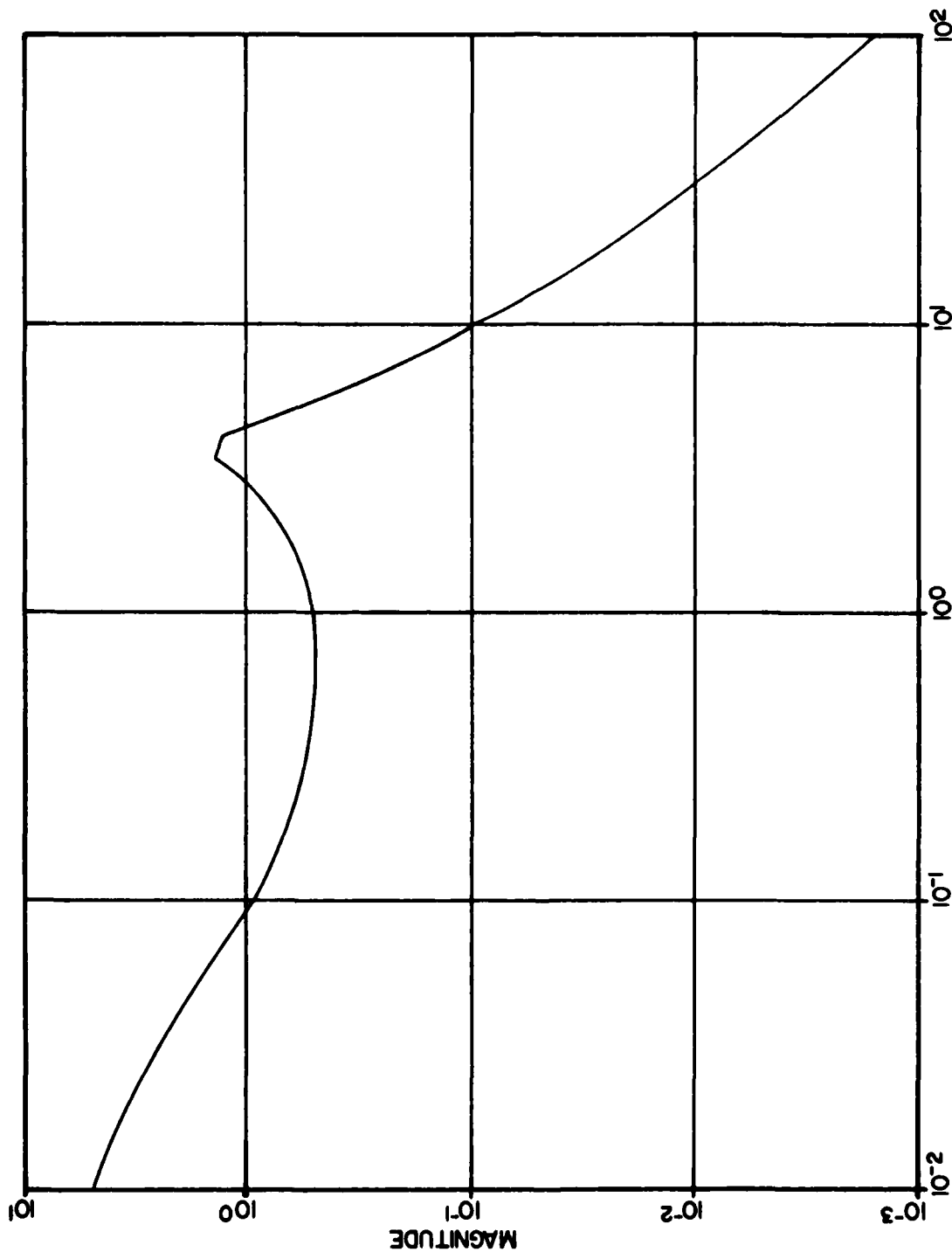


Figure 18a. Bare Airframe Beta/Delta Aileron .8, 10000

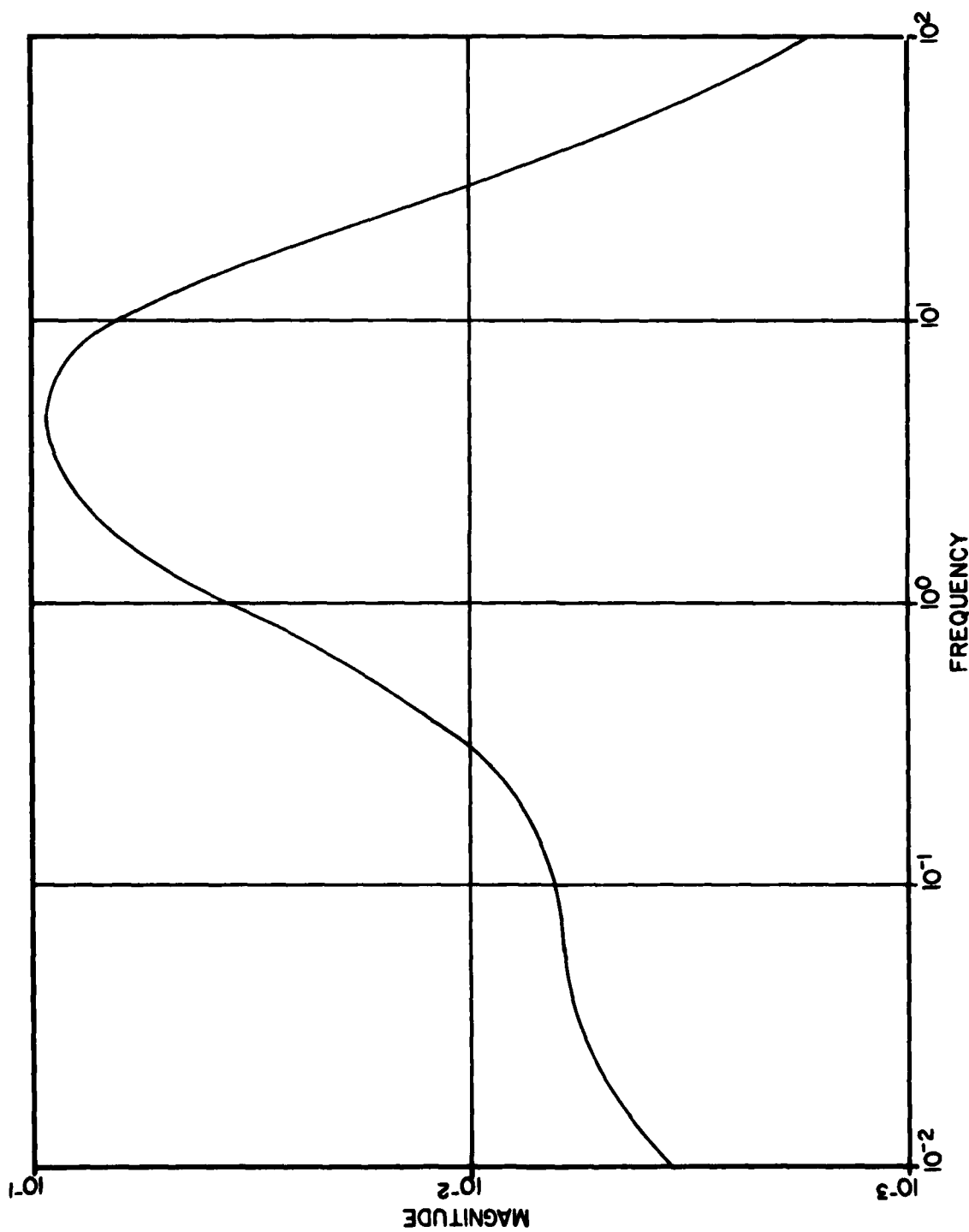


Figure 18b. Standard SAS Beta/Delta Aileron .8, 10000

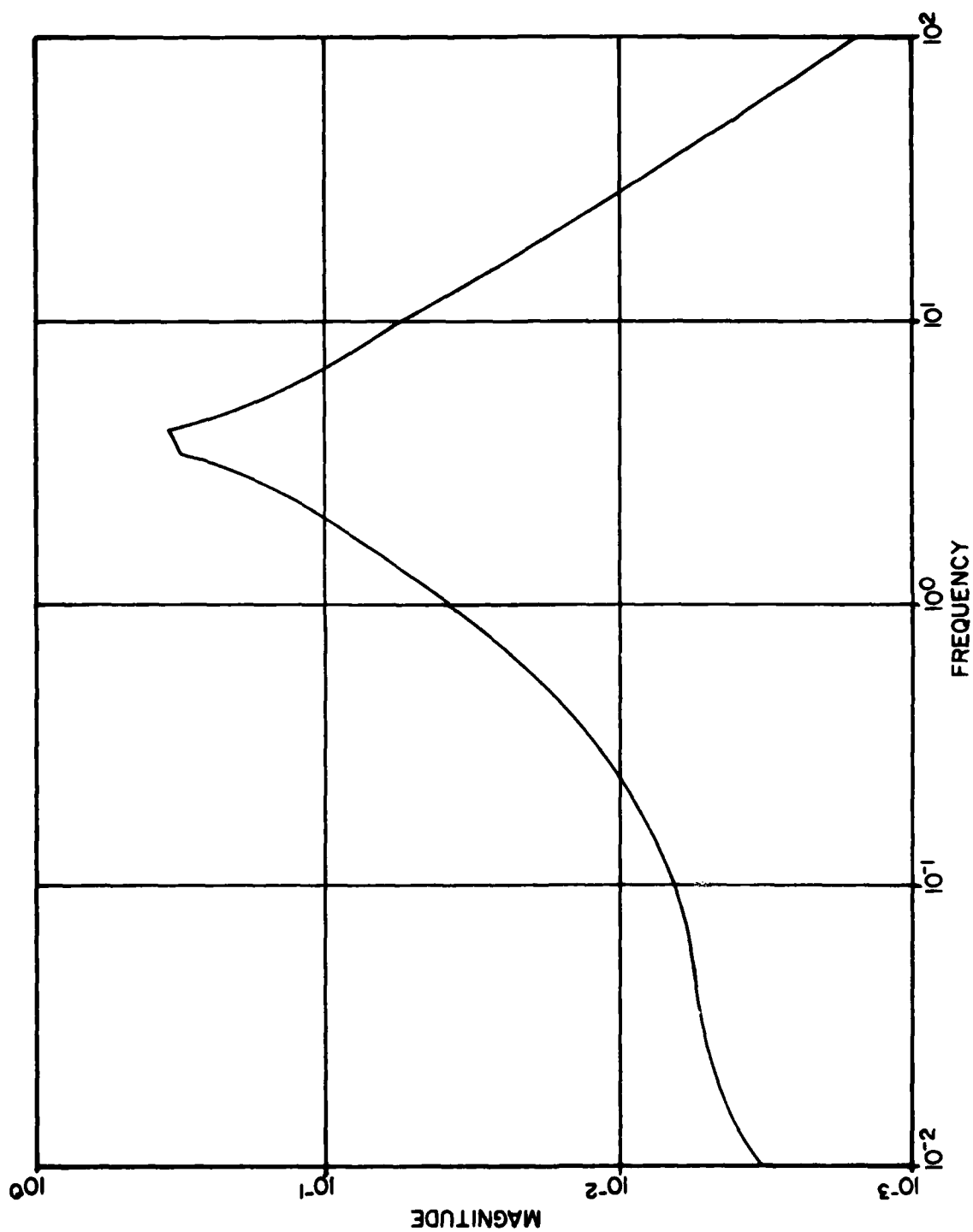


Figure 18c. Betadot SAS Beta/Delta Aileron .8, 10000

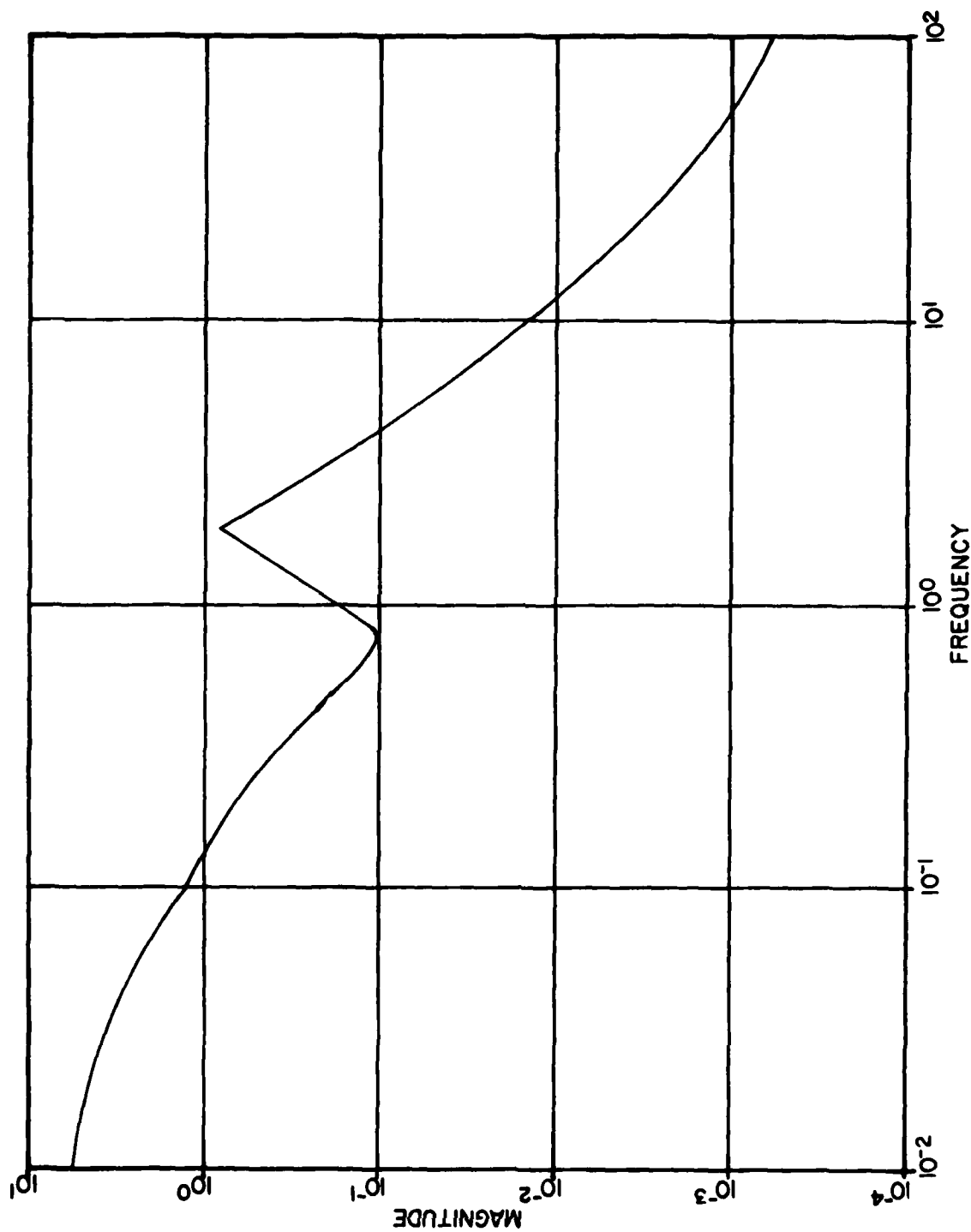


Figure 19a. Bare Airframe Beta/Delta Aileron .6, 30000

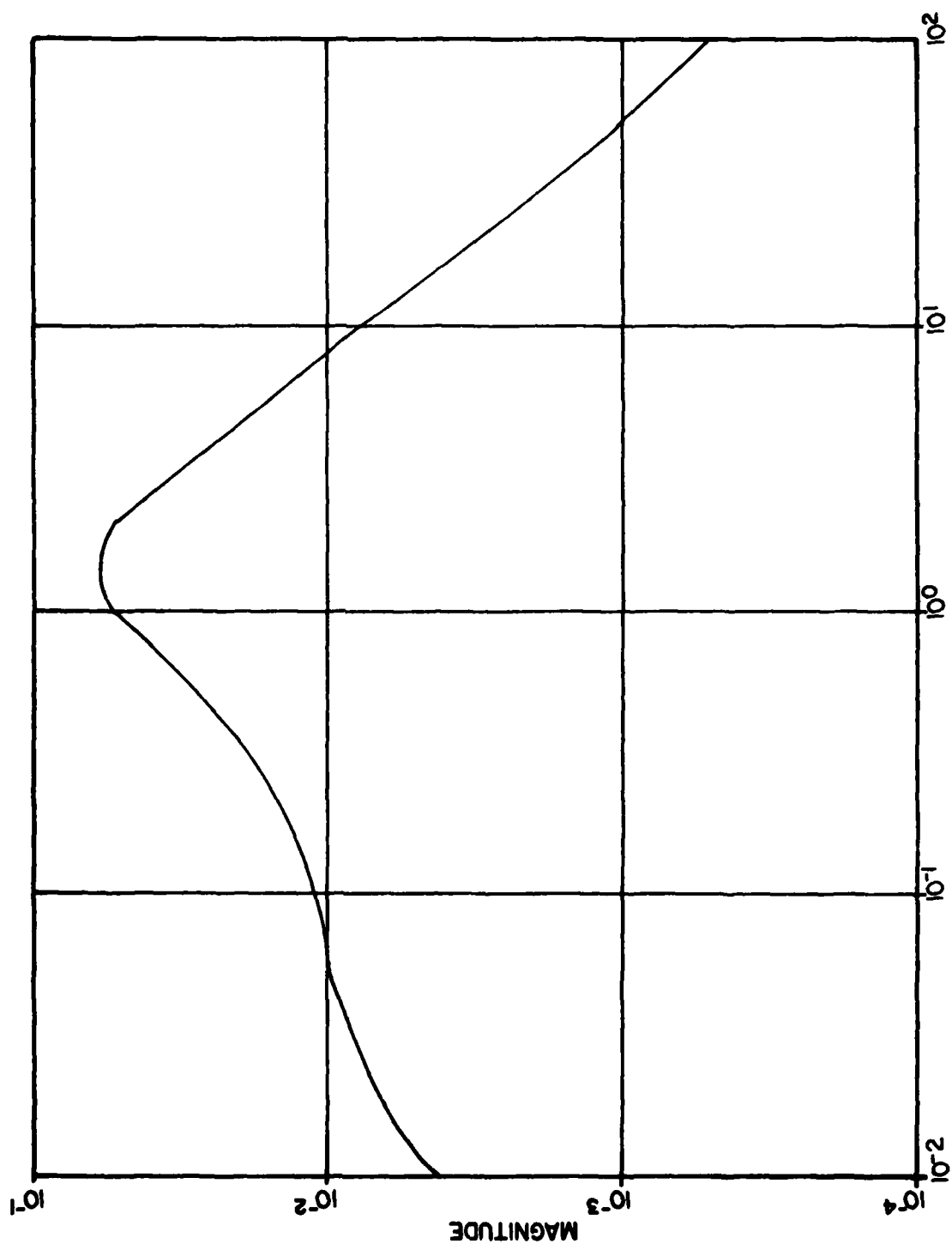


Figure 19b. Standard SAS Beta/Delta Aileron .6, 30000

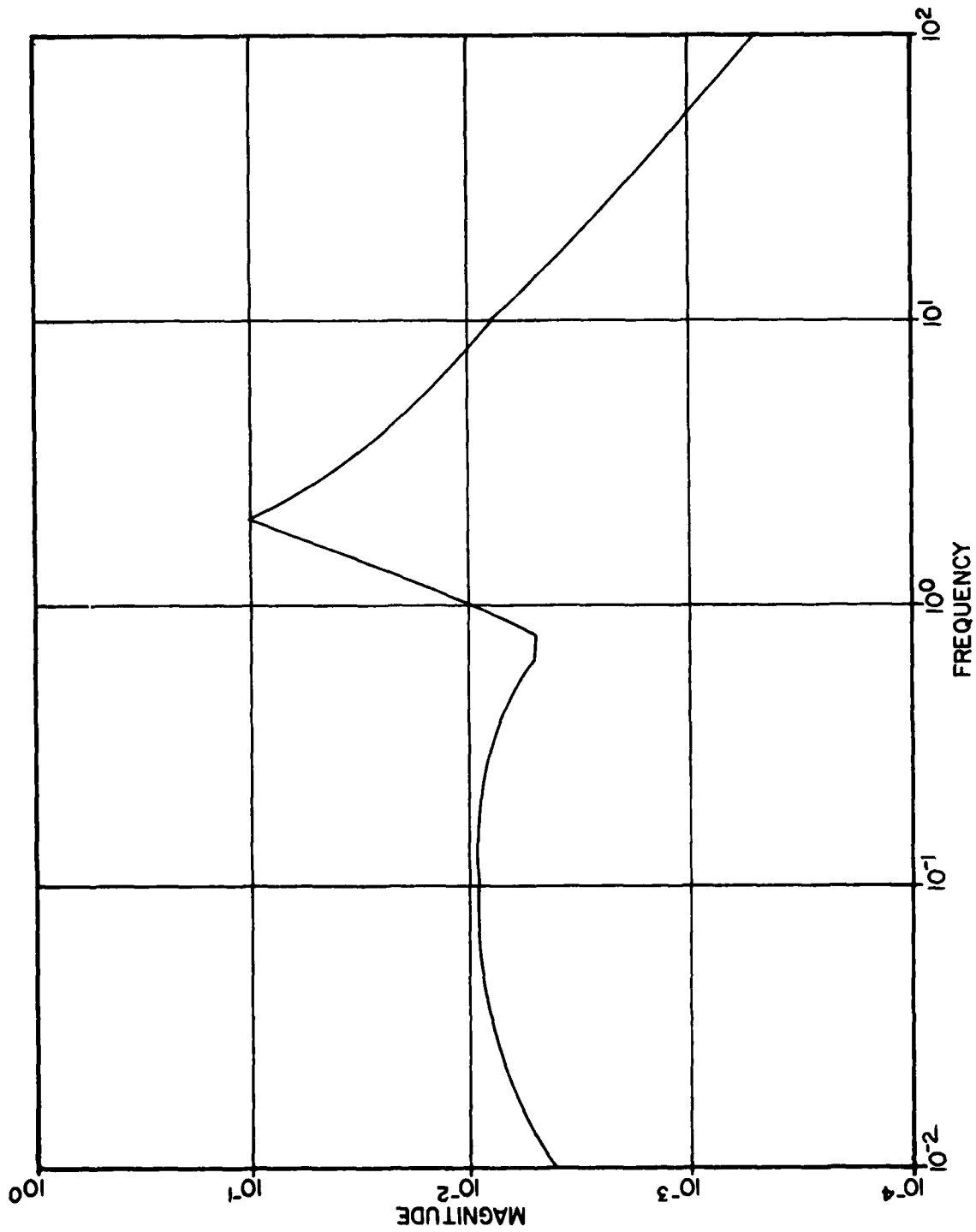


Figure 19c. Betadot SAS Beta/Delta Aileron .6, 30000



Using the definition of  $\beta$ , an approximation of  $\dot{\beta}$  can be derived which consists of parameters measurable on the F-106. Appendix D shows this derivation which provides an approximate, through fairly accurate, synthesis of  $\dot{\beta}$ . The synthesized  $\dot{\beta}$  is shown below:

$$\dot{\beta} = p\alpha - r + \frac{A_{y_{acc}}}{U} + \frac{g \cos \theta \sin \phi}{U}$$

$p$  = roll rate (rad/sec)

$\alpha$  = angle of attack (rad)

$r$  = yaw rate (rad/sec)

$A_{y_{acc}}$  = accelerometer lateral acceleration

$U$  = true airspeed (ft/sec)

$g$  = gravity constant (32.174 ft/sec<sup>2</sup>)

$\theta$  = pitch angle (rad)

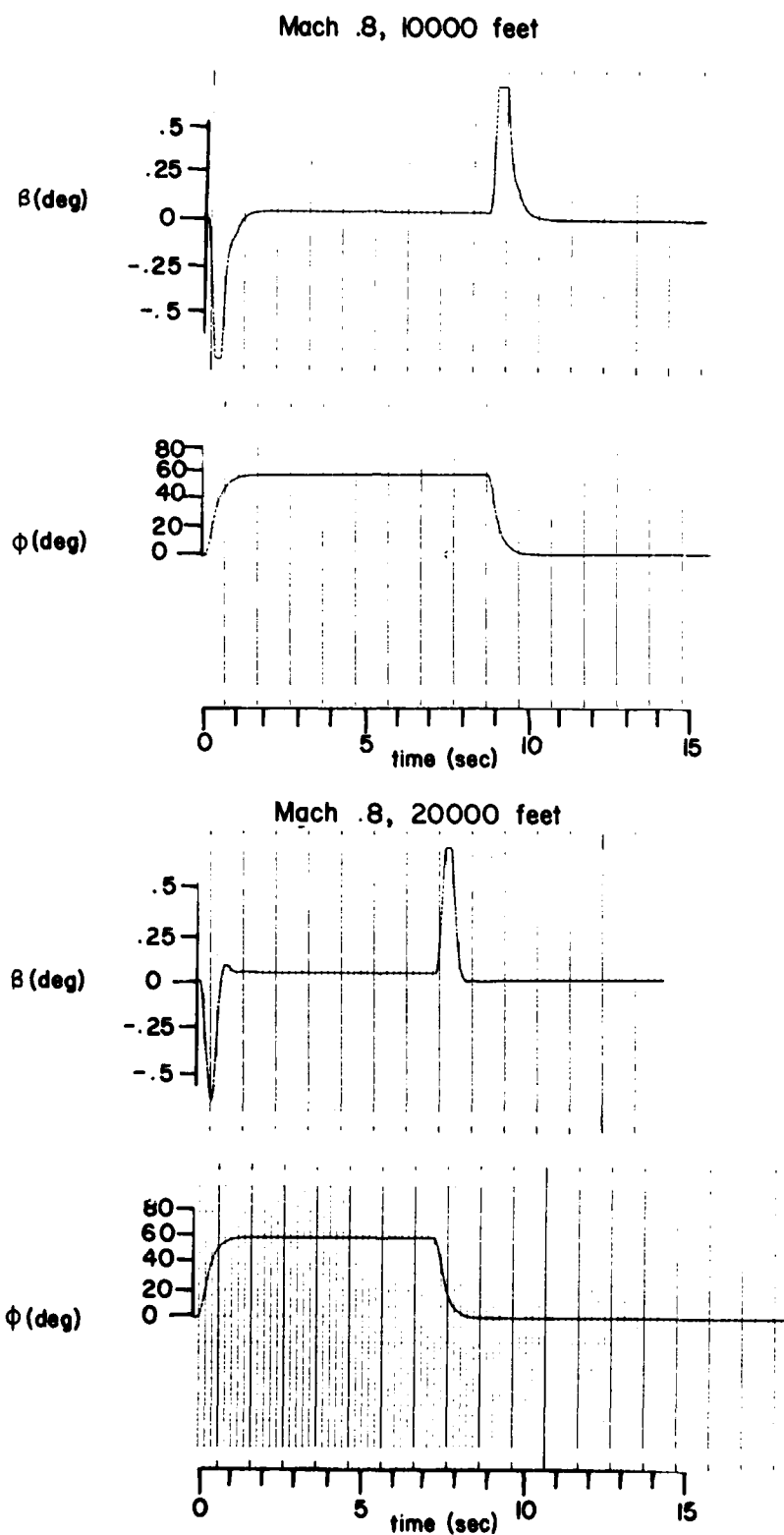
$\phi$  = roll angle (rad)

Based on this synthesis of  $\dot{\beta}$ , a detailed design of the system is shown in Figure 20. Figure 20 includes the  $\pm 6$  degree hardware limits present on the existing F-106 SAS as well as a complementary filter on the  $\beta$  signal. This complementary filter, with time constant  $\tau$ , allows high frequency components of  $\beta$  to come from the  $\dot{\beta}$  signal. The electrical signal from the pilot comes from rudder pedal potentiometers and allows the pilot to command sideslip angle directly or, if  $K_{\beta}$  and  $K_I$  are zero, to command sideslip rate. A value of  $K_p$ , the pilot's gain, cannot be determined in this nonpiloted simulation. A proportional plus integral forward-loop compensator is included to get rid of the steady-state error caused by the feedbacks.



This detailed design of the  $\beta-\dot{\beta}$  SAS was programmed on the Aeronautical Systems Division Hybrid Computer to be compared to the present SAS. Use of the  $\beta-\dot{\beta}$  system showed significant improvement in both sideslip perturbation and dutch roll damping. Figure 21 emphasizes the reduction of sideslip perturbation during a 60 degree roll at different flight conditions. The same response for the bare airframe and the standard SAS were shown previously in Figures 8 and 9. Figure 22 shows the increased speed of response and improved dutch roll damping provided by the  $\beta-\dot{\beta}$  system.

Based on the hybrid simulation runs and previous root locus and frequency response results, Figure 20 shows the configuration of a fixed-gain  $\beta-\dot{\beta}$  SAS which provides significantly better performance than the standard SAS in terms of sideslip perturbations due to roll, speed of response, and dutch roll damping. The system also uses signals realistically available on high performance aircraft, including the F-106.

Figure 21.  $\beta$ - $\dot{\beta}$  SAS Response to 60° Bank Angle

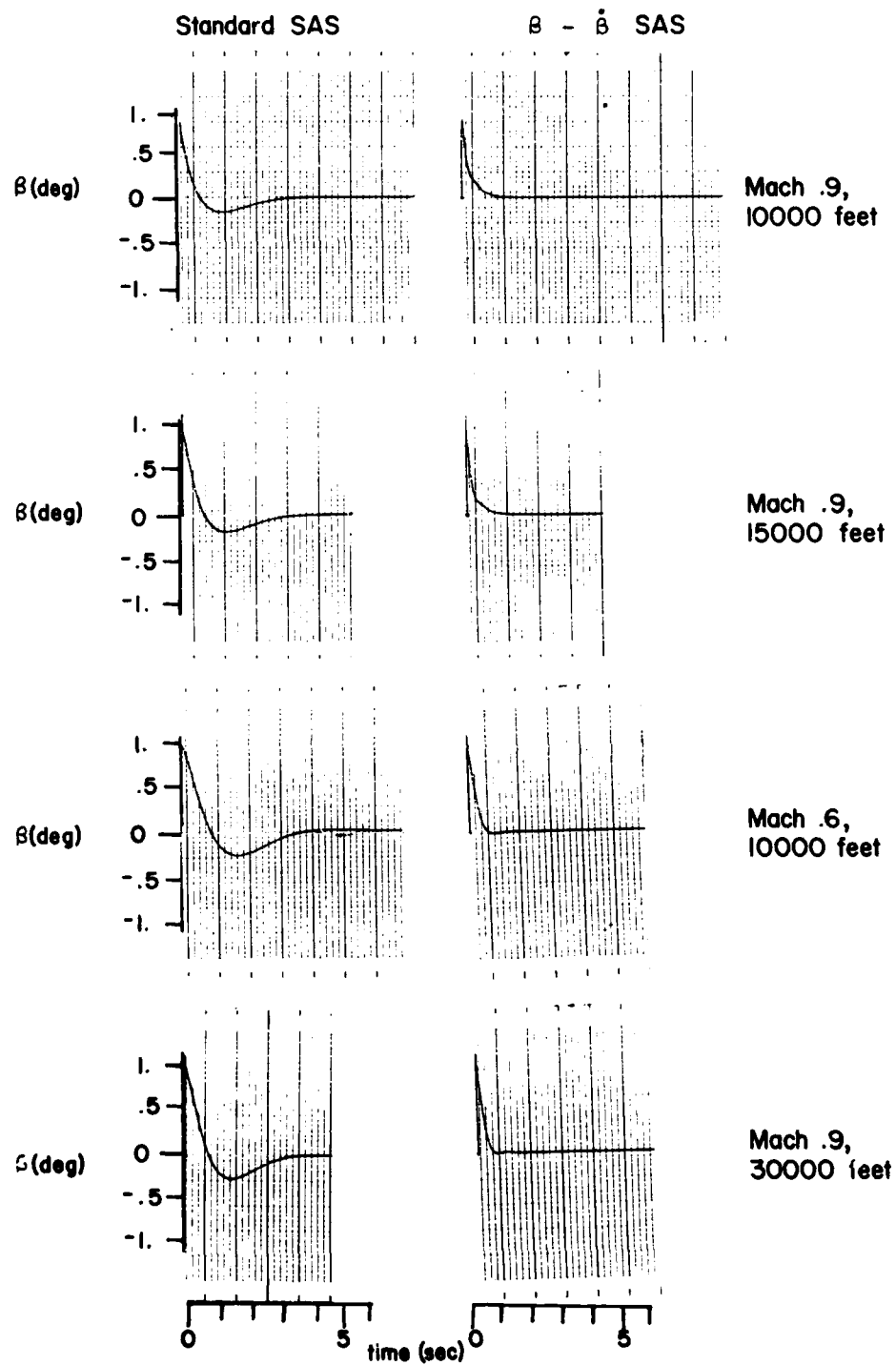


Figure 22. Response to One Degree Sideslip

## SECTION IV

### F-106 LAMARS SIMULATION

#### 1. SIMULATION DESCRIPTION

Based on root locus, frequency response, and time response analysis methods, the  $\beta\text{-}\dot{\beta}$  system appears superior to the standard SAS in terms of sideslip perturbations, speed of response, and dutch roll damping. None of these three measures of merit, however, can be considered the ultimate measure of the system's capability. The ultimate measure of merit is the pilot's ability to track another aircraft. To evaluate these systems using tracking performance as a measure of merit, a man-in-the-loop simulation was used. Using the Flight Dynamics Laboratory's Large Amplitude Multimode Aerospace Research Simulator (LAMARS), an experiment was conducted to evaluate the new system.

The experiment was set up to compare the standard SAS, from Figure 6, and two configurations of the  $\beta\text{-}\dot{\beta}$  SAS, from Figure 20. One configuration is as shown in Figure 20 with  $K_{\beta} = 6.5$  and  $K_{\dot{\beta}} = 1.9$ . The second configuration had  $K_{\beta}$  and  $K_I$  both set to zero with  $K_{\dot{\beta}} = 1.9$ . This configuration, the  $\dot{\beta}$  system, allows only sideslip rate to be fed back to the rudder. This  $\dot{\beta}$  system provides a sideslip rate control capability to the pilot. This configuration is included because the pilots are most familiar with rate control which is provided by the standard SAS. The  $\dot{\beta}$  system also provides a significant reduction in system complexity because the  $\beta$  measurement and all integrations are removed. The value of  $K_{\dot{\beta}}$  was changed from 2.5 to 1.9 after the system was installed and validated in the simulator. The change was based on pilot opinion and engineering judgment. A value of  $K_p$  of 10 was chosen to provide the same steady state sideslip rate as the standard system. The units of  $K_p$  for the  $\dot{\beta}$  configuration are deg/sec sideslip rate per inch of rudder pedal travel. This provides the pilot with the capability to command sideslip rate up to the  $\pm 6^\circ$  SAS rudder actuator limits. The units for  $K_p$  in the  $\beta\text{-}\dot{\beta}$  system are degrees sideslip angle per inch of rudder travel again up to the  $\pm 6^\circ$  actuator limits. Figures 23a and 23b show a comparison of these three systems at a high dynamic pressure, Mach .9 at 10000 feet, and a low dynamic pressure,

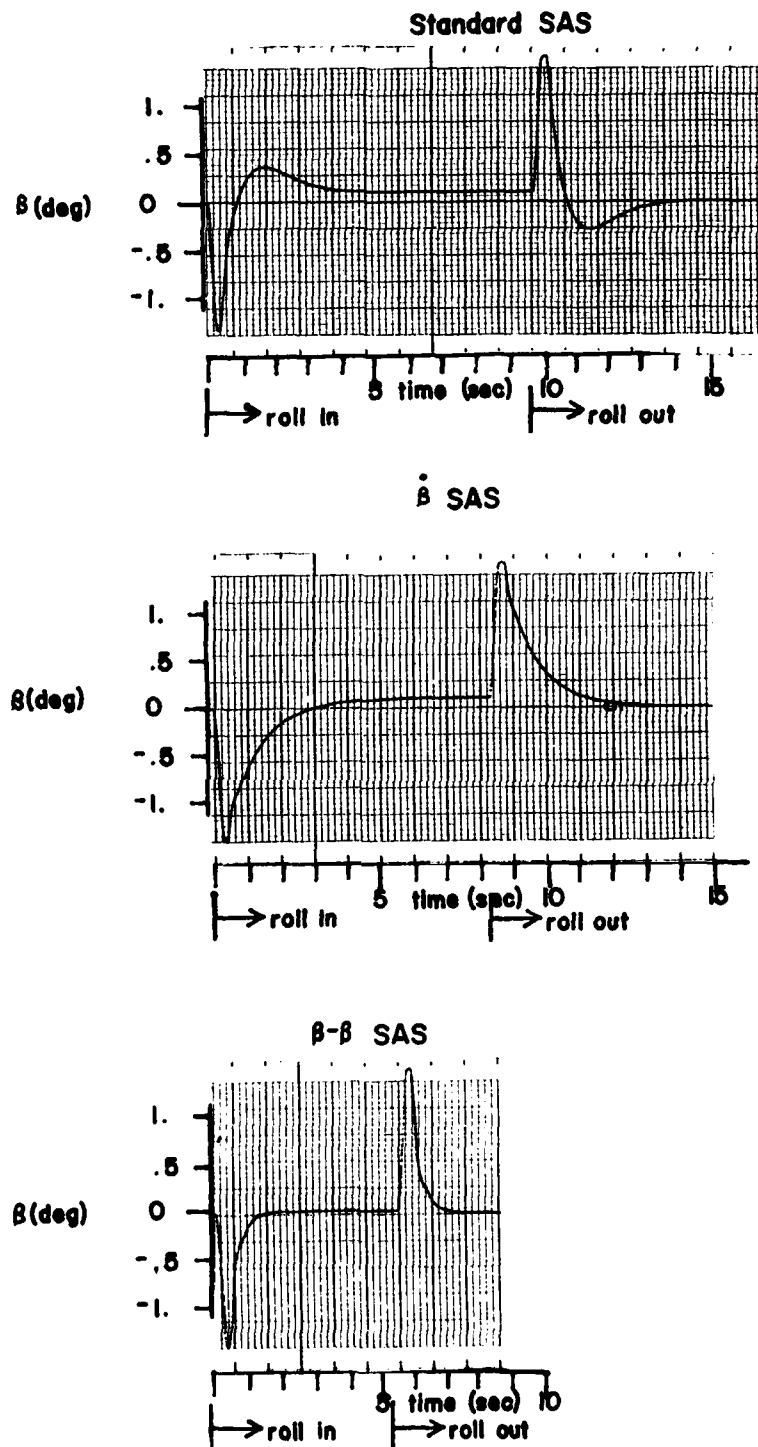


Figure 23a. SAS Comparison at Mach .9, 10000 Feet

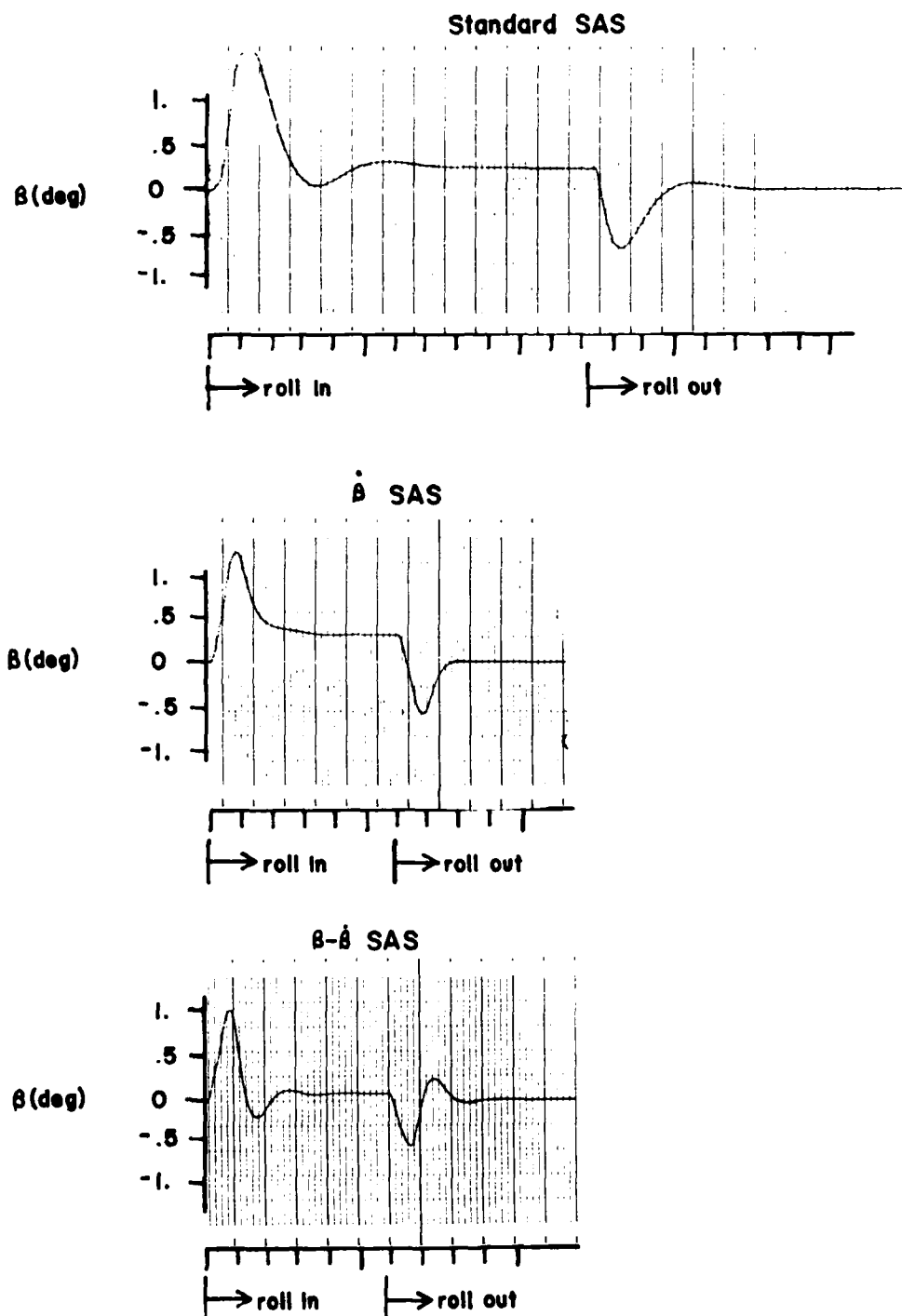


Figure 23b. SAS Comparison at Mach .6, 30000 Feet



Mach .6 at 30000 feet. The responses to a 60° roll input followed by a rollout show that both the  $\dot{\beta}$  and the  $\beta\text{-}\dot{\beta}$  system eliminate the overshoot at high dynamic pressures and reduce maximum sideslip excursion at low dynamic pressure.

The experiment was set up using two pilots flying each of the three control systems four times. The pilots were flight test pilots experienced and current in the F-106. The task performed by the pilots was tracking a constant g target. The experiment was run at the following three flight conditions: Mach .72 at 10000 feet with 3 g target, Mach .9 at 10000 feet with 3 g target, and Mach .9 at 10000 feet with 6 g target. These flight conditions were chosen to provide realistic ATA tracking conditions. The tracking was performed using a fixed reticle depressed 50 milliradians from the waterline.

The experiment was designed specifically to measure the difficulty of the tracking task using the three SAS models and was set up similar to handling qualities during tracking (HQDT) tests, with some minor modifications. As in HQDT tests, the pilot's task was to keep the pipper superimposed on the target. Unlike normal HQDT tests, the pilots were allowed to use rudder pedals for aircraft control. This use of rudder pedals during tracking, not normally allowed in an HQDT test, was allowed because the pilots indicated that the rudder was the main lateral control used at large angles of attack. Initially the pilots were not told which system they were flying; this was done to avoid any biasing of the results. Later and for all the data runs, the pilots were informed of the system being flown. This was necessary because the pilots had developed different techniques for flying with each system.

Since the purpose of the new system is to improve lateral tracking, a quantitative measure of merit for this improvement was needed. This measure of merit was chosen to be the standard deviation of the tracking error. Since the system tested acts only on the lateral modes, the total error was divided into elevation and azimuth errors. The elevation and azimuth means are also included as an indicator of the actual point about which the pilot was tracking. To make the steady state tracking

error statistics valid, the acquisition transients at the beginning of each run were deleted. During this acquisition phase, the pilots often generate large tracking errors while attempting to establish an in-plane steady-state tracking turn behind the target. The errors are extremely difficult to analyze quantitatively and are large relative to the steady tracking errors; therefore, if included, they would have decreased the usefulness of the standard deviation as a quantitative measure of merit. In addition to these quantitative measures, the pilot opinions were obtained in the form of pilot ratings based on the Cooper-Harper Scale (Figure 24). These ratings, along with the means and standard deviations of the tracking errors, provided the measures of merit for evaluating the three SAS's.

## 2. SIMULATION RESULTS

Approximately 75 runs provided data which could be used for evaluating the systems. Table 3 shows the results of these runs in terms of the quantitative measures of merit described earlier. To eliminate the acquisition transients, the middle 30 seconds of the 60-second runs were used for calculating the error statistics for the 3 g runs. For the 6 g runs, the middle 20 seconds of the 45-second runs were used.

Although the mean tracking errors for three SAS's are shown, they provide little insight into the relative merits of the different systems. These mean values are more a function of pilot technique than of the quality of the SAS. This is evident in the azimuth means where Table 3 shows pilot 1 to consistently track left of the target and pilot 2 to consistently track right of the target. These different means could also be due to the position of the pilot's head and his resulting view through the HUD. The elevation means show that the pilots tracked consistently below the target with large error magnitudes as g and airspeed increased with little apparent relation to the SAS's. The elevation means could also have been effected by bias in the data measurement system in the LAMARS facility or again by the pilots' head location.

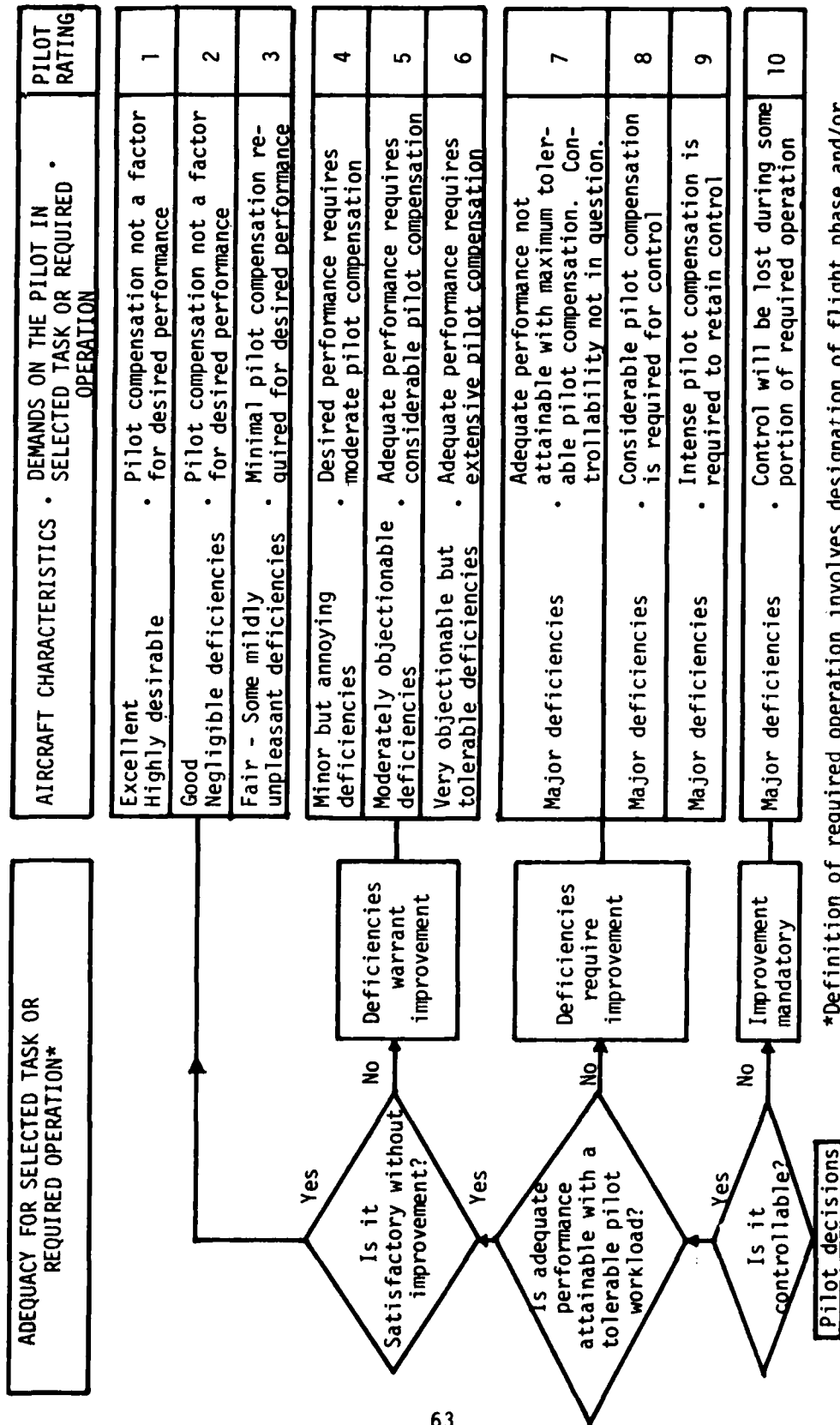


Figure 24. Cooper-Harper Rating Scale

TABLE 3  
SIMULATION RESULTS  
M = .72, 3 g, 10000 FEET

System	Pilot 1			Pilot 2		
	Azimuth Error	Elevation Error	Total Error	Azimuth Error	Elevation Error	Total Error
	Mean	Mean	SD	Mean	Mean	SD
Standard	-4.54	-8.58	12.87	2.21	-1.91	14.56
$\hat{\beta}$	- .47	-10.66	7.38	2.82	-3.06	11.08
$\beta-\hat{\beta}$	-1.27	-9.1	7.09	2.99	-3.57	11.18
	6.3	3.25		9.88	5.23	
	SD	SD	SD	SD	SD	SD
M = .9, 3 g, 10000 FEET						
Standard	-1.91	-9.79	13.72	3.82	-5.52	14.57
$\hat{\beta}$	-1.9	-9.01	9.95	5.36	-4.47	10.73
$\beta-\hat{\beta}$	1.71	-8.97	12.83	.92	-3.74	16.62
	13.14	3.93		13.4	5.71	
	9.08	4.06		9.89	4.15	
	12.11	4.23		15.94	4.71	
	SD	SD	SD	SD	SD	SD
M = .9, 6 g, 10000 FEET						
Standard	-3.75	-17.13	19.6	1.73	-10.95	21.6
$\hat{\beta}$	-2.04	-18.71	17.26	5.48	-7.55	20.1
$\beta-\hat{\beta}$	-1.75	-17.72	20.16	8.87	-8.55	25
	15.02	11.89		17.41	12.79	
	13.01	11.34		17.08	10.59	
	18.72	7.47		21.54	12.67	
	SD	SD	SD	SD	SD	SD

The most important quantitative measure of merit is the standard deviation of the tracking errors. The standard deviation shows the precision with which the pilot can hold the pipper on the target. The smaller the standard deviation, the more precisely the pilot can hold the pipper on the target.

To determine the statistical significance of the SAS effects on the results, a three-way analysis of variance was performed on azimuth, elevation, and total error (vector sum of azimuth and elevation error). The analysis is shown in Appendix E. The three error sources were SAS, pilot, and flight condition. The results are shown in Table 4 (a through c) in terms of level of significance for the different error sources. These levels of significance describe the probability of mistakenly attributing changes in tracking error to one of the error sources when in fact that error source was not the factor causing the change. For instance, the .0173 level of significance of the SAS as an error source in azimuth error means that there is a .0173 probability that the changes, which occurred in azimuth tracking error when the SAS was changed, were not due to the SAS at all but were either random errors or due to some other factor. The results show that the SAS was indeed significant as an error source. The results also show that the pilot and flight condition were even more significant as error sources.

Since the analysis of variance shows the SAS effects to be significant, the results from Table 3 can be examined in more detail. The percentage improvement over the standard SAS, in terms of standard deviation of the tracking error, is shown in Table 5. There are quite large improvements at Mach .72, 10000 feet but as the Mach number and g loading increase, the levels of improvement become smaller. This decrease in percentage improvement is probably due to the increasing difficulty of the task itself, which tends to overwhelm and mask the SAS differences. This is also evident in the analysis of variance, which shows the flight condition to have a highly significant effect on the results. Pilot skill also appears to be important to the results. Pilot 1 consistently had smaller tracking errors and also had consistently higher levels of improvement. As with flight condition, this pilot

TABLE 4  
ANALYSIS OF VARIANCE RESULTS

Error Source	Level of Significance
Pilot	.0163
Flt Cond	.00003
SAS	.0173

a. Azimuth Error

Error Source	Level of Significance
Pilot	.0201
Flt Cond	.00001
SAS	.044

b. Elevation Error

Error Source	Level of Significance
Pilot	.0053
Flt Cond	.00001
SAS	.0135

c. Total Error

TABLE 5  
PERCENT IMPROVEMENTS OVER STANDARD SAS\*

M = .72, 3 g, 10000 FEET

System	Pilot 1			Pilot 2		
	Azimuth Error	Elevation Error	Total Error	Azimuth Error	Elevation Error	Total Error
$\dot{\beta}$	44	39	43	25	20	24
$\beta-\dot{\beta}$	44	49	45	21	29	23

M = .9, 3 g, 10000 FEET

$\dot{\beta}$	31	-3	27	26	27	26
$\beta-\dot{\beta}$	8	-8	6	-19	18	-14

M = .9, 6 g, 10000 FEET

$\dot{\beta}$	13	5	10	2	17	7
$\beta-\dot{\beta}$	-25	37	-5	-24	1	-16

\*Negative value indicates a degradation

effect was evident in the analysis of variance. Based on the quantitative measures of merit in Tables 3 and 5, the  $\dot{\beta}$  SAS appears to be best, followed by the standard SAS and the  $\beta-\dot{\beta}$  SAS.

The three SAS's were also compared qualitatively using the Cooper-Harper rating scale. These ratings, for the 3 g runs, are shown in Table 6. These qualitative measures follow very closely the quantitative measures of Tables 3 and 5. They show the  $\dot{\beta}$  system to be best followed by the standard and the  $\beta-\dot{\beta}$  system. Figures 25a-25c show representative pipper traces at the Mach .9, 3 g flight condition using each of the three SAS's. These pipper traces are from runs flown by pilot 1. The improvement is evident in the  $\dot{\beta}$  SAS, Figure 25c. Figure 26 also shows the improvement provided by the  $\dot{\beta}$  SAS. In Figure 26, the standard SAS was being flown by the pilot as he tracked a 3 g target; at the point shown, the standard SAS was turned off and the  $\dot{\beta}$  SAS turned on. The improvement is evidenced by the elimination of the low frequency oscillation.

TABLE 6  
COOPER-HARPER RATINGS (3 g ENCOUNTERS)

System	Pilot 1	Pilot 2
Standard	3	4
$\dot{\beta}$	2	3
$\beta-\dot{\beta}$	5	5

Although the nonpiloted simulations indicated that the  $\beta-\dot{\beta}$  system was better than the  $\dot{\beta}$  system, in terms of dynamic response, the pilots preferred and performed better with the  $\dot{\beta}$  system, a rate control. This apparent discrepancy can probably be attributed to the fact that the pilots were most familiar with rate control, as with the standard SAS; the position control of the  $\beta-\dot{\beta}$  system was therefore, something new which the pilots had to learn how to use as they evaluated it. This lack of experience in using position control of sideslip might have put a bias on the results. Unfortunately, this possible bias cannot be measured using the data and should not, therefore, enter the results.

In summary, the LAMARS simulation showed that the  $\dot{\beta}$  SAS provides a significant improvement over the standard SAS. This improvement was evidenced by both quantitative measures of merit, tracking error, and qualitative measures of merit, pilot ratings.



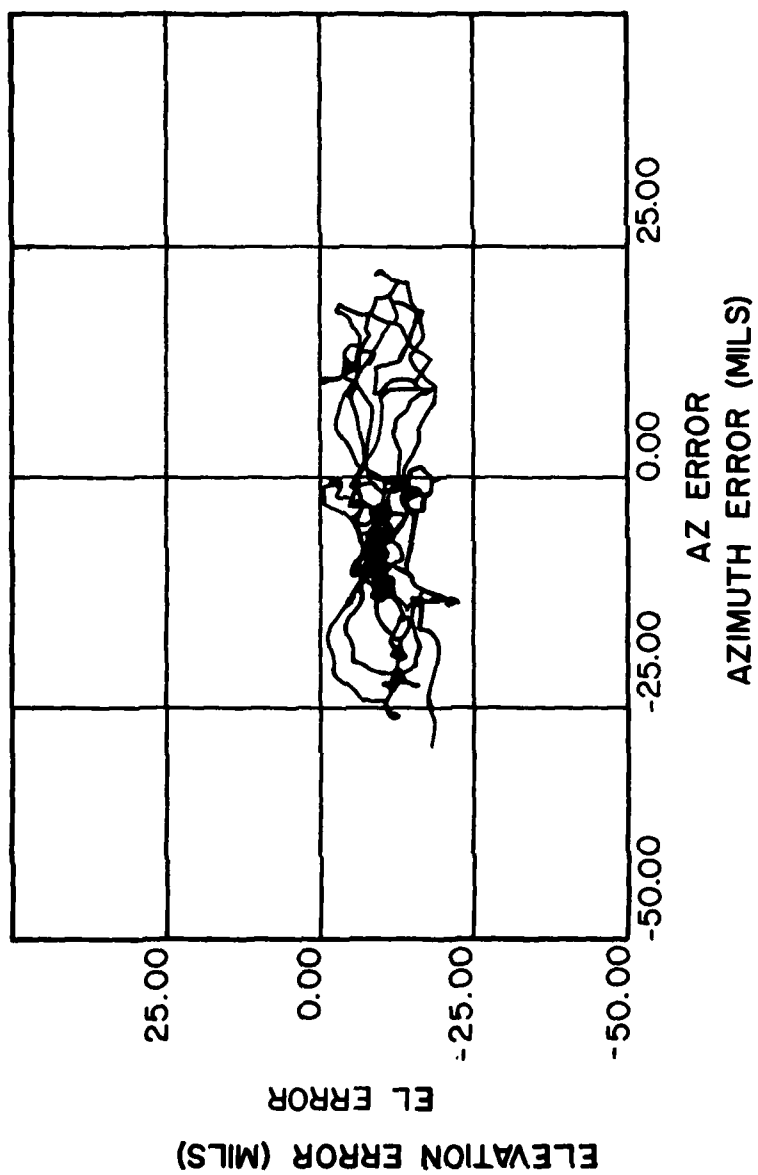


Figure 25a. Standard SAS Pipper Trace at Mach .9, 10000 Feet, 3 g

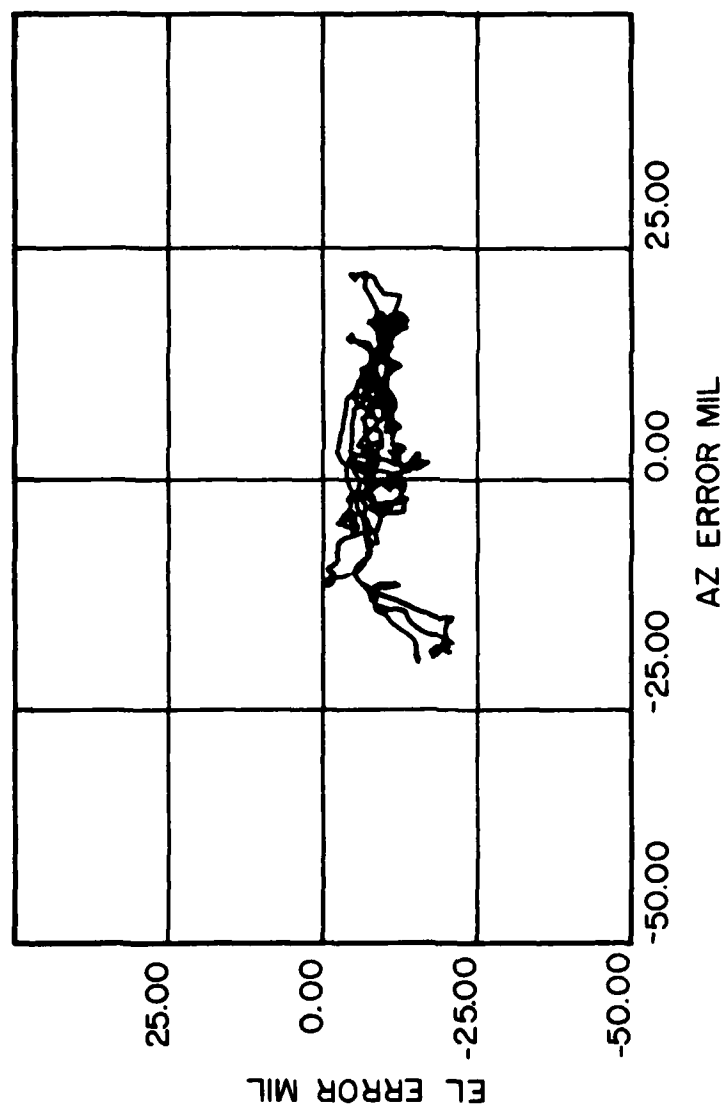


Figure 25b.  $\beta$ - $\beta$  SAS Pipper Trace at Mach .9, 10000 Feet, 3 g

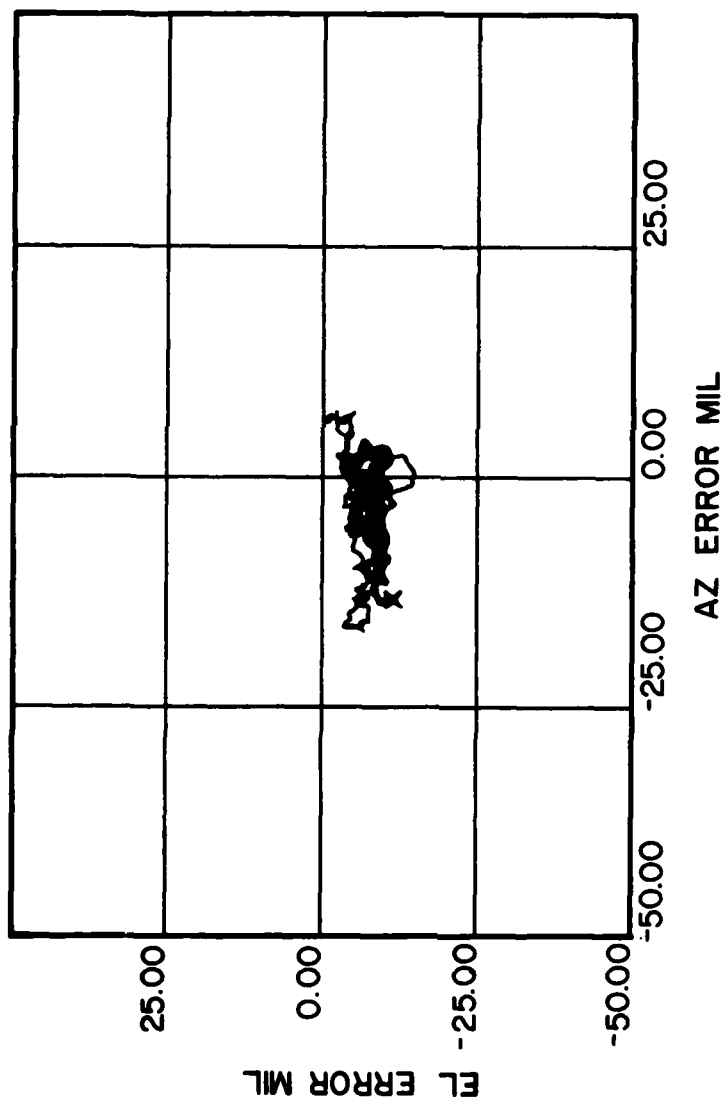


Figure 25c. SAS Pipper Trace at Mach .9, 10000 Feet, 3 g

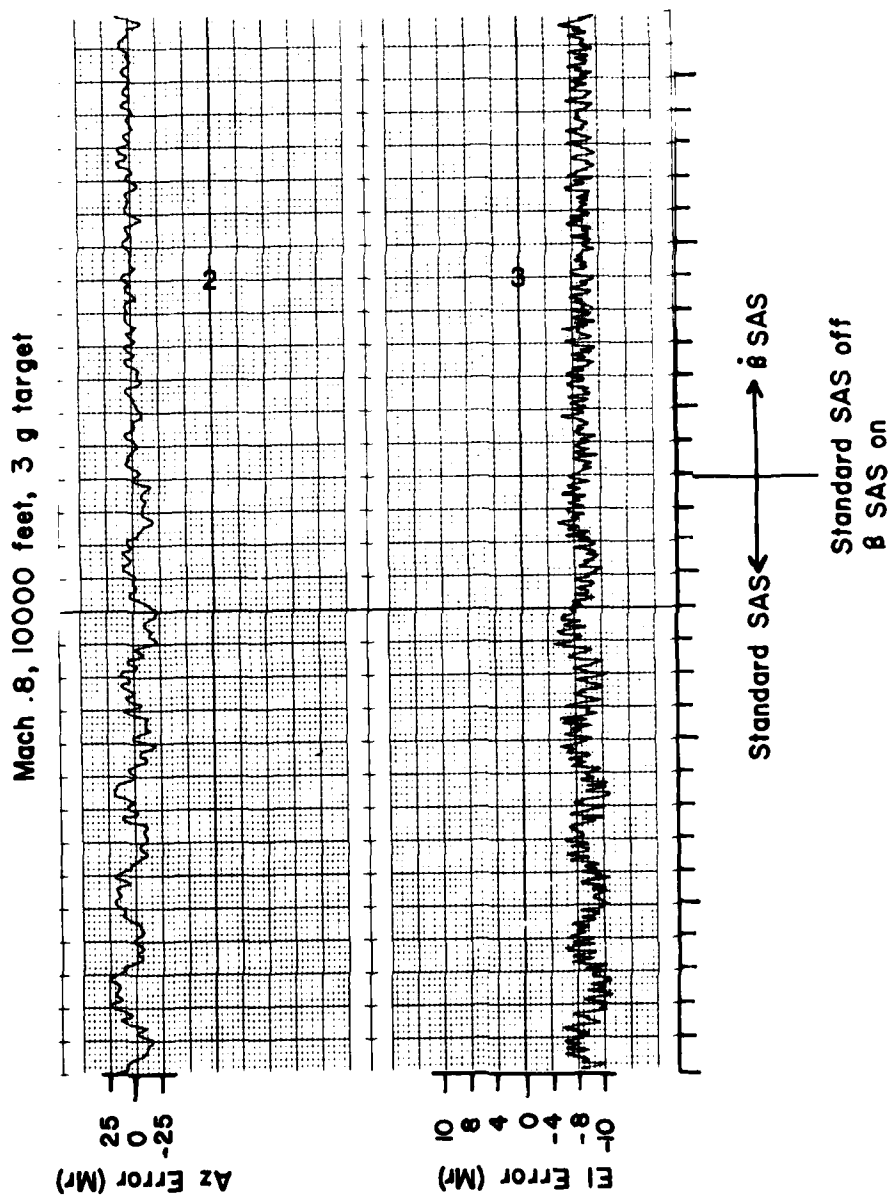


Figure 26. Tracking Error Reduction with  $\beta$  SAS

## SECTION V

## F-106 FLIGHT TEST

## 1. SYSTEM CONFIGURATION AND IMPLEMENTATION

Based on the results of the piloted simulation, both analysis results and pilot comments, the Aerospace Defense Command (ADCOM/DOV) gave the Flight Dynamics Laboratory approval to flight test the modified SAS on an F-106 at Tyndall AFB, Florida. The Flight Dynamics Laboratory, with assistance from the 475th Test Squadron from Tyndall AFB, designed a flight test implementation which allowed for much flexibility during the flight test. The Class II modification package based on this design was approved by Air Force Systems Command. The design for flight test included only provisions to evaluate the sideslip rate ( $\dot{\beta}$ ) feedback. The reasons for looking at only the  $\dot{\beta}$  feedback are twofold. Primarily, the pilot comments and performance measures from the piloted simulation shows this system to have a much greater performance improvement potential than the  $\beta$ - $\dot{\beta}$  system. Also, the cost for implementing the  $\dot{\beta}$  system was considerably less because no integrations were required in the control law.

During the design of the flight test implementation, the Flight Dynamics Laboratory presented an option to ADCOM which would allow for the addition of a roll SAS to the F-106 being tested. The reasons for including this option were that the F-106 did not have roll rate feedback to the SAS, the pilot controlled the elevon position directly, and the change would be very simple, involving only a circuit change to the existing control system. ADCOM/DOV approved this addition to the flight test, and the roll SAS design was included and approved in the Class II modification package.

The F-106 avionics system and flight control system were well suited for testing the  $\dot{\beta}$  SAS and roll SAS because they required only minor modifications to the existing system. The Hughes-built IRAM computer was used for all SAS calculations, both yaw and roll. Since the IRAM computer is part of the MA-1 fire control and automatic intercept system, existing electrical paths from the IRAM computer to

the 464821 flight control interface box were used to carry the calculated SAS commands to the flight control system actuators. Figure 27 shows a conceptual block diagram of the system implementation.

The standard yaw SAS is a single-thread analog system located in the 821 unit. The sensor outputs from the turn rate transmitter (TRT), yaw rate and roll rate, are input to this 821 unit which does the analog SAS calculation for roll and pitch and then sent to the rudder actuator and the two elevon actuators.

The rudder actuator mechanically limits the SAS command rudder movement to  $\pm 6^\circ$ . Likewise, the pitch SAS commands are mechanically limited to  $\pm 1^\circ$  by the elevon actuators. This pitch authority ( $\pm 1^\circ$ ) was also the limit for the roll SAS since the roll SAS consisted of using the existing pitch system but in a differential manner.

The  $\dot{\beta}$  SAS implementation is shown in Figure 28. Figure 29 further describes the inputs and switching used in the  $\dot{\beta}$  SAS. To have all the quantities necessary to solve the  $\dot{\beta}$  equation in the MA-1 IRAM computer, some standard inputs to the computer had to be removed and replaced with sensor measurements needed by the  $\dot{\beta}$  SAS. The pitch rate normally input to the computer was replaced by an angle of attack ( $\alpha$ ) signal from an  $\alpha$  vane located on the pitot-static boom. The lateral acceleration ( $A_y$ ), which came from a Honeywell inertial reference platform (IRP), replaced the existing gunsight sideslip measurement. Rudder pedal position ( $\delta_{rp}$ ) replaced the right elevon position. These three signals,  $\alpha$ ,  $A_y$ , and  $\delta_{rp}$ , were available from instrumentation installed previously for an F-106 parameter identification flight test.

The roll SAS implementation was set up in the same way as the  $\dot{\beta}$  SAS. Figures 30 and 31 show the implementation and switching logic used for the roll SAS. The lateral stick position needed by the roll control law is taken from a lateral stick position potentiometer and input to the computer in the location normally containing left elevon position.

The computer program was set up to enable a maximum amount of flexibility in both system checkout and flight test validation. The program had an option for a ground check by using the aircraft short system

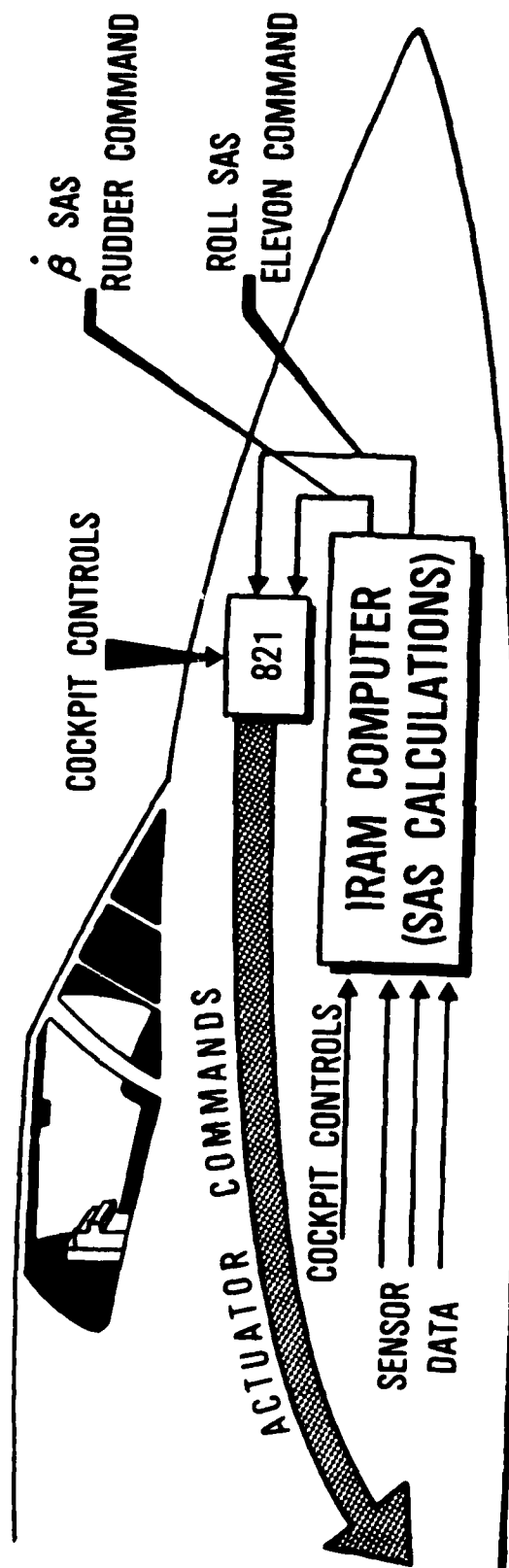


Figure 27. F-106 SAS Conceptual Block Diagram

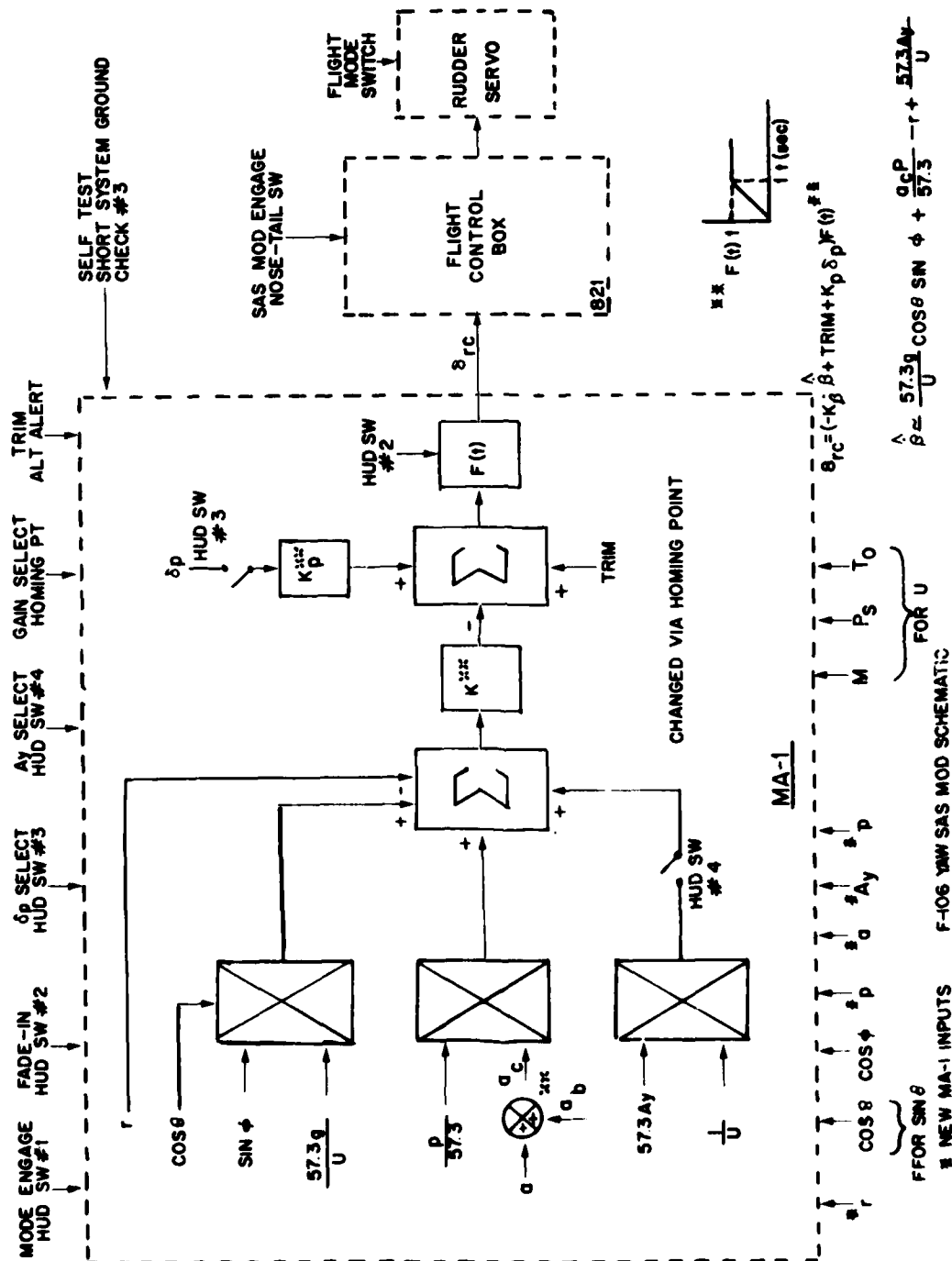


Figure 28.  $\delta$  SAS Implementation



$$\delta_{rc} = (K_p \delta p + \text{TRIM} - K_3 \hat{\delta}) F(t)$$

$$\text{where } \hat{\delta} = \frac{p(\alpha + \alpha_b) - r + 57.3 K_A \dot{A}_y + 57.3 g \cos \alpha \sin \alpha}{57.3 U}$$

$$g = 32.2 \text{ ft/sec}^2$$

COMPUTER OUTPUT	OUTPUT LOCATION	SCALING	RANGE
$\delta_{rc}$	LH Elevon Command (deg)	8.33 V/deg	0-100V, $\pm 6^\circ$
<u>Computer Inputs</u> (Variables)	<u>Source</u>	<u>Input Location</u>	<u>Scaling</u>
p (roll rate, deg/sec)	TRI	existing (E18a)	10 deg/sec/V
$\alpha$ (angle of attack, deg)	boom	pitch rate (E25)	9 deg/volt
r (yaw rate, deg/sec)	TRI	existing (E16a)	4 deg/sec/V
$A_y$ (lateral acceleration, ft/sec)	Honeywell IRP	gunsight $\delta$ (E26)	212 ft/sec/volt
U (airspeed, ft/sec)	existing	existing	$\pm 4.025V$ , $\pm 800 \text{ ft/sec}$
$\sin \theta$ ( $\cos \theta$ calculated from $\sin \theta$ )	existing	existing	
$\sin \phi$ (roll angle)	existing	existing	
$\delta_p$ (rudder pedal position, in)	rudder pot	RT elevon position (A22)	50V $\pm 30V$ , $\pm 3.25 \text{ in}$
TRIM (System electrical trim, deg)	Altitude warning	existing	$\pm 6^\circ$

#### (Variable gains)

$\alpha_b$  (angle of attack, bias deg)

$K_A$  ( $\delta$  gain, deg/deg/sec)

$K_p$  (pilot rudder pedal position gain, deg/in)

#### (Discretes)

HUD Switch #1

HUD Switch #2

HUD Switch #3

HUD Switch #4

These variable gains are set using the Homing Point Selector as a logic indicator to set these gains as shown in Table 1.

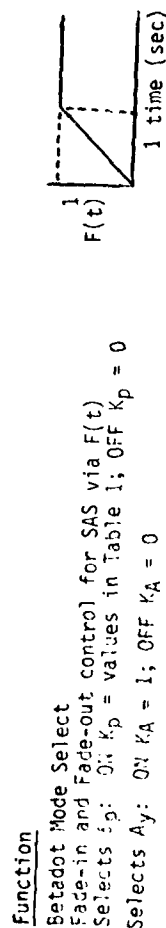


Figure 29.  $\delta$  SAS Inputs and Switching Logic

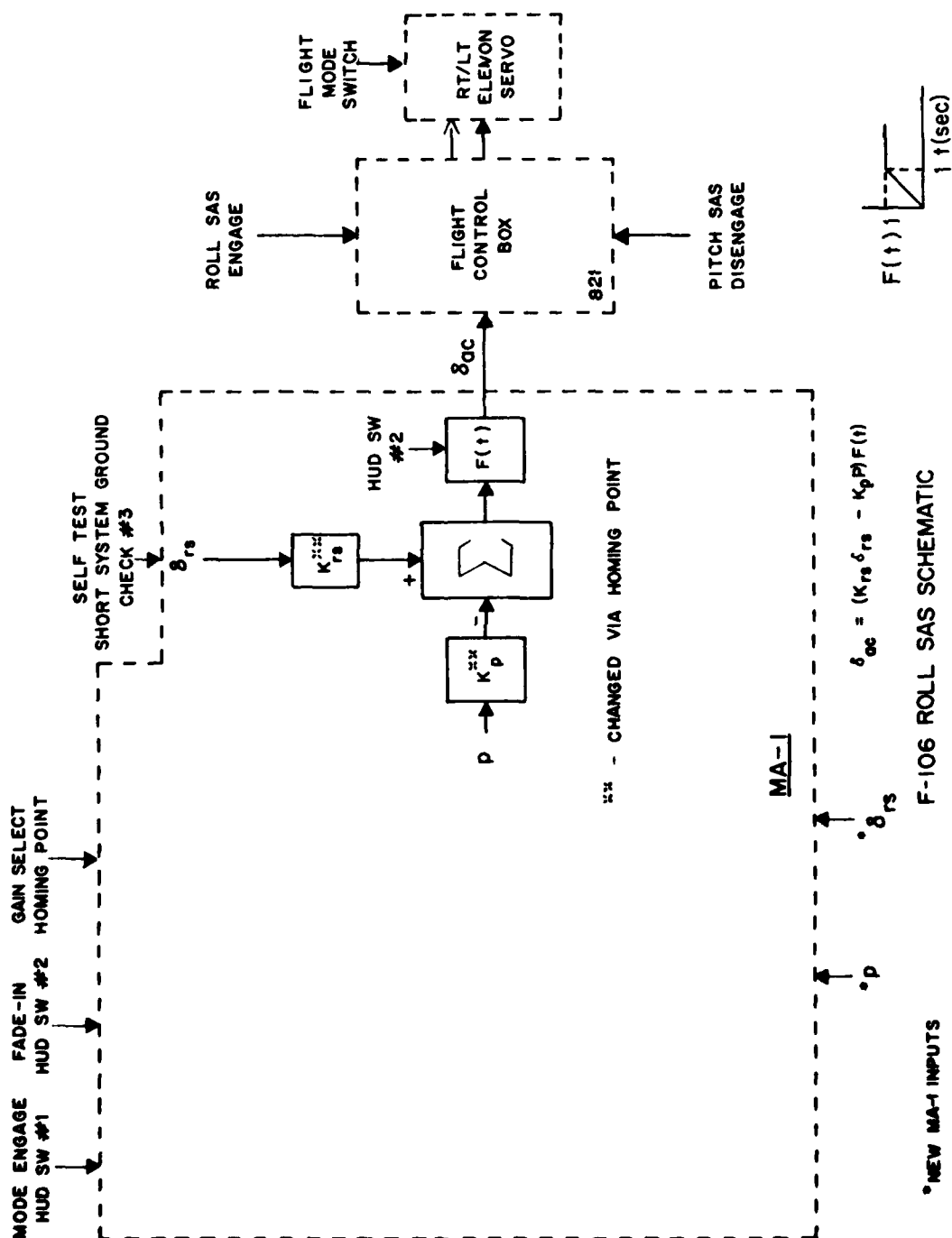


Figure 30. Roll SAS Implementation

$$\delta_{ac} = (K_S \delta_{ps} - K_{rr} P) F(t)$$

<u>COMPUTER OUTPUT</u>		<u>OUTPUT LOCATION</u>	<u>SCALING</u>	<u>RANGE</u>
$\delta_{ac}$		RH Elevon Command (deg)	50 V/deg	0-100V, $\pm 1^\circ$
<u>COMPUTER INPUTS</u>	<u>SOURCE</u>	<u>INPUT LOCATION</u>	<u>SCALING</u>	<u>RANGE</u>
<u>(Variables)</u>				
$P$ (roll rate, deg/sec)	IRP	existing (E25)	10.0 deg/sec/V	$\pm 5V$
$\delta_{ps}$ (lateral stick position, in)	stick potentiometer	LH Elevon Position (A21)	50 $\pm$ 30V	$\pm 3.5$ in

(Variable gains)

$K_S$  (stick gain, deg/in)  
 $K_{rr}$  (roll rate gain, deg/deg/sec)

These gains will be set using the Homing Point Indicator as a logic indicator to set these gains as shown in Table 1.

(Discretes)

HUD Switch #1  
 HUD Switch #2

Function

Selects roll SAS mode  
 Fades in and out control law via  $F(t)$

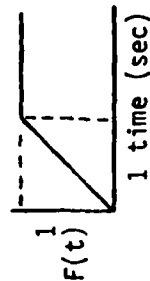


Figure 31. Roll SAS Inputs and Switching Logic

ground check number three (SSGC #3). When SSGC was engaged, the computer would read stored data locations instead of the sensor input. The control law was computed using these values for the sensor measurements. The resulting rudder deflection was then compared with the rudder deflection which should theoretically have occurred. These ground check calculations are shown in Figure 32.

Flight test flexibility was achieved by designing the system with variable gains and SAS mode switching logic. To achieve variable gains in the control law itself, the homing point selector (an existing navigation control) was used as a gain select. For each switch location on the homing point select, a different set of gains were used in the SAS calculations. Table 7 shows the homing point values and the associated gains. In addition to the variable gains, adjusted by the homing point select, an electrical bias or trim was available using the altitude alert switch, an existing digital input to the computer. This electrical bias allowed the pilot to trim out the bias resulting from an accumulation of sensor biases. This electrical trim was used in place of the normal trim because the normal rudder trim uses part of the  $\pm 6^\circ$  SAS authority of rudder actuator. By using the electrical trim, the SAS control law still had even  $\pm 6^\circ$  authority instead of an uneven authority such as  $+5^\circ$ ,  $-7^\circ$  which could occur if a  $1^\circ$  bias was eliminated using the standard rudder trim.

TABLE 7  
HOMING POINT SELECT GAIN VALUES

HD	$K_B$	$K_p$	$a_b$	$K_{rr}$	$K_s$
A	1.9	5	4	.15	3
B	1.9	5	1	.15	3
C	1.25	3.28	4	.15	3
D	2.25	5	4	.15	3
E	1.5	3.45	4	.15	3
F	1.9	5	3	.15	3
G	1.9	5	6.36	.15	3
H	1.9	2.5	4	.15	3
I	1.9	10	4	.25	3
J	1.9	5	2	.15	3
K	1.9	5	4	.15	2
L	1.9	5	4	.15	4
M	1.9	5	4	.1	3
N	1.9	5	4	.2	3

Rudder Check

$$\delta_{rc} = (K_p \delta_p + \text{TRIM} - K_{\dot{\beta}} \hat{\beta})$$

$$\hat{\beta} = \frac{p(\alpha + \alpha_b)}{57.3} - r + \frac{57.3 A_y}{U} + \frac{57.3 g \cos \theta \sin \phi}{U}$$

$$p = 5 \text{ deg/sec}$$

$$\theta = -5^\circ$$

$$\alpha = 7 \text{ deg}$$

$$\phi = -15^\circ$$

$$r = 5 \text{ deg/sec}$$

$$\text{TRIM} = 0$$

$$A_y = -3 \text{ ft/sec}^2$$

$$\delta_p = -1.25 \text{ in}$$

$$U = 862 \text{ ft/sec}^1$$

$$\hat{\beta} = \frac{5(7 + \alpha_b)}{57.3} - 5 + \frac{57.3(-3)}{862} + \frac{57.3(32.2) \cos(-5^\circ) \sin(-15^\circ)}{862}$$

$$= .611 + .0873\alpha_b - 5 - .199 - .552$$

$$= .0873\alpha_b - 5.14$$

$$\delta_{rc} = [K_p * 1.25 + 0 - K_{\dot{\beta}} (.0873\alpha_b - 5.14)]$$

$$= -1.25K_p - K_{\dot{\beta}} (.0873\alpha_b - 5.14)$$

Aileron Check

$$\delta_{ac} = (K_g \delta_{ps} - K_{rr} p)$$

$$p = 5 \text{ deg/sec}$$

$$\delta_{ps} = 0$$

$$\delta_{ac} = 0K_g - 5K_{rr}$$

$$= -5K_{rr}$$

Figure 32. Built-in-Test

The switching logic also allowed some of the parameters in the  $\beta$  SAS control law to be deleted from the control law calculation. Specifically, the heads up display (HUD) switches 3 and 4 were used to delete pilot rudder pedal position ( $\delta_{rp}$ ) and lateral acceleration ( $A_y$ ) respectively. These options proved very helpful, both in debugging the system and in picking the best overall system configuration. HUD switch 1 was used to start the computer calculations and HUD switch 2 was used to fade-in the control law. The fade-in consisted of a 1-second ramp from zero to one. This fade-in is shown as  $F(t)$  on Figures 28-31.

The actual computer program which did the SAS calculations is shown in Appendix F. This IRAM assembly code shown did the  $\beta$  and roll SAS calculations, the rudder trim, gain changes, and also displayed a fixed reticle depressed 50 mils from the water line and 15 mils right of centerline. The cross was placed off center so that the vision splitter on the 106 did not interfere with the HUD camera. The computer program is located on the magnetic memory drum at the same location as the gunsight program; therefore, to load the program, the pilot selected Special Weapons (SPL WPM) on the weapon control panel.

## 2. FLIGHT TEST RESULTS

After several system checkout flights, the system was debugged and data flights were flown. The 475th Test Squadron flew the  $\beta$  and roll SAS during the months of June, July, and August of 1978. The system was flown by three different pilots during this period. Both basic handling qualities tests and handling qualities during tracking (HQDT) tests were flown by all three pilots.

The roll SAS proved to be the least effective of the two systems tested. This ineffectiveness was due primarily to limitations in the way the system was implemented. Since the roll SAS had only  $\pm 1$  degree of elevon authority, small biases in roll rate and lateral stick position measurements saturated the system. This saturation meant that the control law would operate only in one direction. In spite of these limitations, the pilots felt that when the system was operating properly, it was very effective and desirable for air-to-air tracking. Unfortunately, the

stick position and roll rate biases were present during most of the flights, thereby making the roll SAS, on the whole, ineffective. Additionally, instrumentation problems precluded the reduction of aircraft data for the roll SAS flights.

The  $\dot{\beta}$  SAS was shown to be effective in the ATA tracking task by reductions in the tracking error shown on gun camera film. The lateral acceleration ( $A_y$ ) term in the  $\dot{\beta}$  control law was switched out during the data gathering flights because it was very noisy and added no real improvement to the response. The system also showed to be an improvement over the standard SAS in terms of reduction in pilot workload. These conclusions are based primarily on pilot comments and on gun camera film taken during many of the tracking encounters. There is also some strip chart data of aircraft parameters which aided somewhat in system evaluation. Unfortunately, the parameters most critical to the  $\dot{\beta}$  system evaluation,  $\beta$  and  $r$ , were not measured during the tests due to instrumentation problems.

Figures 33 and 34 show a direct comparison between the standard SAS and the  $\dot{\beta}$  SAS with Homing Point E gains ( $K_{\dot{\beta}}=1.5$ ,  $K_p=3.45$ ). The long straight line in the pipper trace of Figure 33 is caused by a data dropout in the instrumentation system. The flight condition was Mach = .8, 10,000 ft. These figures show tracking error data during an aileron reversal. In this case, the difficulty of the task masked much of the SAS differences, although one can see a higher frequency content in the  $\dot{\beta}$  SAS error time plots. This higher frequency content is indicative of the faster response available when the aircraft was flying with the  $\dot{\beta}$  SAS engaged. Pilot comments confirmed the faster response time with the  $\dot{\beta}$  SAS. They also indicated this faster response to be a desirable capability during ATA tracking.

Figures 35 and 36 show similar tracking error comparisons between the standard SAS and the  $\dot{\beta}$  SAS. Both a right and left 4 g turn at Mach .8 and 10,000 feet are shown. The right turn shows little difference between the two systems other than the decreased response time of  $\dot{\beta}$  SAS as indicated qualitatively by the higher frequency content of the error

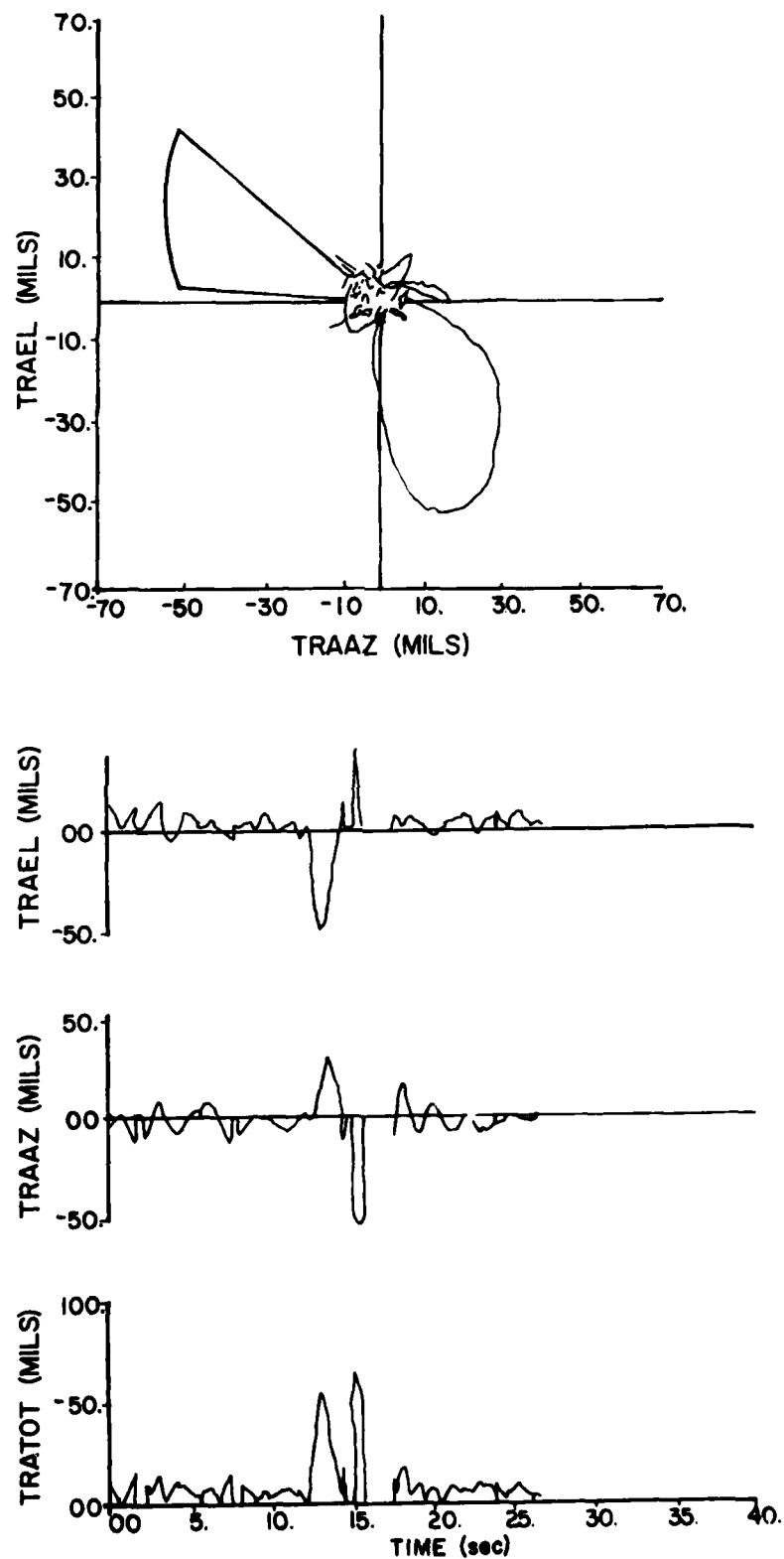


Figure 33. Standard SAS, Aileron Reversal, Mach .8, 10000 Feet



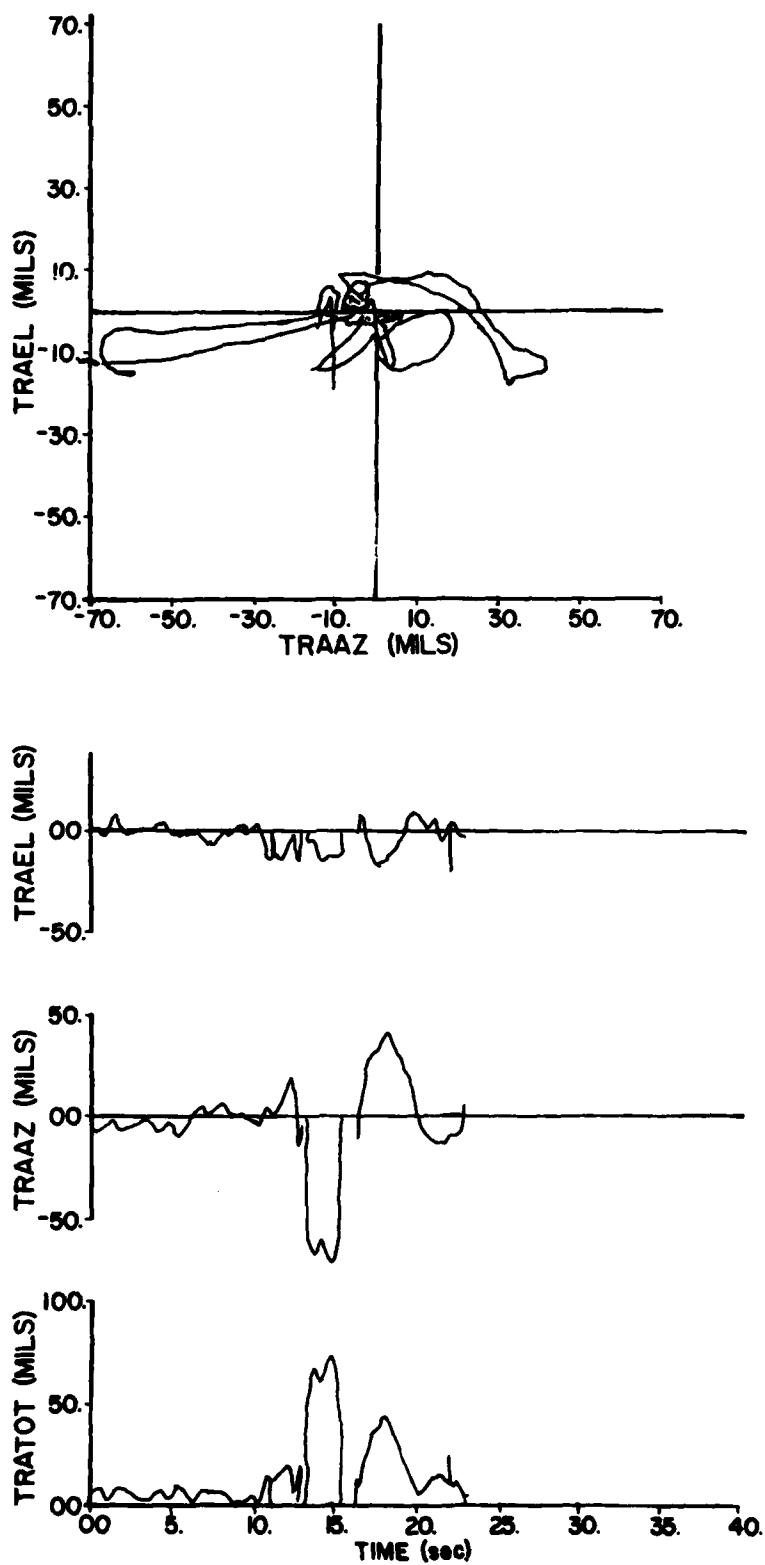


Figure 34.  $K_{\beta} = 1.5$ ,  $K_p = 3.45$ , Aileron Reversal, Mach .8, 10000 Feet

AFWAL-TR-80-3015

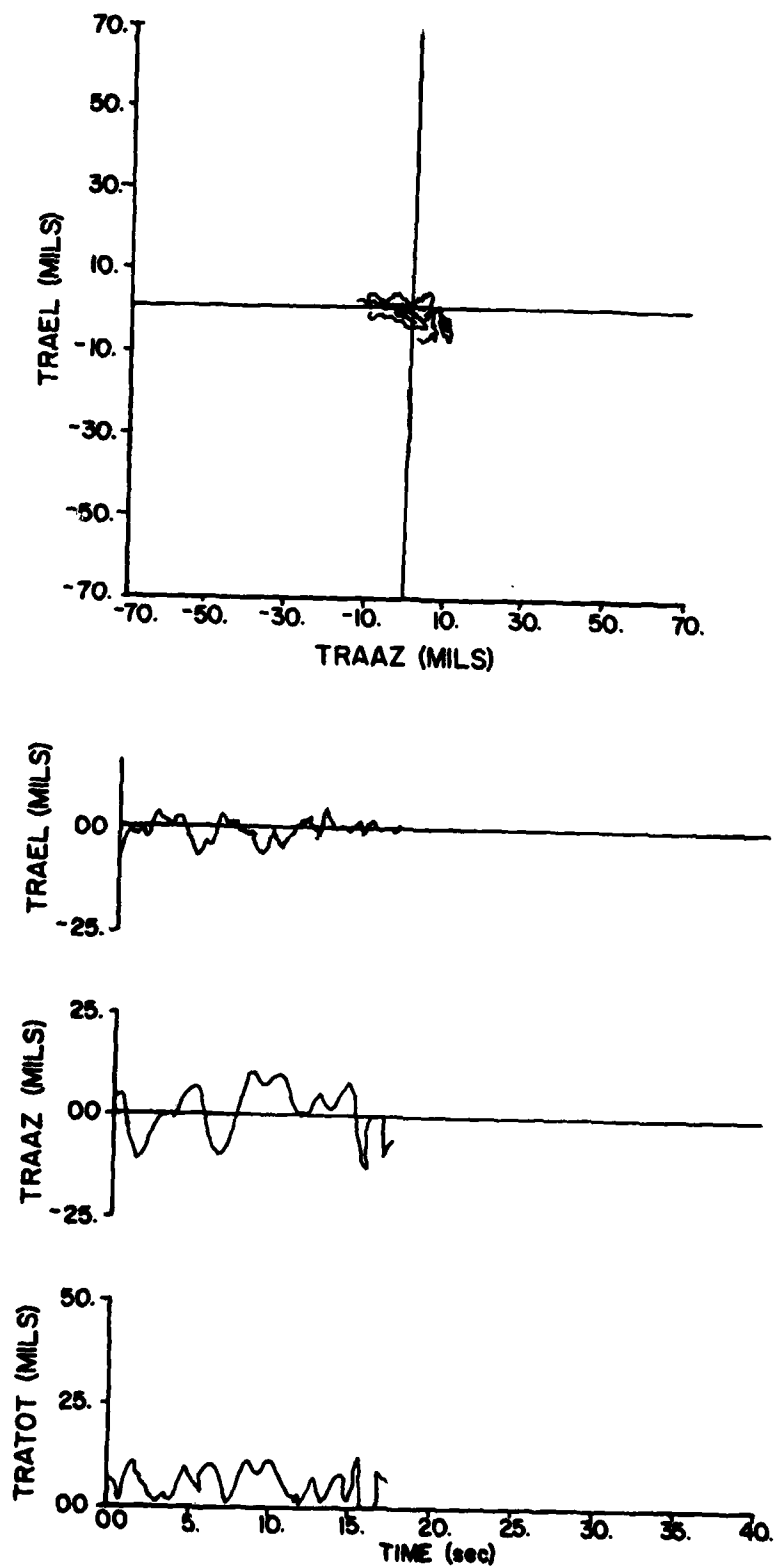


Figure 35. Standard SAS, 4 g Turn, Mach .8, 10000 Feet

AFWAL-TR-80-3015

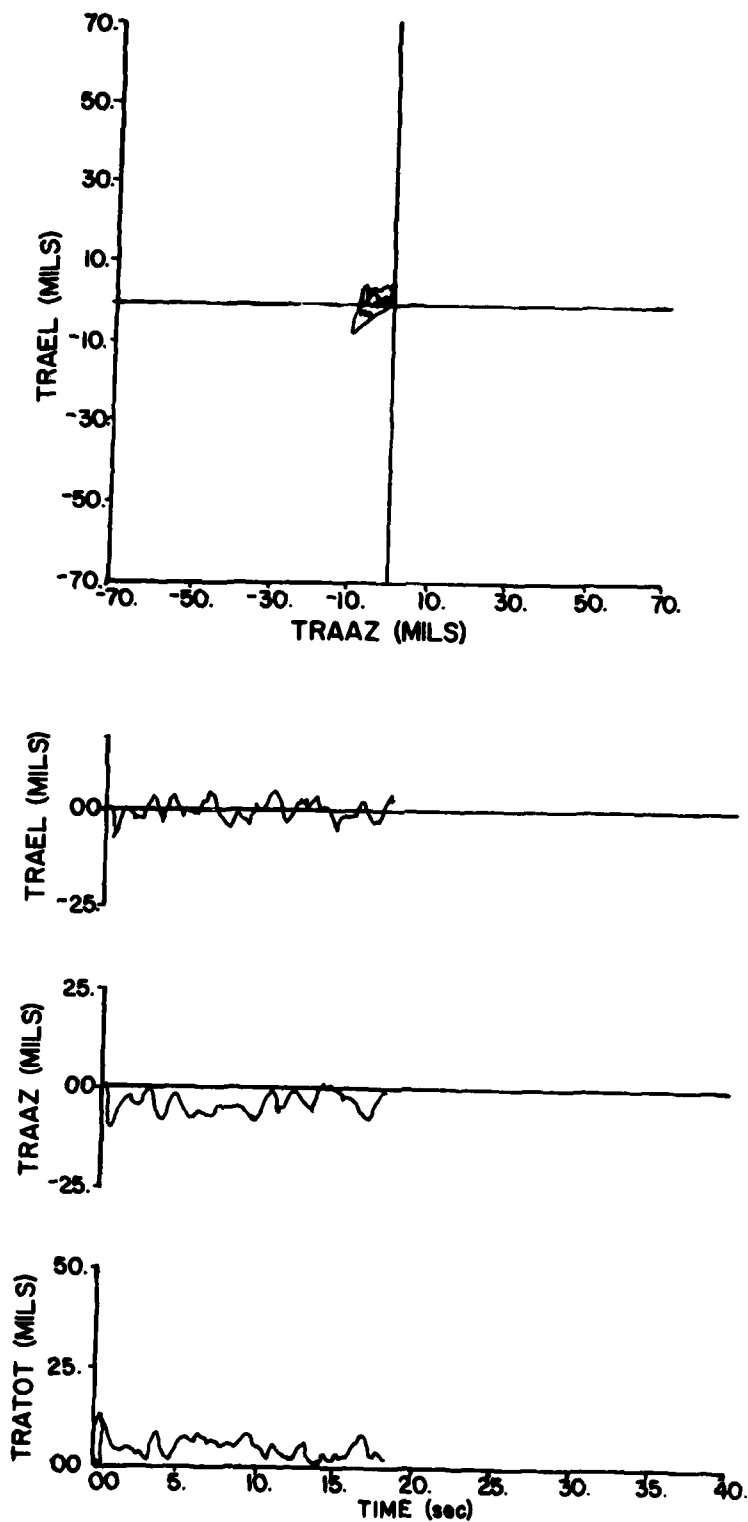


Figure 36.  $K_{\beta} = 1.5$ ,  $K_p = 3.45$ , 4 g Turn, Mach .8, 10000 Feet

time plots. The left turn, however, does show a significant decrease in tracking error on both the pipper plot and the error time plots.

Figures 37 through 42 show additional flight test results for constant 3.5 to 4 g turns. The standard SAS results, Figure 37, show a fairly large pipper trace with excursions as high as  $\pm 25$  mils in both elevation and traverse. The  $\beta$  SAS, Figures 38 through 42, shows significant reduction in this aim wander. The results are especially impressive in Figure 38 with  $K_{\beta}=1.9$  and  $K_p=3.45$ , over 50% reduction in aim wander. Although these plots represent tracking performance for only one flight, they are representative of the performance achieved by all the pilots on all the test missions.

In addition to the improvement evidenced by the pipper plots, Figure 43 shows data which is indicative of the reduction in pilot workloads achieved using the system. The time history strip chart recordings from this figure were taken from the pass whose pipper plot is shown in Figure 42. The reduction in pilot workload is evidenced by the reduction in magnitude of the stick and rudder deflections. The decreased response time is evidenced by the higher frequency content of the control movements using the  $\beta$  SAS. The workload reduction evidenced by Figure 43 is very similar to the workload reduction evidenced by Figure 28 showing simulator results.

A total of three different pilots flew the modified SAS. The roll SAS did not function and was therefore not evaluated. All agreed that the  $\beta$  SAS was an improvement over the standard SAS during ATA tracking. The pilot comments indicated that the improvement in tracking capability was due to the "crisper", faster response available using the  $\beta$  SAS. The consensus was that the gains of  $K_{\beta}=1.9$  and  $K_p=2.5$  were the best of those tested. The pilots felt that these gains made the best system by providing a quick but controllable response.

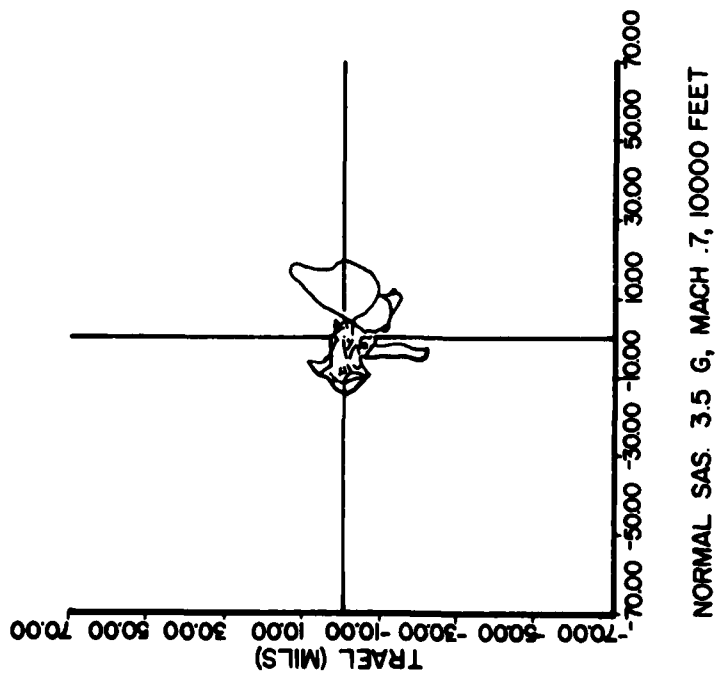
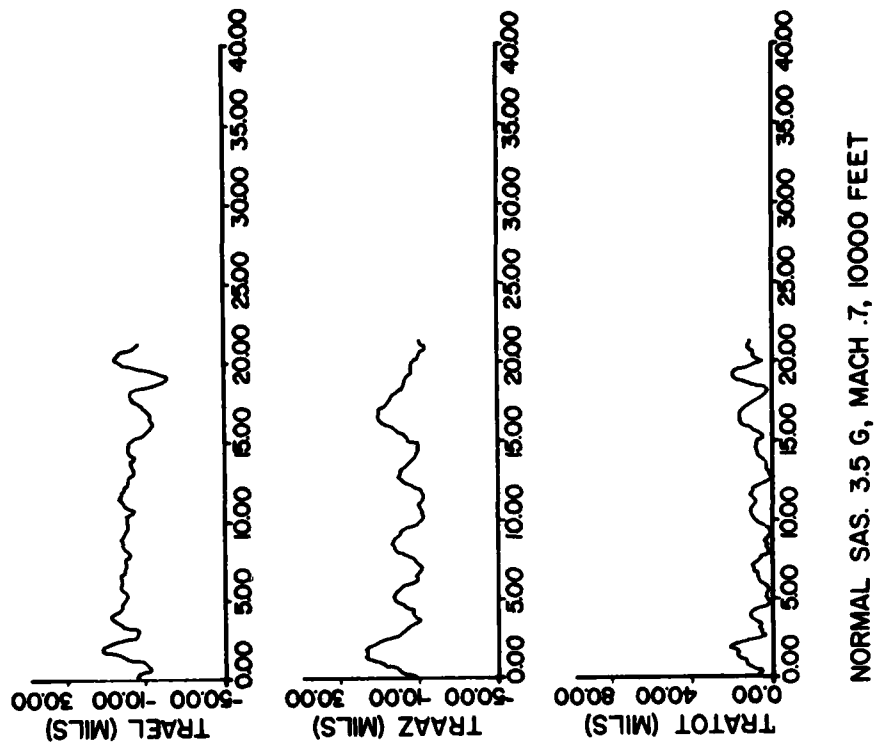
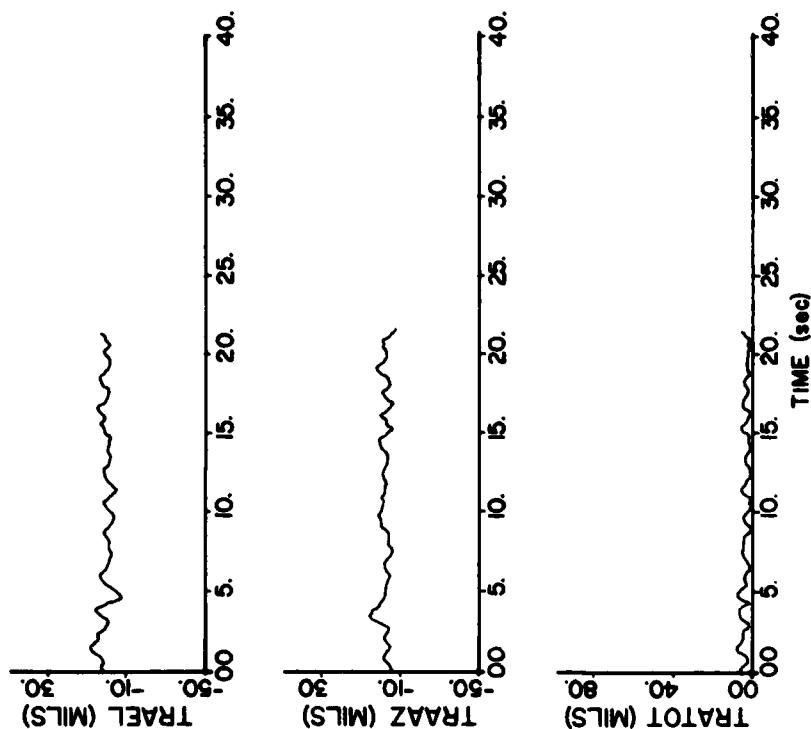


**Figure 37. Standard SAS, 3.5 g, Mach .7, 10000 Feet**



KBO=1.9. KP=5.37 G, MACH .7, 10000 FEET

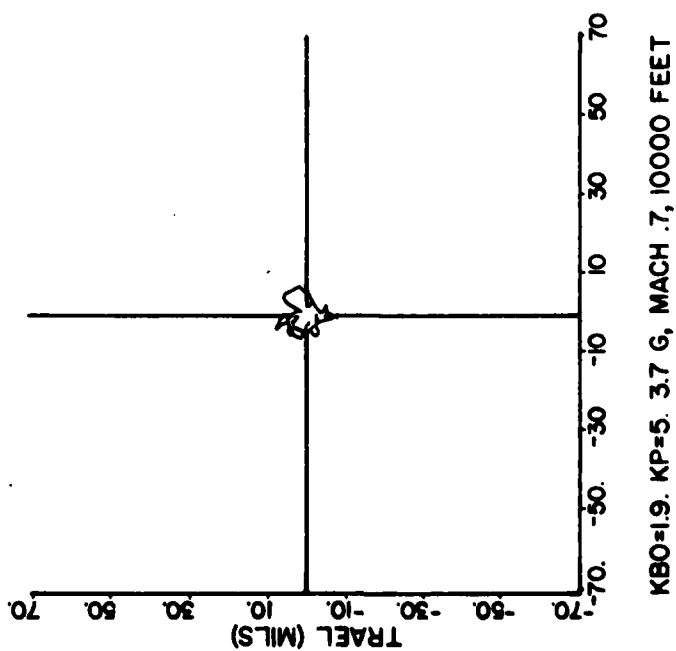
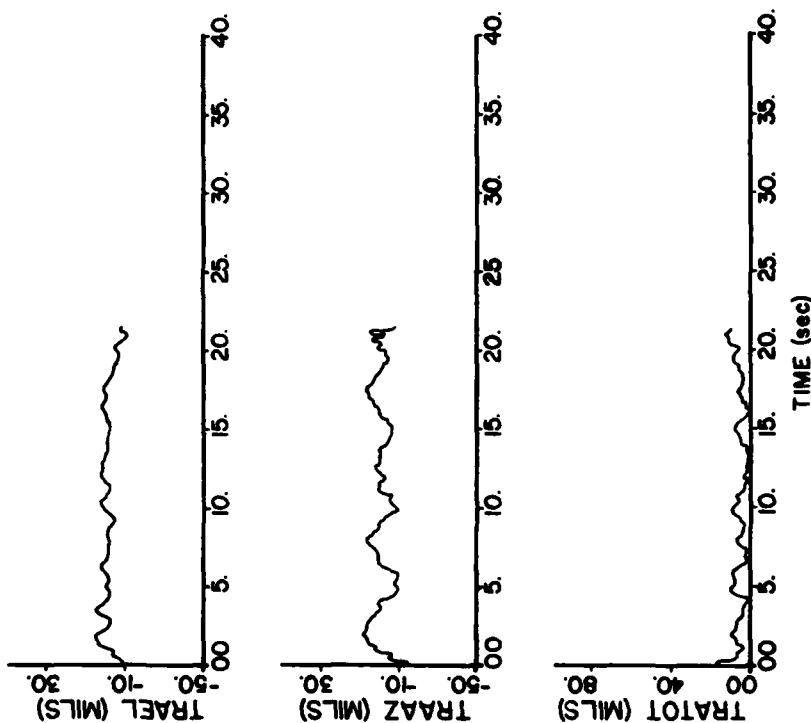
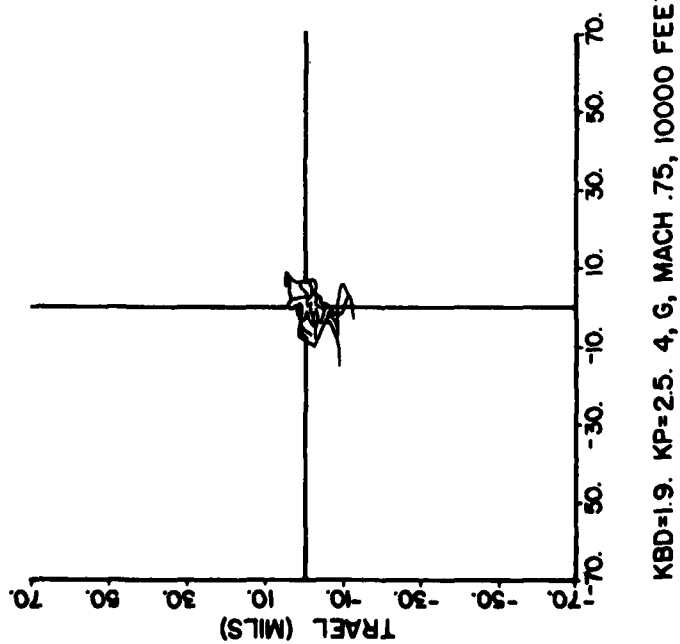


Figure 38.  $K_B=1.9$ ,  $K_p=5$ , 3.7 g, Mach .7, 10000 Feet



KBD=1.9. KP=2.5. 4 G, MACH .75, 10000 FEET

Figure 39.  $K_g=1.9$ ,  $K_p=2.5$ , 4 g, Mach .75, 10000 Feet



KBD=1.9. KP=2.5. 4, G, MACH .75, 10000 FEET

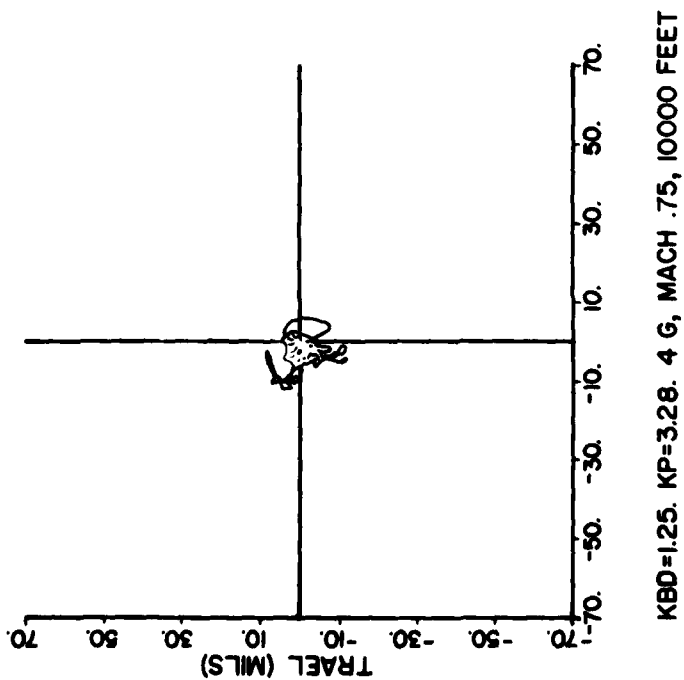
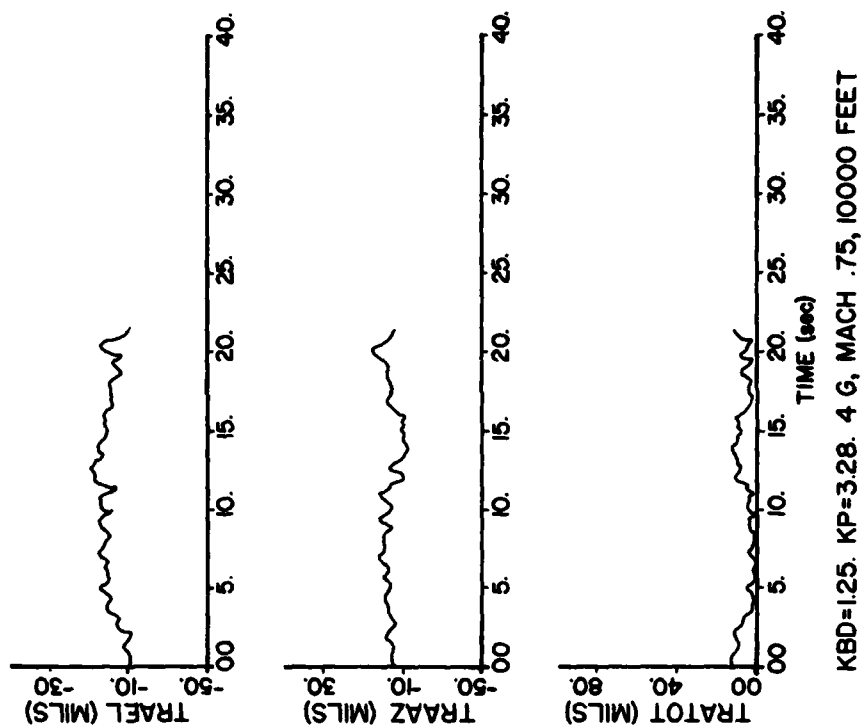


Figure 40.  $K_g=1.25$ ,  $K_p=3.28$ , 4 g, Mach .75, 10000 Feet



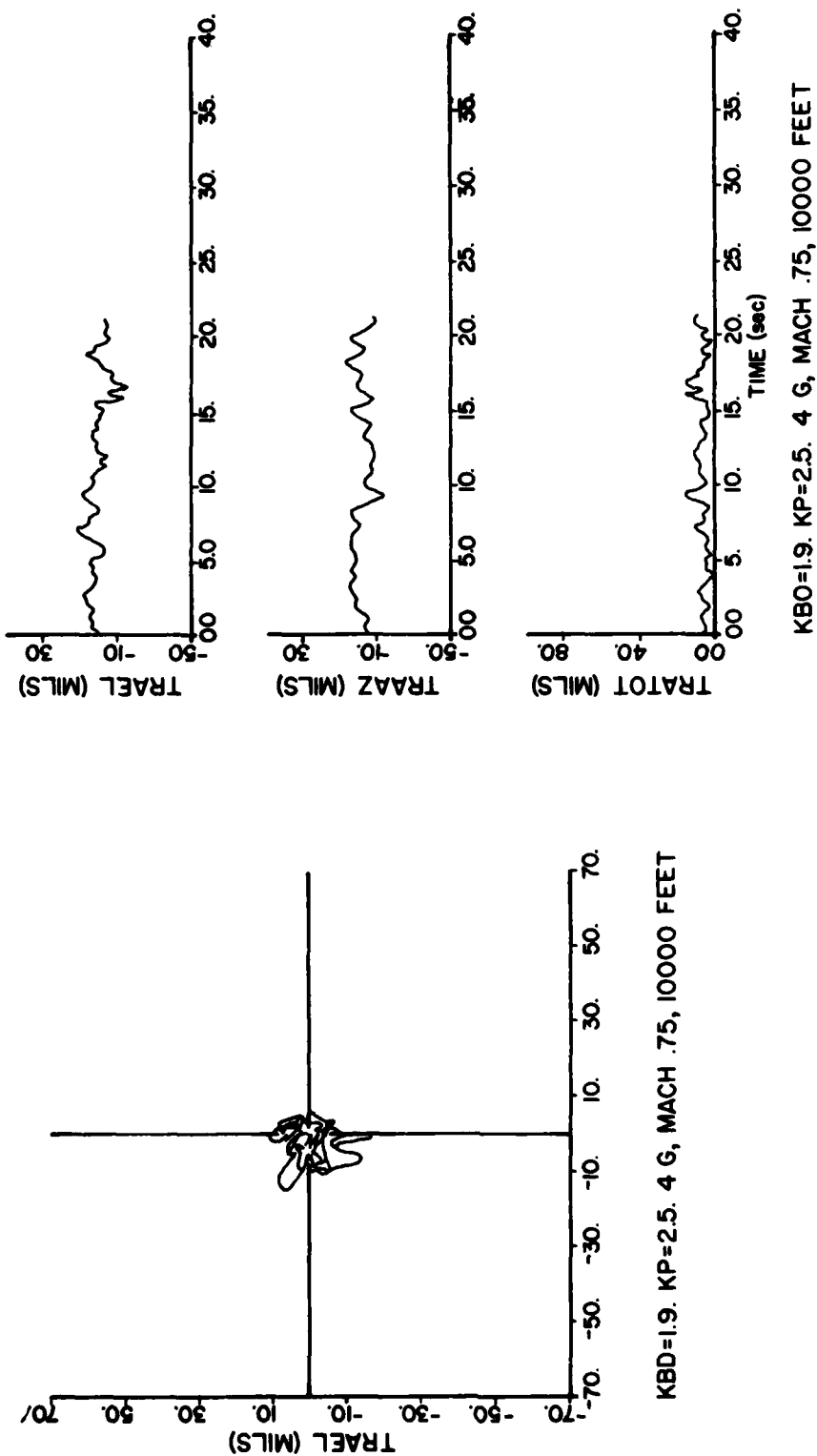


Figure 41.  $K_g=1.9$ ,  $K_p=2.5$ , 4 g, Mach .75, 10000 Feet

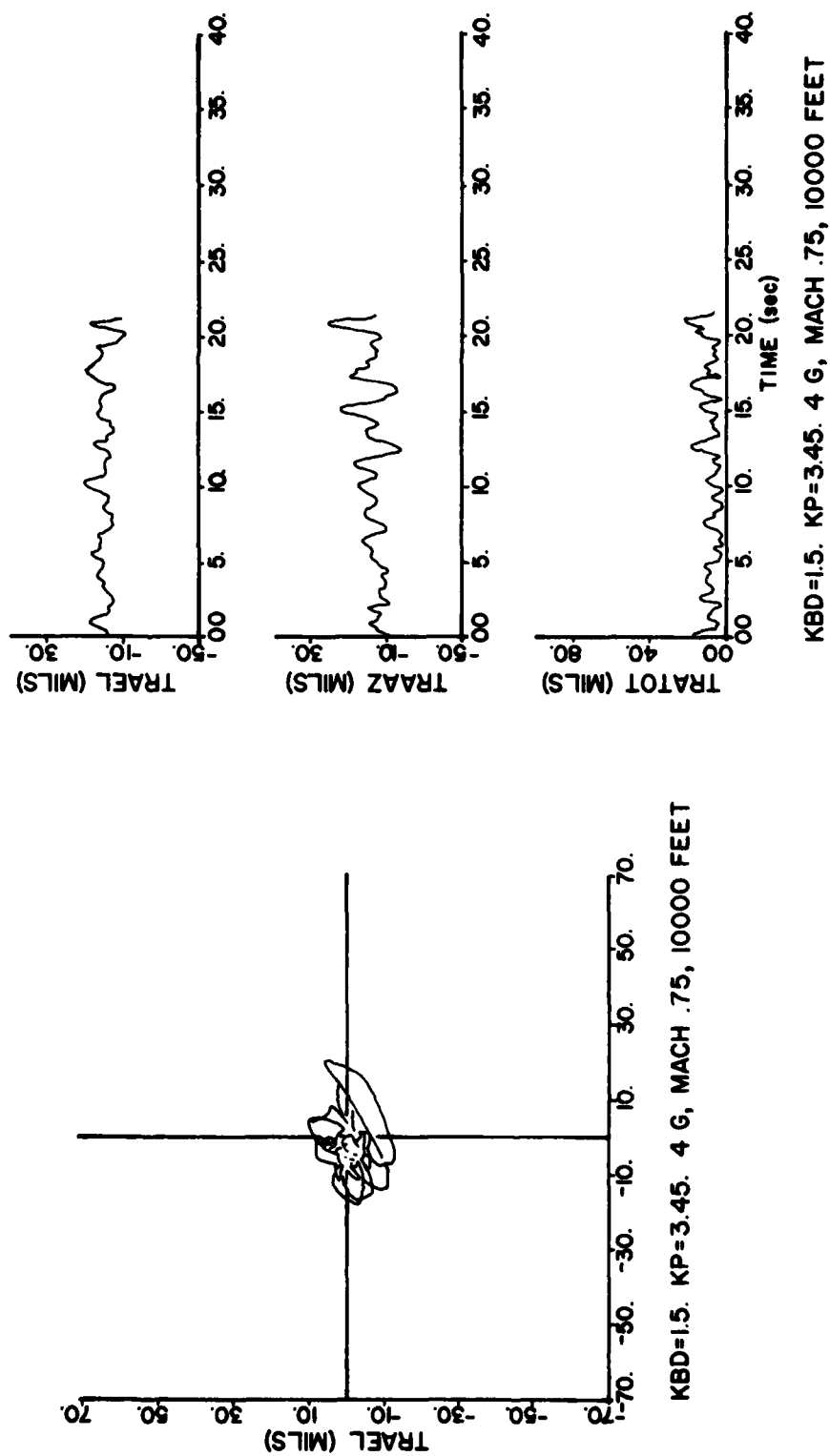


Figure 42.  $K_g=1.5$ ,  $K_p=3.45$ , 4 g, Mach .75, 10000 Feet

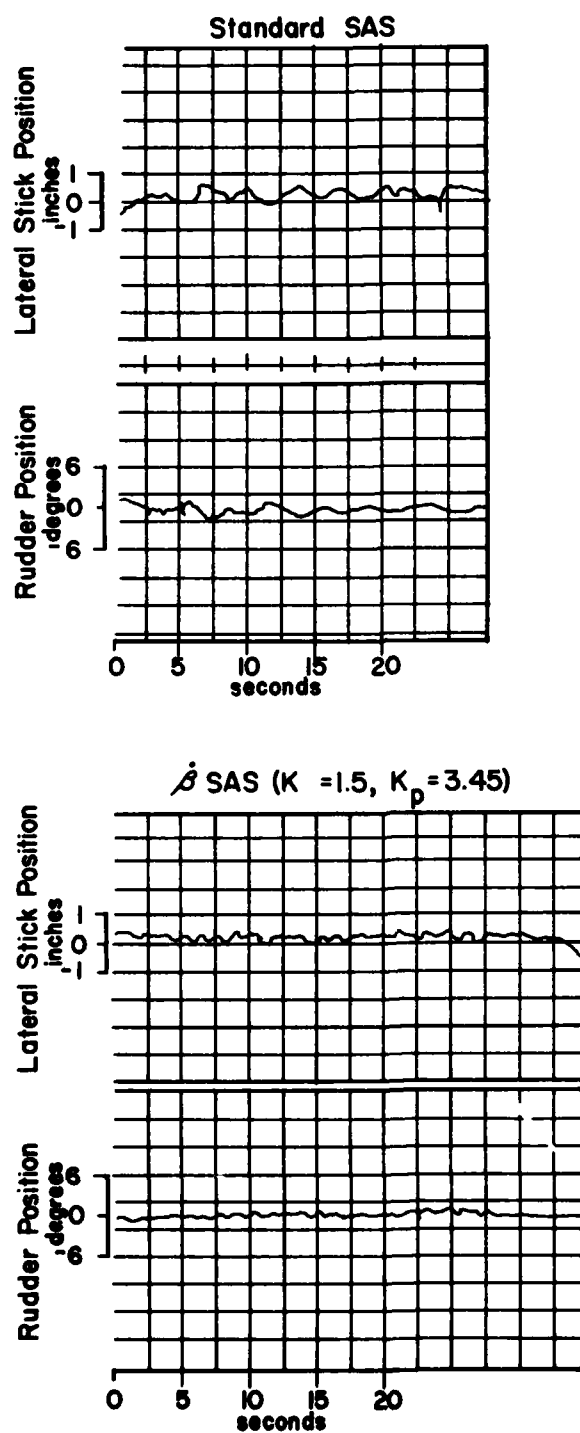


Figure 43. Pilot Workload Comparison, 4 g Tracking Task

## SECTION VI

### CONCLUSIONS AND RECOMMENDATIONS

#### 1. CONCLUSIONS

A lateral stability augmentation system for the F-106 has been designed using sideslip rate and sideslip angle as primary feedbacks. The sideslip rate is synthesized from signals available from sensors on board the aircraft. Both time and frequency domain simulations showed that the dynamic response of the aircraft is improved using the new SAS. A piloted simulation of ATA tracking encounters was also conducted to compare the existing SAS with two configurations of the  $\beta-\dot{\beta}$  SAS. This simulation showed that a configuration of the  $\beta-\dot{\beta}$  SAS which allowed only  $\dot{\beta}$  to be fed to the rudder demonstrated substantial improvement over the standard SAS. This improvement in standard deviation of tracking error varied from 5% to 45% depending on pilot and flight condition. Based on these piloted and non-piloted simulations, the use of a  $\dot{\beta}$  feedback in place of the existing SAS on the F-106 will significantly improve lateral handling qualities during tracking.

To verify this conclusion, this system was flight tested at Tyndall AFB, Florida. The flight test results, in terms of HUD camera film data and pilot comments, confirmed this conclusion that a  $\dot{\beta}$  SAS will improve the F-106 handling qualities during tracking.

#### 2. RECOMMENDATIONS

Based on the flight test results and pilot comments, the Control Systems Development Branch of the Flight Dynamics Laboratory recommended to the Air Defense Command (ADCOM) that this modified system, using  $\dot{\beta}$  as primary feedback, be retrofitted to the F-106's now in the inventory. ADCOM/DOV agreed with the conclusion that such a system would improve the F-106 flight control system; however, fiscal considerations forced a negative decision on retrofit.

# APPENDIX A

## ASD HYBRID SIMULATION

Part of the design process includes looking at the different SAS's in a six degree-of-freedom, nonlinear simulation. This simulation is based on force and moment equations from the GDCA report (Reference 7). The force and moment equations, composed of the aerodynamic coefficients for the F-106, are used in the simulation equations which solve for  $\dot{p}$ ,  $\dot{q}$ ,  $\dot{r}$ ,  $\dot{u}$ ,  $\dot{v}$ , and  $\dot{w}$  (Reference 8). These simulation equations and the force and moment equations are shown below.

### 1. SIMULATION EQUATIONS

The following equations are the basic differential equations used in the ASD hybrid simulation.

$$\dot{p} = \frac{L}{I_x} + \dot{r} \frac{I_{xz}}{I_x} - qr \frac{(I_z - I_y)}{I_y} + pq \frac{I_{xz}}{I_x} \quad (A-1)$$

$$\dot{q} = \frac{M}{I_y} + pr \frac{(I_z - I_x)}{I_y} + (r^2 - p^2) \frac{I_{xz}}{I_y} \quad (A-2)$$

$$\dot{r} = \frac{N}{I_z} + \dot{p} \frac{I_{xz}}{I_z} - pq \frac{(I_y - I_x)}{I_x} - qr \frac{I_{xz}}{I_z} \quad (A-3)$$

$$\dot{u} = \frac{T + Fx}{m} - g \sin \theta + rv - qw \quad (A-4)$$

$$\dot{v} = \frac{Fy}{m} + g \cos \theta \sin \phi + pw - ru \quad (A-5)$$

$$\dot{w} = \frac{Fz}{m} + g \cos \theta \cos \phi + qu - pv \quad (A-6)$$

## 2. FORCE AND MOMENT EQUATIONS

The force and moment equations below are used as inputs to the simulation equations above. The equations include both first and second order aerodynamic effects. A more detailed description of the equations and coefficients is found in Reference 6.

$$F_x = (-C_D \cos \alpha + C_L \sin \alpha) \bar{q} S \quad (A-7)$$

$$F_y = \left\{ C_{y_\beta} \beta + C_{y_{\delta a}} \delta a + C_{y_{\delta r}} \delta r + (C_{y_p} + C_{y_r}) \frac{b}{2U} + \left[ \left( \frac{\partial C_{y_\beta}}{\partial \alpha} \right) \alpha + \left( \frac{\partial C_{y_\beta}}{\partial |\beta|} |\beta| \right) \beta \right] \right\} \bar{q} S \quad (A-8)$$

$$F_z = (-C_L \cos \alpha - C_D \sin \alpha + C_{z_\alpha} \alpha + C_{z_{\delta e}} \delta e) \bar{q} S \quad (A-9)$$

$$L = \left\{ C_{l_p} p + C_{l_r} r \right\} \frac{b}{2U} + C_{l_\beta} \beta + C_{l_{\delta a}} \delta a + C_{l_{\delta r}} \delta r + \left[ \left( \frac{\partial C_{l_\beta}}{\partial \alpha} \right) \alpha + \left( \frac{\partial C_{l_\beta}}{\partial |\beta|} |\beta| \right) \beta + \left[ \left( \frac{\partial C_{l_p}}{\partial \alpha} \right) \alpha + \left( \frac{\partial C_{l_p}}{\partial \alpha} \right) p + \left( \frac{\partial C_{l_r}}{\partial \alpha} \right) r \right] \frac{ab}{2U} \right] \right\} \bar{q} S b \quad (A-10)$$

$$M = [C_m + C_{m_q} \frac{\bar{c}}{2U} (q + \dot{\alpha}) + C_{m_{\delta e}} \delta e] \bar{q} S \bar{c} + (n.p. + \bar{c} - x_{c.g.}) F_z \quad (A-11)$$

$$N = \left\{ C_{n_\beta} \beta + C_{n_{\delta a}} \delta a + C_{n_{\delta r}} \delta r + (C_{n_p} + C_{n_r}) \frac{b}{2U} + \left[ \left( \frac{\partial C_{n_\beta}}{\partial \alpha} \right) \alpha + \left( \frac{\partial C_{n_\beta}}{\partial |\beta|} |\beta| \right) \beta + \left( \frac{\partial C_{n_\beta}}{\partial \alpha} \right) \alpha + \left( \frac{\partial C_{n_\beta}}{\partial \alpha} \right) p + \left( \frac{\partial C_{n_r}}{\partial \alpha} \right) r \right] \frac{ab}{2U} + \left( \frac{\partial C_{n_{\delta a}}}{\partial \alpha} \alpha + \frac{\partial C_{n_{\delta a}}}{\partial \delta a} \delta a \right) \delta a \right\} \bar{q} S b \quad (A-12)$$

## APPENDIX B

## ROOT MAP DATA FOR THE F-106

The root map technique, described in Section III.1, involves finding numerous root loci at each flight condition. Part of the root loci at a given flight condition are generated with fixed values of  $K_\beta$  while the gain  $K_s$  is allowed to vary. The remaining loci have fixed values of  $K_s$  while  $K_\beta$  varies. The transfer function used with a fixed value for  $K_\beta$  is shown below. The derivation is shown in Section III.1.

$$(GH)_{\text{Const } K_\beta} = \frac{K_\beta K_s (s + a)(s + K_I)}{s^3 + bs^2 + cs + d} \quad (B-1)$$

A similar transfer function results when  $K_s$  is held constant and  $K_\beta$  varies.

$$(GH)_{\text{Const } K_s} = \frac{\frac{K_\beta K}{1 + K_\beta K} (s + a)(s + K_I)}{s(s^2 + bs + c)} \quad (B-2)$$

The tables included in this appendix contain the numerator and denominator roots for the transfer functions used to generate the root maps of Section III. The fixed values of  $K_s$  vary from 1 to 7;  $K_\beta$  varies from 1 to 15.

TABLE B-1  
TRANSFER FUNCTION DATA FOR MACH .4, SEA LEVEL

$K_\beta$	Constant $K_\beta$		
	$\frac{K}{1 + K_\beta K}$	Numerator Roots	Denominator Roots
1	.0427	-.2, -53.23 ↓	0, -1.64+ <u>i</u> 1.85
2	.0409		0, -3.57, -1.76
3	.0393		0, -6.17, -1.05
4	.0378		0, -8.16, - .81
5	.0365		0, -9.91, - .68
6	.0352		0, -11.49, -0.6
7	.034		0, -12.96, -.54

Constant $K_\beta$			
$K_\beta$	$K$	Numerator Roots	Denominator Roots
1	.0446 ↓	0, -.2, -53.23 ↓	-.058, -.518+ <u>i</u> 2.82
2			-.090, -.524+ <u>i</u> 3.21
3			-.11 , -.535+ <u>i</u> 3.55
4			-.124, -.551+ <u>i</u> 3.87
5			-.134, -.568+ <u>i</u> 4.16
6			-.142, -.587+ <u>i</u> 4.43
7			-.149, -.606+ <u>i</u> 4.69
8			-.154, -.626+ <u>i</u> 4.93
9			-.158, -.646+ <u>i</u> 5.17
10			-.161, -.667+ <u>i</u> 5.39
11			-.164, -.688+ <u>i</u> 5.6
12			-.167, -.709+ <u>i</u> 5.81
13			-.169, -.730+ <u>i</u> 6.00
14			-.171, -.750+ <u>i</u> 6.20
15			-.173, -.774+ <u>i</u> 6.38



TABLE B-2  
TRANSFER FUNCTION DATA FOR MACH .9, SEA LEVEL


Constant  $K_\beta$ 

$K_\beta$	$\frac{K}{1 + K_\beta K}$	Numerator Roots	Denominator Roots
1	.0641	-.2, -57.34	0, -2.77±i3.98
2	.0602	↓	0, -4.34±i2.0
3	.0568		0, -8.99, -2.46
4	.0538		0, -12.14, -1.78
5	.051		0, -14.72, -1.43
6	.0485		0, -16.94, -1.22
7	.0463		0, -18.91, -1.07

Constant  $K_\beta$ 

$K_\beta$	K	Numerator Roots	Denominator Roots
1	.0685	0, -.2, -57.34	-.028, -1.01 ±i5.22
2	↓	↓	-.049, -1.03 ±i5.57
3			-.066, -1.06 ±i5.90
4			-.079, -1.09 ±i6.22
5			-.090, -1.11 ±i6.53
6			-.099, -1.14 ±i6.82
7			-.106, -1.17 ±i7.06
8			-.113, -1.203±i7.36
9			-.119, -1.236±i7.62
10			-.123, -1.268±i7.86
11			-.128, -1.298±i8.10
12			-.132, -1.329±i8.34
13			-.136, -1.362±i8.57
14			-.139, -1.4 ±i8.79
15			-.142, -1.43 ±i9.0

TABLE B-3  
TRANSFER FUNCTION DATA FOR MACH .7, 10000 FEET

$K_\beta$	$\frac{K}{1 + K_\beta K}$	Constant $K_\beta$ Numerator Roots	Denominator Roots
1	.0495	$-.2, -78.08$ 	0, $-2.471 \pm i2.13$
2	.0472		0, -6.8, -1.6
3	.0451		0, -10.49, -1.06
4	.0431		0, -13.6, -.83
5	.0413		0, -16.37, -.7
6	.0397		0, -18.88, -.62
7	.0382		0, -21.2, -.56



$K_\beta$	K	Constant $K_\beta$ Numerator Roots	Denominator Roots
1	$.0521$ 	$0, -.2, -78.077$ 	$-.056, -.558 \pm i3.75$
2			$-.088, -.566 \pm i4.26$
3			$-.1085, -.584 \pm i4.71$
4			$-.1229, -.603 \pm i5.11$
5			$-.133, -.624 \pm i5.5$
6			$-.141, -.645 \pm i5.85$
7			$-.147, -.67 \pm i6.19$
8			$-.152, -.69 \pm i6.51$
9			$-.156, -.717 \pm i6.81$
10			$-.16, -.74 \pm i7.1$
11			$-.163, -.765 \pm i7.38$
12			$-.165, -.79 \pm i7.64$
13			$-.168, -.82 \pm i7.9$
14			$-.17, -.84 \pm i8.16$
15			$-.171, -.86 \pm i8.4$

TABLE B-4  
TRANSFER FUNCTION DATA FOR MACH .6, 15000 FEET

$K_\beta$	$\frac{K}{1 + K_\beta K}$	Constant $K_\beta$	
		Numerator Roots	Denominator Roots
1	.024	- .2, -102.85 ↓	0, -1.71 + i2.08
2	.0234		0, -3.82, -1.96
3	.0229		0, -6.85, -1.12
4	.0224		0, -9.15, - .86
5	.022		0, -11.2, - .72
6	.0214		0, -13.08, - .63
7	.021		0, -14.83, - .57

$K_\beta$	K	Constant $K_\beta$	
		Numerator Roots	Denominator Roots
1	.0391 ↓	0, - .2, -68.21 ↓	-.056, -.431 ± i3.07
2			-.087, -.435 ± i3.48
3			-.107, -.446 ± i3.84
4			-.121, -.454 ± i4.17
5			-.132, -.469 ± i4.48
6			-.14, -.485 ± i4.76
7			-.146, -.502 ± i5.03
8			-.151, -.519 ± i5.29
9			-.155, -.537 ± i5.54
10			-.159, -.556 ± i5.77
11			-.162, -.574 ± i5.99
12			-.165, -.593 ± i6.21
13			-.167, -.610 ± i6.42
14			-.169, -.630 ± i6.62
15			-.171, -.647 ± i6.82

TABLE B-5  
TRANSFER FUNCTION DATA FOR MACH .9, 15000 FEET

$K_{\beta}$	$\frac{K}{1 + K_{\beta}K}$	Constant $K_{\beta}$ Numerator Roots	Denominator Roots
1	.0443	-.2, -64.51	0, -2.02±i3.19
2	.0424	↓	0, -3.31±i1.81
3	.0407		0, -6.94, -2.04
4	.0391		0, -9.71, -1.45
5	.0376		0, -12.01, -1.17
6	.0362		0, -14.04, -1
7	.035	Constant $K_{\beta}$	0, -15.91, -.88
$K_{\beta}$	K	Numerator Roots	Denominator Roots
1	.0463	0, -.2, -64.51	-.035, -.618±i4.11
2	↓	↓	-.059, -.63 ±i4.45
3			-.077, -.643±i4.77
4			-.091, -.659±i5.08
5			-.102, -.679±i5.36
6			-.11, -.694±i5.63
7			-.12, -.715±i5.88
8			-.13, -.757±i6.13
9			-.13, -.755±i6.37
10			-.13, -.777±i6.6
11			-.14, -.795±i6.82
12			-.14, -.818±i7.03
13			-.15, -.842±i7.23
14			-.15, -.860±i7.44
15			-.15, -.884±i7.63

TABLE B-6  
TRANSFER FUNCTION DATA FOR MACH 1.2, 15000 FEET

$K_\beta$	$\frac{K}{1 + K_\beta K}$	Constant $K_\beta$ Numerator Roots	Denominator Roots
1	.0376	-.2, -88.21	0, -1.91 $\pm$ i4.66
2	.0363	↓	0, -3.07 $\pm$ i3.97
3	.035		0, -4.18 $\pm$ i2.77
4	.0338		0, -6.79, -3.68
5	.0327		0, -10.01, -2.49
6	.0317		0, -12.4, -2
7	.0307	Constant $K_\beta$	0, -14.61, -1.69

$K_\beta$	K	Numerator Roots	Denominator Roots
1	.0246	0, -.2, -102.85	-.018, -.686 $\pm$ i5.24
2	↓	↓	-.033, -.688 $\pm$ i5.48
3			-.046, -.697 $\pm$ i5.70
4			-.057, -.702 $\pm$ i5.92
5			-.067, -.712 $\pm$ i6.12
6			-.075, -.717 $\pm$ i6.33
7			-.082, -.729 $\pm$ i6.52
8			-.089, -.739 $\pm$ i6.72
9			-.095, -.748 $\pm$ i6.90
10			-.100, -.755 $\pm$ i7.08
11			-.105, -.768 $\pm$ i7.25
12			-.109, -.775 $\pm$ i7.42
13			-.113, -.786 $\pm$ i7.59
14			-.117, -.797 $\pm$ i7.75
15			-.120, -.807 $\pm$ i7.91

TABLE B-7  
TRANSFER FUNCTION DATA FOR MACH .6, 30000 FEET

$K_\beta$	$\frac{K}{1 + K_\beta K}$	Constant $K_\beta$	Denominator Roots
		Numerator Roots	
1	.0221	$-.2, 78.67$ $\downarrow$	0, -1.18, $\pm 12.01$
2	.0216		0, -2.013, $\pm 11.272$
3	.0212		0, -4.21, -1.4
4	.0207		0, -6.14, -.99
5	.0203		0, -7.78, -.808
6	.0122		0, -9.82, -.7
7	.0195		0, -10.71, -.62

$K_\beta$	K	Constant $K_\beta$	Denominator Roots
		Numerator Roots	
1	$.0226$ $\downarrow$	$0, -.2, -78.67$ $\downarrow$	-.051, $-.31 \pm 12.62$
2			-.081, $-.3 \pm 12.94$
3			-.1, $-.36 \pm 13.23$
4			-.12, $-.36 \pm 13.48$
5			-.13, $-.31 \pm 13.74$
6			-.135, $-.32 \pm 13.97$
7			-.14, $-.33 \pm 14.18$
8			-.147, $-.34 \pm 14.39$
9			-.151, $-.35 \pm 14.59$
10			-.155, $-.36 \pm 14.78$
11			-.157, $-.37 \pm 14.96$
12			-.16, $-.38 \pm 15.13$
13			-.16, $-.39 \pm 15.3$
14			-.166, $-.40 \pm 15.47$
15			-.167, $-.41 \pm 15.63$

TABLE B-8  
TRANSFER FUNCTION DATA FOR MACH .9, 30000 FEET

Constant  $K_\beta$

$K_\beta$	$\frac{K}{1 + K_\beta K}$	Numerator Roots	Denominator Roots
1	.0274	-.2, -76.56	0, -1.416±12.551
2	.0267	↓	0, -2.401±11.712
3	.026		0, -4.834, -1.83
4	.0253		0, -7.183, -1.257
5	.0247		0, -9.118, -1.007
6	.0241		0, -10.869, -.859

Constant  $K_\beta$

$K_\beta$	K	Numerator Roots	Denominator Roots
1	.0282	0, -.2, -76.56	-.0413, -.37 ±i3.21
2	↓	↓	-.0686, -.37 ±i3.53
3			-.088, -.37 ±i3.82
4			-.1, -.38 ±i4.09
5			-.11, -.39 ±i4.34
6			-.12, -.40 ±i4.59
7			-.13, -.41 ±i4.81
8			-.135, -.42 ±i5.03
9			-.14, -.43 ±i5.24
10			-.145, -.44 ±i5.44
11			-.149, -.46 ±i5.635
12			-.152, -.47 ±i5.82
13			-.155, -.48 ±i6.0
14			-.157, -.494±i6.2
15			-.159, -.51 ±i6.35

TABLE B-9  
TRANSFER FUNCTION DATA FOR MACH 1.4, 30000 FEET

	$\frac{K}{1 + K_\beta K}$	Constant $K_\beta$	
$K_\beta$		Numerator Roots	Denominator Roots
1	.0148	- .2, -81.67 ↓	0, -1.045±i4.017
2	.0146		0, -1.626±i3.817
3	.0144		0, -2.191±i3.522
4	.0142		0, -2.739±i3.113
5	.014		0, -3.272±i2.544
6	.0138		0, -3.79 ±i1.673
7	.0136		0, -5.43 -3.1593
Constant K			
$K_\beta$	K	Numerator Roots	Denominator Roots
1	.015 ↓	0, -.2, -81.67 ↓	-.013 , -.448±i4.27
2			-.025 , -.45 ±i4.413
3			-.035 , -.452±i4.55
4			-.044 , -.455±i4.68
5			-.053 , -.458±i4.81
6			-.06 , -.462±i4.93
7			-.067 , -.467±i5.056
8			-.073 , -.471±i5.174
9			-.078 , -.475±i5.29
10			-.083 , -.48 ±i5.14
11			-.088 , -.49 ±i5.52
12			-.0921, -.49 ±i5.625
13			-.096 , -.50 ±i5.73
14			-.1 , -.50 ±i5.836
15			-.103 , -.51 ±i5.94



## APPENDIX C

### EASY DYNAMIC ANALYSIS PROGRAM

Under contract to the USAF, The Boeing Aircraft Company developed the Environmental Systems Analysis (EASY) digital computer program. The program was originally developed to use in designing environmental control systems. It has since been extended to allow time and frequency domain analysis of aircraft systems.

The program is used to describing the system to be analyzed through the use of block diagrams and the associated interconnections. The program supplies generic block diagrams of the airframe and engine and the user supplies the aerodynamic data and the block diagrams representing the control system, pilot model, gunsight algorithm or any aircraft subsystem desired in the analysis. The F-106 was programmed using the same set of force and moment equations as used in the ASD Hybrid Simulation described in Appendix A.

The included listings show an example of the data required to generate the F-106 aircraft system model with both standard and  $\beta$ - $\dot{\beta}$  SAS. Also shown are the models resulting from the data and the data decks required to produce the Bode plots at .8 Mach and 10000 feet. Figures C-1 and C-2 contain the input data and resulting models for the  $\beta$ - $\dot{\beta}$  and standard SAS. Figures C-3 and C-4 contains the analysis data used to draw the Bode plots.

```

MODEL DESCRIPTION      FLTA GETA00T AND GETA SAS MODEL
ADD TABLES=CYA1,-53,CYB1,-53,CYMAA,-53,CYMAOF,-53
ADD TABLES=CL7,153,CL8,153,CL9,113,CL9A2,153,CL9D,153,CL9A,153,
CL9F,153,CLP,153,CLP42,153,CLP,153,CLRA,153,CNMF,153,CN0,153,CN0,153,
CN0,153,CN0A2,153,CN0,153,CN0A,153,CN0,113,CN0,153,CN0,153,CN0,153,
CN0A2,153,CN0,153,CN0A,153,CN0,153,CN0,153,CN0,153,CLJ,153,CL9E,153,
THP,153,CLPA,153,C01,327,C025,327,C05,327,C010,327,C015,327
ADD PARAMETERS=,XCS,YPCS,YCS,ZDEF,7CG,RPD
ADD VARIABLE=AX,AY,AZ,REFANOT
LOCATION=66      AV      INPUTS=60
LOCATION=76      FV      INPUTS=60(ALT=X),AV(MAC=X)
LOCATION=52      MA      INPUTS=FV(X=C1),LGTT,
LOCATION=2       FN      INPUTS=MA(V=THP)
FORTRAN STATEMENTS
C
C      COMPUTE ACCELERATIONS IN G'S
C
      G=32.2
      AX=50 1V/G
      AY=5V 1V/G
      AZ=5V 1V/G
C
C      COMPUTE LONGITUDINAL FORCE TERMS% FZ EN AND FX EN
C
C      INTERPOLATE TO FIND LIFT COEFFICIENTS
C
      CL0=TRLU2(MACAV,ALTS0,CLZ(9),CLZ(4),CLZ(34),1,1,-25,-5,25,5)
      CL0A=TRLU2(MACAV,ALTS0,CLA(9),CLA(4),CLA(34),1,1,-25,-5,25,5)
      CL0F=TRLU2(MACAV,ALTS0,CLF(9),CLF(4),CLF(34),1,1,-25,-5,25,5)
C
C      COMPUTE LIFT, DRAG COEFFICIENTS AND BODY AXIS FORCES
C
      ELEV= (C LA *PPH)
      ALPHA= AL AM*PPH
      CL= CL0 + CL0A*ALPHA + CL0F*ELEV
C
C      LINEAR INTERPOLATION OF DRAG BETWEEN ELEVATOR SETTINGS
C
      DE=X2 LA E
      IF (DE.GT.2.5) GO TO 19
      DEL=1.
      DEL=1.5
      CL=TRLU2(CL1,MACAV,C05(16),C05(4),C05(40),1,1,24,12,24,12)
      CLU=TRLU2(CL1,MACAV,C025(16),C025(4),C025(40),1,1,24,12,24,12)
      GO TO 40
19  IF (DE.GT.5.) GO TO 29
      DEL=2.5
      DEL=3.
      CL=TRLU2(CL1,MACAV,C05(16),C05(4),C05(40),1,1,24,12,24,12)
      CLU=TRLU2(CL1,MACAV,C025(16),C025(4),C025(40),1,1,24,12,24,12)
      GO TO 40
29  IF (DE.GT.10) GO TO 39
      DEL=5.
      DEL=7.
      CL=TRLU2(CL1,MACAV,C05(16),C05(4),C05(40),1,1,24,12,24,12)
      CLU=TRLU2(CL1,MACAV,C025(16),C025(4),C025(40),1,1,24,12,24,12)
      GO TO 40
39  DEL=11.
      DEL=12.
      CL=TRLU2(CL1,MACAV,C05(16),C05(4),C05(40),1,1,24,12,24,12)
      CLU=TRLU2(CL1,MACAV,C025(16),C025(4),C025(40),1,1,24,12,24,12)
      GO TO 40
40  FTO=TRLU2(C001-C002-C003-C004-C005-C006-C007-C008-C009-C010-C011-C012-C013-C014-C015-C016-C017-C018-C019-C020-C021-C022-C023-C024-C025-C026-C027-C028-C029-C030-C031-C032-C033-C034-C035-C036-C037-C038-C039-C040-C041-C042-C043-C044-C045-C046-C047-C048-C049-C050-C051-C052-C053-C054-C055-C056-C057-C058-C059-C060-C061-C062-C063-C064-C065-C066-C067-C068-C069-C070-C071-C072-C073-C074-C075-C076-C077-C078-C079-C080-C081-C082-C083-C084-C085-C086-C087-C088-C089-C090-C091-C092-C093-C094-C095-C096-C097-C098-C099-C100-C101-C102-C103-C104-C105-C106-C107-C108-C109-C110-C111-C112-C113-C114-C115-C116-C117-C118-C119-C120-C121-C122-C123-C124-C125-C126-C127-C128-C129-C130-C131-C132-C133-C134-C135-C136-C137-C138-C139-C140-C141-C142-C143-C144-C145-C146-C147-C148-C149-C150-C151-C152-C153-C154-C155-C156-C157-C158-C159-C160-C161-C162-C163-C164-C165-C166-C167-C168-C169-C170-C171-C172-C173-C174-C175-C176-C177-C178-C179-C180-C181-C182-C183-C184-C185-C186-C187-C188-C189-C190-C191-C192-C193-C194-C195-C196-C197-C198-C199-C200-C201-C202-C203-C204-C205-C206-C207-C208-C209-C210-C211-C212-C213-C214-C215-C216-C217-C218-C219-C220-C221-C222-C223-C224-C225-C226-C227-C228-C229-C230-C231-C232-C233-C234-C235-C236-C237-C238-C239-C240-C241-C242-C243-C244-C245-C246-C247-C248-C249-C250-C251-C252-C253-C254-C255-C256-C257-C258-C259-C260-C261-C262-C263-C264-C265-C266-C267-C268-C269-C270-C271-C272-C273-C274-C275-C276-C277-C278-C279-C280-C281-C282-C283-C284-C285-C286-C287-C288-C289-C290-C291-C292-C293-C294-C295-C296-C297-C298-C299-C300-C301-C302-C303-C304-C305-C306-C307-C308-C309-C310-C311-C312-C313-C314-C315-C316-C317-C318-C319-C320-C321-C322-C323-C324-C325-C326-C327-C328-C329-C330-C331-C332-C333-C334-C335-C336-C337-C338-C339-C340-C341-C342-C343-C344-C345-C346-C347-C348-C349-C350-C351-C352-C353-C354-C355-C356-C357-C358-C359-C360-C361-C362-C363-C364-C365-C366-C367-C368-C369-C370-C371-C372-C373-C374-C375-C376-C377-C378-C379-C380-C381-C382-C383-C384-C385-C386-C387-C388-C389-C390-C391-C392-C393-C394-C395-C396-C397-C398-C399-C400-C401-C402-C403-C404-C405-C406-C407-C408-C409-C410-C411-C412-C413-C414-C415-C416-C417-C418-C419-C420-C421-C422-C423-C424-C425-C426-C427-C428-C429-C430-C431-C432-C433-C434-C435-C436-C437-C438-C439-C440-C441-C442-C443-C444-C445-C446-C447-C448-C449-C450-C451-C452-C453-C454-C455-C456-C457-C458-C459-C460-C461-C462-C463-C464-C465-C466-C467-C468-C469-C470-C471-C472-C473-C474-C475-C476-C477-C478-C479-C480-C481-C482-C483-C484-C485-C486-C487-C488-C489-C490-C491-C492-C493-C494-C495-C496-C497-C498-C499-C500-C501-C502-C503-C504-C505-C506-C507-C508-C509-C510-C511-C512-C513-C514-C515-C516-C517-C518-C519-C520-C521-C522-C523-C524-C525-C526-C527-C528-C529-C530-C531-C532-C533-C534-C535-C536-C537-C538-C539-C540-C541-C542-C543-C544-C545-C546-C547-C548-C549-C550-C551-C552-C553-C554-C555-C556-C557-C558-C559-C560-C561-C562-C563-C564-C565-C566-C567-C568-C569-C570-C571-C572-C573-C574-C575-C576-C577-C578-C579-C580-C581-C582-C583-C584-C585-C586-C587-C588-C589-C590-C591-C592-C593-C594-C595-C596-C597-C598-C599-C600-C601-C602-C603-C604-C605-C606-C607-C608-C609-C610-C611-C612-C613-C614-C615-C616-C617-C618-C619-C620-C621-C622-C623-C624-C625-C626-C627-C628-C629-C630-C631-C632-C633-C634-C635-C636-C637-C638-C639-C640-C641-C642-C643-C644-C645-C646-C647-C648-C649-C650-C651-C652-C653-C654-C655-C656-C657-C658-C659-C660-C661-C662-C663-C664-C665-C666-C667-C668-C669-C670-C671-C672-C673-C674-C675-C676-C677-C678-C679-C680-C681-C682-C683-C684-C685-C686-C687-C688-C689-C690-C691-C692-C693-C694-C695-C696-C697-C698-C699-C700-C701-C702-C703-C704-C705-C706-C707-C708-C709-C710-C711-C712-C713-C714-C715-C716-C717-C718-C719-C720-C721-C722-C723-C724-C725-C726-C727-C728-C729-C730-C731-C732-C733-C734-C735-C736-C737-C738-C739-C740-C741-C742-C743-C744-C745-C746-C747-C748-C749-C750-C751-C752-C753-C754-C755-C756-C757-C758-C759-C760-C761-C762-C763-C764-C765-C766-C767-C768-C769-C770-C771-C772-C773-C774-C775-C776-C777-C778-C779-C780-C781-C782-C783-C784-C785-C786-C787-C788-C789-C790-C791-C792-C793-C794-C795-C796-C797-C798-C799-C800-C801-C802-C803-C804-C805-C806-C807-C808-C809-C810-C811-C812-C813-C814-C815-C816-C817-C818-C819-C820-C821-C822-C823-C824-C825-C826-C827-C828-C829-C830-C831-C832-C833-C834-C835-C836-C837-C838-C839-C840-C841-C842-C843-C844-C845-C846-C847-C848-C849-C850-C851-C852-C853-C854-C855-C856-C857-C858-C859-C860-C861-C862-C863-C864-C865-C866-C867-C868-C869-C870-C871-C872-C873-C874-C875-C876-C877-C878-C879-C880-C881-C882-C883-C884-C885-C886-C887-C888-C889-C890-C891-C892-C893-C894-C895-C896-C897-C898-C899-C900-C901-C902-C903-C904-C905-C906-C907-C908-C909-C910-C911-C912-C913-C914-C915-C916-C917-C918-C919-C920-C921-C922-C923-C924-C925-C926-C927-C928-C929-C930-C931-C932-C933-C934-C935-C936-C937-C938-C939-C940-C941-C942-C943-C944-C945-C946-C947-C948-C949-C950-C951-C952-C953-C954-C955-C956-C957-C958-C959-C960-C961-C962-C963-C964-C965-C966-C967-C968-C969-C970-C971-C972-C973-C974-C975-C976-C977-C978-C979-C980-C981-C982-C983-C984-C985-C986-C987-C988-C989-C990-C991-C992-C993-C994-C995-C996-C997-C998-C999
      CALP= C03 (ALPHA)
      SALP= SINT(CALP)
      FZCAY= FZ CN

```

Figure C-1. EASY Model Generation Data and Resulting Model for B-B SAS

[illegible]

Figure C-1. (Cont'd)

[illegible]

**Figure C-1. (Cont'd)**

**Figure C-1. (Cont'd)**

PAPA DETASONT AND META SAS MODEL										PAGE 1
101	102	103	104	105	106	107	108	109	110	111
112	113	114	115	116	117	118	119	120	121	122
123	124	125	126	127	128	129	130	131	132	133
134	135	136	137	138	139	140	141	142	143	144
145	146	147	148	149	150	151	152	153	154	155
156	157	158	159	160	161	162	163	164	165	166
167	168	169	170	171	172	173	174	175	176	177
178	179	180	181	182	183	184	185	186	187	188
189	190	191	192	193	194	195	196	197	198	199
200	201	202	203	204	205	206	207	208	209	210
211	212	213	214	215	216	217	218	219	220	221
222	223	224	225	226	227	228	229	230	231	232
233	234	235	236	237	238	239	240	241	242	243
244	245	246	247	248	249	250	251	252	253	254
255	256	257	258	259	260	261	262	263	264	265
266	267	268	269	270	271	272	273	274	275	276
277	278	279	280	281	282	283	284	285	286	287
288	289	290	291	292	293	294	295	296	297	298
299	300	301	302	303	304	305	306	307	308	309
310	311	312	313	314	315	316	317	318	319	320
321	322	323	324	325	326	327	328	329	330	331
332	333	334	335	336	337	338	339	340	341	342
343	344	345	346	347	348	349	350	351	352	353
354	355	356	357	358	359	360	361	362	363	364
365	366	367	368	369	370	371	372	373	374	375
376	377	378	379	380	381	382	383	384	385	386
387	388	389	390	391	392	393	394	395	396	397
398	399	400	401	402	403	404	405	406	407	408
409	410	411	412	413	414	415	416	417	418	419
420	421	422	423	424	425	426	427	428	429	430
431	432	433	434	435	436	437	438	439	440	441
442	443	444	445	446	447	448	449	450	451	452
453	454	455	456	457	458	459	460	461	462	463
464	465	466	467	468	469	470	471	472	473	474
475	476	477	478	479	480	481	482	483	484	485
486	487	488	489	490	491	492	493	494	495	496
497	498	499	500	501	502	503	504	505	506	507
508	509	510	511	512	513	514	515	516	517	518
519	520	521	522	523	524	525	526	527	528	529
530	531	532	533	534	535	536	537	538	539	540
541	542	543	544	545	546	547	548	549	550	551
552	553	554	555	556	557	558	559	560	561	562
563	564	565	566	567	568	569	570	571	572	573
574	575	576	577	578	579	580	581	582	583	584
585	586	587	588	589	590	591	592	593	594	595
596	597	598	599	600	601	602	603	604	605	606
607	608	609	610	611	612	613	614	615	616	617
618	619	620	621	622	623	624	625	626	627	628
629	630	631	632	633	634	635	636	637	638	639
640	641	642	643	644	645	646	647	648	649	650
651	652	653	654	655	656	657	658	659	660	661
662	663	664	665	666	667	668	669	670	671	672
673	674	675	676	677	678	679	680	681	682	683
684	685	686	687	688	689	690	691	692	693	694
695	696	697	698	699	700	701	702	703	704	705
706	707	708	709	710	711	712	713	714	715	716
717	718	719	720	721	722	723	724	725	726	727
728	729	730	731	732	733	734	735	736	737	738
739	740	741	742	743	744	745	746	747	748	749
750	751	752	753	754	755	756	757	758	759	760
761	762	763	764	765	766	767	768	769	770	771
772	773	774	775	776	777	778	779	780	781	782
783	784	785	786	787	788	789	790	791	792	793
794	795	796	797	798	799	800	801	802	803	804
805	806	807	808	809	810	811	812	813	814	815
816	817	818	819	820	821	822	823	824	825	826
827	828	829	830	831	832	833	834	835	836	837
838	839	840	841	842	843	844	845	846	847	848
849	850	851	852	853	854	855	856	857	858	859
860	861	862	863	864	865	866	867	868	869	870
871	872	873	874	875	876	877	878	879	880	881
882	883	884	885	886	887	888	889	890	891	892
893	894	895	896	897	898	899	900	901	902	903
904	905	906	907	908	909	910	911	912	913	914
915	916	917	918	919	920	921	922	923	924	925
926	927	928	929	930	931	932	933	934	935	936
937	938	939	940	941	942	943	944	945	946	947
948	949	950	951	952	953	954	955	956	957	958
959	960	961	962	963	964	965	966	967	968	969
970	971	972	973	974	975	976	977	978	979	980
981	982	983	984	985	986	987	988	989	990	991
992	993	994	995	996	997	998	999	1000	1001	1002

Figure C-1. (Cont'd)

PICK DETACTANT AND META SAS MPM-L									
X2 MA A									
201	202	203	204	205	206	207	208	209	210
211	212	213	214	215	216	217	218	219	220
221	222	223	224	225	226	227	228	229	230
231	232	233	234	235	236	237	238	239	240
241	242	243	244	245	246	247	248	249	250
251	252	253	254	255	256	257	258	259	260
261	262	263	264	265	266	267	268	269	270
271	272	273	274	275	276	277	278	279	280

Figure C-1. (Cont'd)

FILE STADANT AND DATA SAS MODEL

301	302	303	304	305	306	307	308	309	310
311	312	313	314	315	316	317	318	319	320
321	322	323	324	325	326	327	328	329	330
331	332	333	334	335	336	337	338	339	340
341	342	343	344	345	346	347	348	349	350
351	352	353	354	355	356	357	358	359	360
361	362	363	364	365	366	367	368	369	370
371	372	373	374	375	376	377	378	379	380
381	382	383	384	385	386	387	388	389	390
391	392	393	394	395	396	397	398	399	400

Figure C-1. (Cont'd)



F10A DETADOT AND DATA SAS MODEL										PAGE 4
601	602	603	604	605	606	607	608	609	610	611
612	613	614	615	616	617	618	619	620	621	622
623	624	625	626	627	628	629	630	631	632	633
634	635	636	637	638	639	640	641	642	643	644
645	646	647	648	649	650	651	652	653	654	655
656	657	658	659	660	661	662	663	664	665	666
667	668	669	670	671	672	673	674	675	676	677
678	679	680	681	682	683	684	685	686	687	688
689	690	691	692	693	694	695	696	697	698	699
700	701	702	703	704	705	706	707	708	709	710

Figure C-1. (Concluded)

```

MODEL DESCRIPTION ----- F105 STANDARD SAS MODEL -----
ADD TABLES=CYBA,-53,CNCA,-53,CNCAA,-53,CNDACE,-53
ADD TABLES=CLZ,158,CLP,158,CLPA2,158,CLL,158,CLRA,158,CMD,158,CND,158,CMQ,158,
CLDR,158,CLP,158,CLPA2,158,CLL,158,CLRA,158,CMD,158,CND,158,CMQ,158,
GNB,158,GNBA2,158,GNB3,158,GNB4,158,GNB5,158,GNB6,158,GNB7,158,GNB8,158,
CYBA2,158,CYB3,158,CYBA,158,CYD,158,CYP,158,CYR,158,CL1,158,CLOE,158,
TNP,158,CLPA,158,GB0,327,GB25,327,GB5,327,GB10,327,GB15,327
ADD PARAMETERS=,XCG,YREF,TCG,ZREF,ZCG,RPD
*DO VARIABLE=AX,AY,AZ
LOCATION=N=56 AV INPTS=SQ
LOCATION=N=76 FV INPTS=SQ(ALT=X),A+(MAC=X)
LOCATION=N=52 MA INPTS=F,(X=C1),LGTT,
LOCATION=N=2 EN INPTS=MA(X=THR)
FORTRAN STATEMENTS
C
C COMPUTE ACCELERATIONS IN G'S
C
Z=32.2
IX=EU-AY/G
IY=EV-AY/G
IZ=EN-AY/G
CCCCCCCC
C COMPUTE LONGITUDINAL FORCE TERMS% FZ-EN AND FX-EN
CCCCCCCC
C INTERPOLATE TO FIND LIFT COEFFICIENTS
C
ZL= TBLU2(MACAV,ALTSD,CL(9),CL(4),Z-Z(4),1,1,-25,-5,25,5)
ZLAO= TBLU2(MACAV,ALTSD,CL(9),CL(4),ZLA(3),1,1,-25,-5,25,5)
ZLEO= TBLU2(MACAV,ALTSD,CL(9),CL(4),ZLE(3),1,1,-25,-5,25,5)
C
C COMPUTE LIFT, DRAG COEFFICIENTS AND BODY AXIS FORCES
C
ELEV= XZ LA E*RPD
ALPHA= AL-AY*RPD
CL1= CL0 + CLAO*ALPHA + CLEO*ELEV
C
C LINEAR INTERPOLATION OF DRAG BETWEEN ELEVATOR SETTINGS
C
DE=-XZ LA E
IF(DE.GT.2.5) GO TO 10
DEL=3.
DOE=.4
COL= TBLU2(CL1,MACAV,C03(16),C03(4),C03(40),1,1,24,12,24,12)
COU= TBLU2(CL1,MACAV,C025(16),C025(4),C025(40),1,1,24,12,24,12)
GO TO 40
10 IF(DE.GT.5.) GO TO 20
DEL=2.5
DOE=.4
COL= TBLU2(CL1,MACAV,C025(16),C025(4),C025(40),1,1,24,12,24,12)
COU= TBLU2(CL1,MACAV,C05(16),C05(4),C05(40),1,1,24,12,24,12)
GO TO 40
20 IF(DE.GT.10) GO TO 30
DEL=2.
DOE=.2
COL= TBLU2(CL1,MACAV,C05(16),C05(4),C05(40),1,1,24,12,24,12)
COU= TBLU2(CL1,MACAV,C010(16),C010(4),C010(40),1,1,24,12,24,12)
GO TO 40
30 DEL=1.
DOE=.2
COL= TBLU2(CL1,MACAV,C010(16),C010(4),C010(40),1,1,24,12,24,12)
COU= TBLU2(CL1,MACAV,C015(16),C015(4),C015(40),1,1,24,12,24,12)
GO TO 40
40 COU= COL + (COU - COL)*DOE*(DE - DEL)
200 *ALP= COS(ALPHA)
*ALP= SIN(ALPHA)

```

Figure C-2. EASY Model Generation Data and Resulting Model for Standard SAS

```

130000 14 EN
* XSA = FX EN
* Z EN = QS AV * (CL1 * SA.P + CJO * CALP) + FZ EN
* X EN = QS AV * (CL1 * SA.P - CJO * CALP) + FX EN
CCCCCG:CG
C      COMBINE LONGITUDINAL DYNAMICS IN "LO"
CCCCCG:CG
10 LO = TBLU2(MACAV, A.TSD, CM0(9), CM0(4), CM0(34), 1, 1, -25, -5, 25, 5)
11 LO = 2 * TBLU2(MACAV, A.TSD, CM2(9), CM2(4), CM2(34), 1, 1, -25, -5, 25, 5)
12 LO = 10 LO
13 LO = TBLU2(MACAV, A.TSD, CM3(9), CM3(4), CM3(34), 1, 1, -25, -5, 25, 5)
LOCATIONN=4 LO INPTS=AV, LA E(X=ELE), EN
FORTRAN STATEMENTS
CCCCCG:CG
C      ADJUST LONGITUDINAL MOMENTS FOR CG LOCATION
CCCCCG:CG
14 PO = TBLU2(MACAV, A.TSD, INP(9), INP(4), INP(34), 1, 1, -25, -5, 25, 5)
15 ZLO = TYZLO + (ZREF - ZCG) * (FXZLO - FXSAV) - (TNPO * C LO - XCG) *
      (FZLO - FZSAV)
CCCCCG:CG
C      COMPUTE LATERAL DIRECTIONAL NONLINEAR TERMS FY1LO, TX1LO, TZ1LO
CCCCCG:CG
C      INTERPOLATE TO FIND FY DERIVATIVES
C
16 Y3A20 = TBLU2(MACAV, A.TSD, CY3A2(9), CY3A2(4), CY3A2(34), 1, 1,
      -25, -5, 25, 5)
17 Y3A0 = TBLU2(MACAV, A.TSD, CY3A(9), CY3A(4), CY3A(34), 1, 1, -25, -5, 25, 5)
18 Y9B0 = TBLU2(MACAV, A.TSD, CY9B(9), CY9B(4), CY9B(34), 1, 1,
      -25, -5, 25, 5)
C
C      COMPUTE NONLINEAR Y FORCES
BETA = BE AV * RPD
FY1LO = QS AV * (BETA * (ALPHA *
1  (CY3A20 * ALP14 + CY3A0) + CY9B0 * AGS(BETA)))
C
C      INTERPOLATE TO FIND L=TX DERIVATIVES
19 L3A20 = TBLU2(MACAV, A.TSD, CL3A2(9), CL3A2(4), CL3A2(34), 1, 1,
      -25, -5, 25, 5)
20 L3A0 = TBLU2(MACAV, A.TSD, CL3A(9), CL3A(4), CL3A(34), 1, 1, -17, -5, 17, 5)
21 L3B0 = TBLU2(MACAV, A.TSD, CL3B(9), CL3B(4), CL3B(34), 1, 1, -25, -5, 25, 5)
22 L3A20 = TBLU2(MACAV, A.TSD, CL3A2(9), CL3A2(4), CL3A2(34), 1, 1,
      -25, -5, 25, 5)
23 L3A0 = TBLU2(MACAV, A.TSD, CL3A(9), CL3A(4), CL3A(34), 1, 1, -25, -5, 25, 5)
24 L3B0 = TBLU2(MACAV, A.TSD, CL3B(9), CL3B(4), CL3B(34), 1, 1, -25, -5, 25, 5)
C
C      COMPUTE NONLINEAR L=TX TORQUES
25 NOLIN = (CL3A20 * A3S(ALPHA) + CL3A0 * A3S(ALPHA) + CL3B0 * A3S(BETA))
      * BETA + (CL3A20 * ALPHA + CL3A0) * P SD + CL3B0 * R SU
26 NOLIN = QS AV * B LO * NOLIN
TX1LO = QS AV * B LO * NOLIN
C
C      INTERPOLATE TO FIND N=TZ DERIVATIVES
27 N3A20 = TBLU2(MACAV, A.TSD, CN3A2(9), CN3A2(4), CN3A2(34), 1, 1,
      -25, -5, 25, 5)
28 N3A0 = TBLU2(MACAV, A.TSD, CN3A(9), CN3A(4), CN3A(34), 1, 1, -25, -5, 25, 5)
29 N3B0 = TBLU2(MACAV, A.TSD, CN3B(9), CN3B(4), CN3B(34), 1, 1, -25, -5, 25, 5)
30 N3A20 = TBLU2(MACAV, A.TSD, CN3A2(9), CN3A2(4), CN3A2(34), 1, 1,
      -25, -5, 25, 5)
31 N3A0 = TBLU2(MACAV, A.TSD, CN3A(9), CN3A(4), CN3A(34), 1, 1, -25, -5, 25, 5)
32 N3B0 = TBLU2(MACAV, A.TSD, CN3B(9), CN3B(4), CN3B(34), 1, 1, -25, -5, 25, 5)
C
C      COMPUTE NONLINEAR N=TZ TORQUES
33 NOLIN = (CN3A20 * A3S(ALPHA) + CN3A0 * A3S(ALPHA) + CN3B0 * A3S(BETA))
      * BETA + (CN3A20 * ALPHA + CN3A0) * P SD + CN3B0 * R SU
34 NOLIN = QS AV * B LO * NOLIN
TZ1LO = QS AV * B LO * NOLIN
CCCCCG:CG
C      LOOK UP LATERAL DIRECTIONAL LINEAR COEFFICIENTS FOR CG
CCCCCG:CG

```

Figure C-2. (Cont'd)

120

FAUG STANDARD SAS MODEL									
EN	PC	RY	LO	LO	LO	LO	LO	LO	LO
1	1	1	1	1	1	1	1	1	1
2	2	2	2	2	2	2	2	2	2
3	3	3	3	3	3	3	3	3	3
4	4	4	4	4	4	4	4	4	4
5	5	5	5	5	5	5	5	5	5
6	6	6	6	6	6	6	6	6	6
7	7	7	7	7	7	7	7	7	7
8	8	8	8	8	8	8	8	8	8
9	9	9	9	9	9	9	9	9	9
10	10	10	10	10	10	10	10	10	10
11	11	11	11	11	11	11	11	11	11
12	12	12	12	12	12	12	12	12	12
13	13	13	13	13	13	13	13	13	13
14	14	14	14	14	14	14	14	14	14
15	15	15	15	15	15	15	15	15	15
16	16	16	16	16	16	16	16	16	16
17	17	17	17	17	17	17	17	17	17
18	18	18	18	18	18	18	18	18	18
19	19	19	19	19	19	19	19	19	19
20	20	20	20	20	20	20	20	20	20
21	21	21	21	21	21	21	21	21	21
22	22	22	22	22	22	22	22	22	22
23	23	23	23	23	23	23	23	23	23
24	24	24	24	24	24	24	24	24	24
25	25	25	25	25	25	25	25	25	25
26	26	26	26	26	26	26	26	26	26
27	27	27	27	27	27	27	27	27	27
28	28	28	28	28	28	28	28	28	28
29	29	29	29	29	29	29	29	29	29
30	30	30	30	30	30	30	30	30	30
31	31	31	31	31	31	31	31	31	31
32	32	32	32	32	32	32	32	32	32
33	33	33	33	33	33	33	33	33	33
34	34	34	34	34	34	34	34	34	34
35	35	35	35	35	35	35	35	35	35
36	36	36	36	36	36	36	36	36	36
37	37	37	37	37	37	37	37	37	37
38	38	38	38	38	38	38	38	38	38
39	39	39	39	39	39	39	39	39	39
40	40	40	40	40	40	40	40	40	40
41	41	41	41	41	41	41	41	41	41
42	42	42	42	42	42	42	42	42	42
43	43	43	43	43	43	43	43	43	43
44	44	44	44	44	44	44	44	44	44
45	45	45	45	45	45	45	45	45	45
46	46	46	46	46	46	46	46	46	46
47	47	47	47	47	47	47	47	47	47
48	48	48	48	48	48	48	48	48	48
49	49	49	49	49	49	49	49	49	49
50	50	50	50	50	50	50	50	50	50
51	51	51	51	51	51	51	51	51	51
52	52	52	52	52	52	52	52	52	52
53	53	53	53	53	53	53	53	53	53
54	54	54	54	54	54	54	54	54	54
55	55	55	55	55	55	55	55	55	55
56	56	56	56	56	56	56	56	56	56
57	57	57	57	57	57	57	57	57	57
58	58	58	58	58	58	58	58	58	58
59	59	59	59	59	59	59	59	59	59
60	60	60	60	60	60	60	60	60	60
61	61	61	61	61	61	61	61	61	61
62	62	62	62	62	62	62	62	62	62
63	63	63	63	63	63	63	63	63	63
64	64	64	64	64	64	64	64	64	64
65	65	65	65	65	65	65	65	65	65
66	66	66	66	66	66	66	66	66	66
67	67	67	67	67	67	67	67	67	67
68	68	68	68	68	68	68	68	68	68
69	69	69	69	69	69	69	69	69	69
70	70	70	70	70	70	70	70	70	70
71	71	71	71	71	71	71	71	71	71
72	72	72	72	72	72	72	72	72	72
73	73	73	73	73	73	73	73	73	73
74	74	74	74	74	74	74	74	74	74
75	75	75	75	75	75	75	75	75	75
76	76	76	76	76	76	76	76	76	76
77	77	77	77	77	77	77	77	77	77
78	78	78	78	78	78	78	78	78	78
79	79	79	79	79	79	79	79	79	79
80	80	80	80	80	80	80	80	80	80

Figure C-2. (Cont'd)

F200 STANDARD SAS MODEL										PAGE 1
101	102	103	104	105	106	107	108	109	110	111
111	112	113	114	115	116	117	118	119	120	121
122	123	124	125	126	127	128	129	130	131	132
133	134	135	136	137	138	139	140	141	142	143
144	145	146	147	148	149	150	151	152	153	154
155	156	157	158	159	160	161	162	163	164	165
166	167	168	169	170	171	172	173	174	175	176
177	178	179	180	181	182	183	184	185	186	187
188	189	190	191	192	193	194	195	196	197	198
199	200	201	202	203	204	205	206	207	208	209
210	211	212	213	214	215	216	217	218	219	220
221	222	223	224	225	226	227	228	229	230	231
232	233	234	235	236	237	238	239	240	241	242
243	244	245	246	247	248	249	250	251	252	253
254	255	256	257	258	259	260	261	262	263	264
265	266	267	268	269	270	271	272	273	274	275
276	277	278	279	280	281	282	283	284	285	286
287	288	289	290	291	292	293	294	295	296	297
298	299	300	301	302	303	304	305	306	307	308
309	310	311	312	313	314	315	316	317	318	319
320	321	322	323	324	325	326	327	328	329	330
331	332	333	334	335	336	337	338	339	340	341
342	343	344	345	346	347	348	349	350	351	352
353	354	355	356	357	358	359	360	361	362	363
364	365	366	367	368	369	370	371	372	373	374
375	376	377	378	379	380	381	382	383	384	385
386	387	388	389	390	391	392	393	394	395	396
397	398	399	400	401	402	403	404	405	406	407
408	409	410	411	412	413	414	415	416	417	418
419	420	421	422	423	424	425	426	427	428	429
430	431	432	433	434	435	436	437	438	439	440
441	442	443	444	445	446	447	448	449	450	451
452	453	454	455	456	457	458	459	460	461	462
463	464	465	466	467	468	469	470	471	472	473
474	475	476	477	478	479	480	481	482	483	484
485	486	487	488	489	490	491	492	493	494	495
496	497	498	499	500	501	502	503	504	505	506
507	508	509	510	511	512	513	514	515	516	517
518	519	520	521	522	523	524	525	526	527	528
529	530	531	532	533	534	535	536	537	538	539
540	541	542	543	544	545	546	547	548	549	550
551	552	553	554	555	556	557	558	559	560	561
562	563	564	565	566	567	568	569	570	571	572
573	574	575	576	577	578	579	580	581	582	583
584	585	586	587	588	589	590	591	592	593	594
595	596	597	598	599	600	601	602	603	604	605
606	607	608	609	610	611	612	613	614	615	616
617	618	619	620	621	622	623	624	625	626	627
628	629	630	631	632	633	634	635	636	637	638
639	640	641	642	643	644	645	646	647	648	649
650	651	652	653	654	655	656	657	658	659	660
661	662	663	664	665	666	667	668	669	670	671
672	673	674	675	676	677	678	679	680	681	682
683	684	685	686	687	688	689	690	691	692	693
694	695	696	697	698	699	700	701	702	703	704
705	706	707	708	709	710	711	712	713	714	715
716	717	718	719	720	721	722	723	724	725	726
727	728	729	730	731	732	733	734	735	736	737
738	739	740	741	742	743	744	745	746	747	748
749	750	751	752	753	754	755	756	757	758	759
760	761	762	763	764	765	766	767	768	769	770
771	772	773	774	775	776	777	778	779	780	781
782	783	784	785	786	787	788	789	790	791	792
793	794	795	796	797	798	799	800	801	802	803
804	805	806	807	808	809	810	811	812	813	814
815	816	817	818	819	820	821	822	823	824	825
826	827	828	829	830	831	832	833	834	835	836
837	838	839	840	841	842	843	844	845	846	847
848	849	850	851	852	853	854	855	856	857	858
859	860	861	862	863	864	865	866	867	868	869
870	871	872	873	874	875	876	877	878	879	880
881	882	883	884	885	886	887	888	889	890	891
892	893	894	895	896	897	898	899	900	901	902
903	904	905	906	907	908	909	910	911	912	913
914	915	916	917	918	919	920	921	922	923	924
925	926	927	928	929	930	931	932	933	934	935
936	937	938	939	940	941	942	943	944	945	946
947	948	949	950	951	952	953	954	955	956	957
958	959	960	961	962	963	964	965	966	967	968
969	970	971	972	973	974	975	976	977	978	979
980	981	982	983	984	985	986	987	988	989	990
991	992	993	994	995	996	997	998	999	1000	1001

Figure C-2. (Cont'd)

FILE STANDARD SAS MODEL									
101	207	MA A	12 MA A	LA A	208	209	210	211	212
*****									
*****									
111	213	214	215	216	217	218	219	220	221
*****									
*****									
121	227	228	229	230	231	232	233	234	235
*****									
*****									
131	243	244	245	246	247	248	249	250	251
*****									
*****									
141	263	264	265	266	267	268	269	270	271
*****									
*****									
151	283	284	285	286	287	288	289	290	291
*****									
*****									
161	303	304	305	306	307	308	309	310	311
*****									
*****									
171	323	324	325	326	327	328	329	330	331
*****									
*****									

Figure C-2. (Cont'd)

Page 3

STANDARD SAS MODEL

194	302	303	304	305	306	307	308	309	310
111	317	318	319	320	321	322	323	324	325
112	326	327	328	329	330	331	332	333	334
113	335	336	337	338	339	340	341	342	343
114	344	345	346	347	348	349	350	351	352
115	353	354	355	356	357	358	359	360	361
116	362	363	364	365	366	367	368	369	370
117	371	372	373	374	375	376	377	378	379
118	380	381	382	383	384	385	386	387	388
119	389	390	391	392	393	394	395	396	397
120	398	399	400	401	402	403	404	405	406
121	407	408	409	410	411	412	413	414	415
122	416	417	418	419	420	421	422	423	424
123	425	426	427	428	429	430	431	432	433
124	434	435	436	437	438	439	440	441	442
125	443	444	445	446	447	448	449	450	451
126	452	453	454	455	456	457	458	459	460
127	461	462	463	464	465	466	467	468	469
128	470	471	472	473	474	475	476	477	478
129	479	480	481	482	483	484	485	486	487
130	488	489	490	491	492	493	494	495	496
131	497	498	499	500	501	502	503	504	505
132	506	507	508	509	510	511	512	513	514
133	515	516	517	518	519	520	521	522	523
134	524	525	526	527	528	529	530	531	532
135	533	534	535	536	537	538	539	540	541
136	542	543	544	545	546	547	548	549	550
137	551	552	553	554	555	556	557	558	559
138	560	561	562	563	564	565	566	567	568
139	569	570	571	572	573	574	575	576	577
140	578	579	580	581	582	583	584	585	586
141	587	588	589	590	591	592	593	594	595
142	596	597	598	599	600	601	602	603	604
143	605	606	607	608	609	610	611	612	613
144	614	615	616	617	618	619	620	621	622
145	623	624	625	626	627	628	629	630	631
146	632	633	634	635	636	637	638	639	640
147	641	642	643	644	645	646	647	648	649
148	650	651	652	653	654	655	656	657	658
149	659	660	661	662	663	664	665	666	667
150	668	669	670	671	672	673	674	675	676
151	677	678	679	680	681	682	683	684	685
152	686	687	688	689	690	691	692	693	694
153	695	696	697	698	699	700	701	702	703
154	704	705	706	707	708	709	710	711	712
155	713	714	715	716	717	718	719	720	721
156	722	723	724	725	726	727	728	729	730
157	731	732	733	734	735	736	737	738	739
158	740	741	742	743	744	745	746	747	748
159	749	750	751	752	753	754	755	756	757
160	758	759	760	761	762	763	764	765	766
161	767	768	769	770	771	772	773	774	775
162	776	777	778	779	780	781	782	783	784
163	785	786	787	788	789	790	791	792	793
164	794	795	796	797	798	799	800	801	802
165	803	804	805	806	807	808	809	810	811
166	812	813	814	815	816	817	818	819	820
167	821	822	823	824	825	826	827	828	829
168	830	831	832	833	834	835	836	837	838
169	839	840	841	842	843	844	845	846	847
170	848	849	850	851	852	853	854	855	856
171	857	858	859	860	861	862	863	864	865
172	866	867	868	869	870	871	872	873	874
173	875	876	877	878	879	880	881	882	883
174	884	885	886	887	888	889	890	891	892
175	893	894	895	896	897	898	899	900	901
176	902	903	904	905	906	907	908	909	910
177	911	912	913	914	915	916	917	918	919
178	920	921	922	923	924	925	926	927	928
179	929	930	931	932	933	934	935	936	937
180	938	939	940	941	942	943	944	945	946
181	947	948	949	950	951	952	953	954	955
182	956	957	958	959	960	961	962	963	964
183	965	966	967	968	969	970	971	972	973
184	974	975	976	977	978	979	980	981	982
185	983	984	985	986	987	988	989	990	991
186	992	993	994	995	996	997	998	999	1000

Figure C-2. (Cont'd)



```

.400, .400, .500, .500, .600, .600, .700, .700, .800, .800
.650, .475, .920, .920, .950, .975, 1.000, 1.025, 1.050, 1.075
1.100, 1.125, 1.150, 1.175, 1.200,
.00157800, .00167600, .00163960, .00167600, .00172000
.00178200, .00184120, .00189700, .00195000, .00200100
.00206000, .00211700, .00217200, .00223000, .00229000
.00235000, .00241000, .00247000, .00253000, .00259000
.00265000, .00271000, .00277000, .00283000, .00289000
TITLE=F126-NONLINEAR-8-ONE-POINT ANALYSIS
PARAMETER VALUES
Q=1.13, Q=23.755, S=6.95
TCOFN=1, GAXEN=0, GAXEN=1, XC EN=-11.8, ZC EN=0.
XREF=0.72000, Y00=0.72000, Y00=0.72000, PU=0.174532
IQ1AV=1, ALSAV=0.
AN FUD=1, AN FUD=1, ZC LE=0
C1 SA Q=1, C2 SA Q=1, E=6, C3 SA Q=1, C4 SA Q=1, C5 SA Q=1, E=6,
GAILA Q=1, GAILA Q=1, GAILA Q=1, GAILA Q=1, GAILA Q=1
C1 MC P=1, C2 MC P=1, C3 MC P=1, C4 MC P=1, C5 MC P=1
C1 SA E=1, C2 SA E=1, E=6, C3 SA E=1, C4 SA E=1, C5 SA E=1, E=6
C4 SA E=1, C5 SA E=1, E=6, C6 SA E=-25
GAILA E=1, GAILA E=1, GAILA E=1, GAILA E=1, GAILA E=1
PARAMETER VALUES
AN FV=1, AN FV=1, AN FV=1, AN FV=1, AN FV=1
C2 MA A=0, GAILA A=1, GAILA A=1, GAILA A=1, GAILA A=1
GATE R=1, GATE R=1, GATE R=1, GATE R=1, GATE R=1
C1 MC P=1, C2 MC P=1, C3 MC P=1, C4 MC P=1, C5 MC P=1
GAILA R=1, GAILA R=1, GAILA R=1, GAILA R=1, GAILA R=1
C1 MAIT=-1, C2 MAIT=-1, C3 MAIT=-1, C4 MAIT=-1, C5 MAIT=-1
C1 MAIT=-1, C2 MAIT=-1, C3 MAIT=-1, C4 MAIT=-1, C5 MAIT=-1
TABLE, F126, A=11
0.50, 1.00, 1.50, 2.00, 2.50, 3.00, 3.50, 4.00, 4.50, 5.00
1.3, 3.1, 2.6, 1.8, 1.2, 0.7, 1.1, 1.25, 1.5, 1.5
TABLE, F126, P=11
0.50, 1.00, 1.50, 2.00, 2.50, 3.00, 3.50, 4.00, 4.50, 5.00
1.3, 3.1, 2.6, 1.8, 1.2, 0.7, 1.1, 1.25, 1.5, 1.5
TABLE, F126, Q=4
0.50, 1.00, 1.50, 2.00, 2.50, 3.00, 3.50, 4.00, 4.50, 5.00
1.3, 3.1, 2.6, 1.8, 1.2, 0.7, 1.1, 1.25, 1.5, 1.5
TABLE, F126, R=4
0.50, 1.00, 1.50, 2.00, 2.50, 3.00, 3.50, 4.00, 4.50, 5.00
1.3, 3.1, 2.6, 1.8, 1.2, 0.7, 1.1, 1.25, 1.5, 1.5
PARAMETER VALUES
GAILA Q=1, GAXEN=0, GAXEN=1, XC EN=-11.8, ZC EN=0.
X00=-6.34, VS AV=697.
C2 MAIT=-1, C3 MAIT=-1, C4 MAIT=-1, C5 MAIT=-1
INITIAL CONDITIONS
ALTSQ=0.0001, POLSQ=0.00, SO=500.
INT CONTROL=Y4450=0.
TITLE=F126-CASEAL-DYNAMICS-FOR-M=0-AT-10K-FT
PRINT CONTROL=3
STEADY STATE
XIC-X
NO-STATE
INT CONTROL=2 SO=1.0 SO=1.0 SO=1.0 SO=1.0 SO=1.0 SO=1.0
GAILA Q=0, GAXEN=0, GAILA A=0, GAILA R=0, GAILA E=0, GAXEN=0
INT CONTROL=1
INT CONTROL=2
INT CONTROL=3
INT CONTROL=X1 LE 2=1, X2 LA Q=1, X2 LA E=1
PARAMETER VALUES GAILA A=1
INT CONTROL=X2 LA A=1
PARAMETER VALUES GAILA A=1
INT CONTROL=X1 LE 2=1, X1 LE 2=1, X2 LA R=1
PARAMETER VALUES GAILA R=1
INT CONTROL=ALTSQ=1

```

Figure C-3. EASY  $\beta$ - $\beta$  SAS Analysis Data

```

PARAMETER VALUES=GAILEN=1
INT CONTROL=X2 LA B=1,XI LEBU=1,X2 LA R=1
PARAMETER VALUES=GAILEN=1,GAILEBO=1,GAILE R=1
INT CONTROL=ALTSO=1
INT CONTROL=TH EN=1
PARAMETER VALUES=GAXEN=1
PLOT OF
TITLE=JETA00T SAS BETA/DELTA RUDDER .8,10000
TF INPUT=X2 LA R,TF OUTPUT=BE A/
FREQ MIN=.01,FREQ MAX=100.
TRANSFER FUNCTION
TITLE=JETA00T SAS PHI/DELTA RUDDER .8,10000
TF INPUT=X2 LA R,TF OUTPUT=ROCSO
FREQ MIN=.01,FREQ MAX=100.
TRANSFER FUNCTION
TITLE=JETA00T SAS BETA/DELTA AILERON .8,10000
TF INPUT=X2 LA A,TF OUTPUT=BE A/
FREQ MIN=.01,FREQ MAX=100.
TRANSFER FUNCTION

```

Figure C-3. (Concluded)

127

```

INI CONTINUE IN C=1
PARAMETER VALUES=TAKE=1
PL07-07
TITLE=STANDARD SAS BETA/DELTA RUDDER .6,30000
IF INPUT=12 LA 0,IF OUTPUT=1E AV
FREQ MIN=.01,FREQ MAX=100.
TRANSFER FUNCTION
TITLE=STANDARD SAS PHI/DELTA RUDDER .6,30000
IF INPUT=12 LA 0,IF OUTPUT=1E AV
FREQ MIN=.01,FREQ MAX=100.
TRANSFER FUNCTION
TITLE=STANDARD SAS BETA/DELTA AILERON .6,30000
IF INPUT=12 LA 0,IF OUTPUT=1E AV
FREQ MIN=.01,FREQ MAX=100.
TRANSFER FUNCTION

```

Figure C-4. (Concluded)

## APPENDIX D

## DERIVATION OF SIDESLIP RATE

The  $\beta$ - $\dot{\beta}$  system uses as feedbacks both sideslip ( $\beta$ ) and sideslip rate ( $\dot{\beta}$ ). Sideslip can be measured with a vane attached to the aircraft. Sideslip rate, on the other hand, cannot be measured directly. The  $\beta$  signal is too noisy to differentiate, so  $\dot{\beta}$  must come from some other source. The solution to this problem begins with the definition of  $\beta$ .

$$\beta = \arcsin v/U \quad (D-1)$$

$v$  and  $U$  are the side and total velocity of the aircraft in body axis coordinates differentiating with respect to time.

$$\dot{\beta} = \frac{U\dot{v} - v\dot{U}}{U^2 + v^2} \quad (D-2)$$

The terms in D-2 are normalized using total velocity,  $U$ .

$$\dot{\beta} = \frac{\frac{U}{U} \frac{\dot{v}}{U} - \frac{v}{U} \frac{\dot{U}}{U}}{\frac{U^2}{U^2} + \frac{v^2}{U^2}} \quad (D-3)$$

An order of magnitude analysis is performed on Equation D-3 using the assumptions below.

$$\frac{\dot{v}}{U} \ll 1$$

$$\frac{v}{U} \ll 1$$

$$\frac{\dot{U}}{U} \ll 1$$

Using these assumptions,  $\dot{\beta}$  is reduced to D-4.

$$\dot{\beta} = \frac{\dot{v}}{U} \quad (D-4)$$

The  $\dot{\bar{v}}$  term in Equation D-4 is the side acceleration as seen by an observer in the body coordinate frame. This term cannot be measured; it must be synthesized from aircraft states which can be measured by sensors onboard the aircraft.

The total rate of change of the velocity in the inertial frame must be derived in order to get  $\dot{\bar{v}}$  in terms of measurable variables.

$$\dot{\bar{v}}_I = \dot{\bar{v}}_b + \bar{\omega} \times \bar{v}_b \quad (D-5)$$

$$\dot{\bar{v}}_I = \begin{bmatrix} \dot{u} \\ \dot{v} \\ \dot{w} \end{bmatrix}_I \quad \text{the inertial acceleration vector in body axis coordinates}$$

$$\dot{\bar{v}}_b = \begin{bmatrix} \dot{u} \\ \dot{v} \\ \dot{w} \end{bmatrix}_b \quad \text{the acceleration vector observed in the body frame in body axis coordinates}$$

$$\bar{\omega} = \begin{bmatrix} p \\ q \\ r \end{bmatrix} \quad \text{the body angular rate vector in body axis coordinates}$$

$$\bar{v}_b = \begin{bmatrix} u \\ v \\ w \end{bmatrix}_b \quad \text{the body velocity vector in body axis coordinates}$$

The y-coordinate scalar equation resulting from Equation D-5 is shown below.

$$\dot{\bar{v}}_I = \dot{\bar{v}} - pw + ur \quad (D-6)$$

The inertial side acceleration  $\dot{v}_I$  is a measurable quantity consisting of lateral accelerometer output,  $A_y)_{acc}$ , summed with the gravitational component in the y-direction.

$$\dot{v}_I = A_y)_{acc} + g \cos\theta \sin\phi \quad (D-7)$$

Using Equation D-6 and Equation D-7,  $\dot{v}$  is shown below.

$$\dot{v} = pw - ur + A_y)_{acc} + g \cos\theta \sin\phi \quad (D-8)$$

Dividing by V.

$$\frac{\dot{v}}{V} = \frac{pw}{V} - \frac{ur}{V} + \frac{A_y)_{acc}}{V} + \frac{g}{V} \cos\theta \sin\phi \quad (D-9)$$

Equation D-9 is further simplified by assuming  $\frac{w}{V}$  equal to angle of attack and  $\frac{u}{V}$  equal to one.

$$\frac{\dot{v}}{V} = p\alpha - r + \frac{A_y)_{acc}}{V} + \frac{g}{V} \cos\theta \sin\phi \quad (D-10)$$

Substituting, using Equation D-4,

$$\dot{\beta} = p\alpha - r + \frac{A_y)_{acc}}{V} + \frac{g}{V} \cos\theta \sin\phi \quad (D-11)$$

Equation D-11 represents a synthesis of sideslip rate based on measurable variables.

## APPENDIX E

## ANALYSIS OF VARIANCE OF TRACKING DATA

A three-way analysis of variance was conducted on azimuth error, elevation error, and total error. The three error sources considered were pilot, flight condition, and SAS. Since no replications were available, the error source interactions were not examined. The analysis is based on the method described by Miller and Freund.

The model used for the analysis is shown below.

$$Y_{ijk} = \mu + \alpha_i + \beta_j + \gamma_k + \epsilon_{ijk}$$

$$\alpha_i = \text{Effect due to } i^{\text{th}} \text{ pilot} \quad i = 1, 2$$

$$\beta_j = \text{Effect due to } j^{\text{th}} \text{ SAS} \quad j = 1, 2, 3$$

$$\gamma_k = \text{Effect due to } k^{\text{th}} \text{ flight condition} \quad k = 1, 2, 3$$

$$\epsilon_{ijk} = \text{Effect due to interactions and error}$$

$$SSTO = \sum_{ijk} Y_{ijk}^2 - C$$

$$SS(\text{Pilot}) = \frac{(\sum Y_{\text{pilot } 1})^2 + (\sum Y_{\text{pilot } 2})^2}{N_{\text{pilot}}} - C$$

$$SS(\text{SAS}) = \frac{(\sum Y_{\text{SAS1}})^2 + (\sum Y_{\text{SAS2}})^2 + (\sum Y_{\text{SAS3}})^2}{N_{\text{SAS}}} - C$$

$$SS(\text{FC}) = \frac{(\sum Y_{\text{FC1}})^2 + (\sum Y_{\text{FC2}})^2 + (\sum Y_{\text{FC3}})^2}{N_{\text{FL}}} - C$$

$$C = \frac{(\sum Y)^2}{N_{\text{total}}}$$



TABLE E-1  
AZIMUTH ERROR ANOVA

Source	SS	DOF	MS	F	Level of Significance
Pilot	26.68	1	26.68	7.8	.0163
Flt Cond	188.6	2	94.3	27.6	.00003
SAS	39.66	2	19.83	5.8	.0173
Error	41.02	12	3.42		
Total	296	17			

TABLE E-2  
ELEVATION ERROR ANOVA

Source	SS	DOF	MS	F	Level of Significance
Pilot	8.76	1	8.76	7.18	.0201
Flt Cond	157.6	2	78.8	64.55	.00001
SAS	10.08	2	5.01	4.1	.044
Error	14.65	12	1.22		
Total	191.09	17			

TABLE E-3  
TOTAL ERROR ANOVA

Source	SS	DOF	MS	F	Level of Significance
Pilot	33.49	1	33.49	10.97	.0053
Flt Cond	317.28	2	158.6	52	.00001
SAS	38.45	2	19.23	6.3	.0135
Error	36.65	12	3.05		
Total	425.87	17			

APPENDIX F

ASSEMBLY LISTING OF FLIGHT TEST OPERATIONAL FLIGHT PROGRAM

This appendix contains an assembled listing of the IRAM computer program used to perform the SAS calculations and the built-in test. The Hughes-built IRAM (improved reliability and maintainability) computer is a fixed-point, two's complement airborne digital computer in the F-106 fire control system.

'SAS CHANNEL 40 C3043 01	28 JUN 1978'	
LOCATION INSTRUCTION SEQUENCE LARFL INST OPERANDS	C3043	
		CHANNEL 40, BLOCK A PAGE 1

```

00001 START/ELV AUGMENTATION SYSTEM (949) INCORPORATED IN 03042
00002 THIS PROGRAM HAS REVISED SCALING IN THE DIFFERENTIAL ELEVON
00003 IT AS FOLLOWS: TRIM IS IN ADDER IN THE DIFFERENTIAL ELEVON
00004 AS (1/40) TRIM IS IN ADDER IN THE DIFFERENTIAL ELEVON
00005 THE (1/40) TRIM IS USED TO DIFFERENTIAL ELEVON TRIM, POS 2 =
00006 TRIMMING THE ELEVONS OR RUDDER... POS 1 = ELEVON TRIM,
00007 RUDDER TRIM FOR THIS PROGRAM;
00008 CYCLE TIME FOR 5.32 MS
00009 IN SSGC3 15.9 MS
00010 NOT SSGC3
00011
00012 THE MAIN PROGRAM STARTS AT SECTOR 0400
00013
00014
00015
00016
00017
00018
00019
00020
00021
00022
00023
00024
00025
00026
00027
00028
00029
00030
00031
00032
00033
00034
00035
00036
00037
00038
00039
00040
00041
00042
00043
00044
00045
00046
00047
00048
00049
00050
00051
00052
00053
00054
00055
00056
00057
00058
00059
00060
00061
00062
00063
00064
00065
00066
00067
00068
00069
00070
00071
00072
00073
00074
00075
00076
00077
00078
00079
00080
00081
00082
00083
00084
00085
00086
00087
00088
00089
00090
00091
00092
00093
00094
00095
00096
00097
00098
00099
00100
00101
00102
00103
00104
00105
00106
00107
00108
00109
00110
00111
00112
00113
00114
00115
00116
00117
00118
00119
00120
00121
00122
00123
00124
00125
00126
00127
00128
00129
00130
00131
00132
00133
00134
00135
00136
00137
00138
00139
00140
00141
00142
00143
00144
00145
00146
00147
00148
00149
00150
00151
00152
00153
00154
00155
00156
00157
00158
00159
00160
00161
00162
00163
00164
00165
00166
00167
00168
00169
00170
00171
00172
00173
00174
00175
00176
00177
00178
00179
00180
00181
00182
00183
00184
00185
00186
00187
00188
00189
00190
00191
00192
00193
00194
00195
00196
00197
00198
00199
00200
00201
00202
00203
00204
00205
00206
00207
00208
00209
00210
00211
00212
00213
00214
00215
00216
00217
00218
00219
00220
00221
00222
00223
00224
00225
00226
00227
00228
00229
00230
00231
00232
00233
00234
00235
00236
00237
00238
00239
00240
00241
00242
00243
00244
00245
00246
00247
00248
00249
00250
00251
00252
00253
00254
00255
00256
00257
00258
00259
00260
00261
00262
00263
00264
00265
00266
00267
00268
00269
00270
00271
00272
00273
00274
00275
00276
00277
00278
00279
00280
00281
00282
00283
00284
00285
00286
00287
00288
00289
00290
00291
00292
00293
00294
00295
00296
00297
00298
00299
00300
00301
00302
00303
00304
00305
00306
00307
00308
00309
00310
00311
00312
00313
00314
00315
00316
00317
00318
00319
00320
00321
00322
00323
00324
00325
00326
00327
00328
00329
00330
00331
00332
00333
00334
00335
00336
00337
00338
00339
00340
00341
00342
00343
00344
00345
00346
00347
00348
00349
00350
00351
00352
00353
00354
00355
00356
00357
00358
00359
00360
00361
00362
00363
00364
00365
00366
00367
00368
00369
00370
00371
00372
00373
00374
00375
00376
00377
00378
00379
00380
00381
00382
00383
00384
00385
00386
00387
00388
00389
00390
00391
00392
00393
00394
00395
00396
00397
00398
00399
00400
00401
00402
00403
00404
00405
00406
00407
00408
00409
00410
00411
00412
00413
00414
00415
00416
00417
00418
00419
00420
00421
00422
00423
00424
00425
00426
00427
00428
00429
00430
00431
00432
00433
00434
00435
00436
00437
00438
00439
00440
00441
00442
00443
00444
00445
00446
00447
00448
00449
00450
00451
00452
00453
00454
00455
00456
00457
00458
00459
00460
00461
00462
00463
00464
00465
00466
00467
00468
00469
00470
00471
00472
00473
00474
00475
00476
00477
00478
00479
00480
00481
00482
00483
00484
00485
00486
00487
00488
00489
00490
00491
00492
00493
00494
00495
00496
00497
00498
00499
00500
00501
00502
00503
00504
00505
00506
00507
00508
00509
00510
00511
00512
00513
00514
00515
00516
00517
00518
00519
00520
00521
00522
00523
00524
00525
00526
00527
00528
00529
00530
00531
00532
00533
00534
00535
00536
00537
00538
00539
00540
00541
00542
00543
00544
00545
00546
00547
00548
00549
00550
00551
00552
00553
00554
00555
00556
00557
00558
00559
00560
00561
00562
00563
00564
00565
00566
00567
00568
00569
00570
00571
00572
00573
00574
00575
00576
00577
00578
00579
00580
00581
00582
00583
00584
00585
00586
00587
00588
00589
00590
00591
00592
00593
00594
00595
00596
00597
00598
00599
00600
00601
00602
00603
00604
00605
00606
00607
00608
00609
00610
00611
00612
00613
00614
00615
00616
00617
00618
00619
00620
00621
00622
00623
00624
00625
00626
00627
00628
00629
00630
00631
00632
00633
00634
00635
00636
00637
00638
00639
00640
00641
00642
00643
00644
00645
00646
00647
00648
00649
00650
00651
00652
0065
```

CHANNEL 40, BLOCK A PAGE 2

LOCATION	INSTRUCTION	SEQUENCE	LABEL	INST	OPERANDS	C3043
0027	10	0000		TRA	S3	
0028	12	0021	/DSPL	RTI	G87	0170,171,172,173
0029	48	3750		STO	TEMP2	
0030	72	2722		RDI	G88	0180,181,182,183
0031	72	2722		ANA	B211	
0032	02	2766		ALS	04	
0033	24	0004		ADD	TEMP2	
0034	04	3750		STO	TEMP2	
0035	44	3750		RDI	G86	0180,181,170,171,172,173
0036	72	0020		ANA	R211	0165,166,167,168
0037	02	2772		STO	R211	
0038	44	3010		SUNZ	D3A1	0166,167,168
0039	12	3747		TNZ	TEMP2	0101 = 1200 MBS
0040	12	3750		CLA	TEMP2	NOT INPUTING MBS, TRY L8887
0041	04	0050		ALS	06	STORE THE MBS OF THE
0042	24	0050		STO	TEMP2	LOCATION THAT IS TO
0043	04	3017		TRA	TEMP2	BE DISPLAYED.
0044	30	0027		ADD	TEMP2	
0045	04	3750		STO	TEMP2	
0046	04	3750		STO	TEMP2	
0047	30	0027		TRA	TEMP2	
0048	04	3750		STO	TEMP2	
0049	04	3750		STO	TEMP2	
0050	04	3750		STO	TEMP2	
0051	04	3750		STO	TEMP2	
0052	04	3750		STO	TEMP2	
0053	04	3750		STO	TEMP2	
0054	04	3750		STO	TEMP2	
0055	04	3750		STO	TEMP2	
0056	04	3750		STO	TEMP2	

IS DS = 01007  
TRANSFR IF NOT 0100  
INPUT L888  
AND MBS  
DISPLAY THE DUDE

137

LOCATION INSTRUCTION SEQUENCE LABEL INST OPERANDS C3043 CHANNEL 40, BLOCK 8 PAGE 4

[illegible]

LOCATION	INSTRUCTION	SEQUENCE	LABEL	INST	OPERANDS	C3043	CHANNEL 40, BLOCK 8 PAGE 5
0000	LD	0001	START	0001	R1, 0001		
0001	LD	0002	START	0002	R2, 0002		
0002	LD	0003	START	0003	R3, 0003		
0003	LD	0004	START	0004	R4, 0004		
0004	LD	0005	START	0005	R5, 0005		
0005	LD	0006	START	0006	R6, 0006		
0006	LD	0007	START	0007	R7, 0007		
0007	LD	0008	START	0008	R8, 0008		
0008	LD	0009	START	0009	R9, 0009		
0009	LD	0010	START	0010	R10, 0010		
0010	LD	0011	START	0011	R11, 0011		
0011	LD	0012	START	0012	R12, 0012		
0012	LD	0013	START	0013	R13, 0013		
0013	LD	0014	START	0014	R14, 0014		
0014	LD	0015	START	0015	R15, 0015		
0015	LD	0016	START	0016	R16, 0016		
0016	LD	0017	START	0017	R17, 0017		
0017	LD	0018	START	0018	R18, 0018		
0018	LD	0019	START	0019	R19, 0019		
0019	LD	0020	START	0020	R20, 0020		
0020	LD	0021	START	0021	R21, 0021		
0021	LD	0022	START	0022	R22, 0022		
0022	LD	0023	START	0023	R23, 0023		
0023	LD	0024	START	0024	R24, 0024		
0024	LD	0025	START	0025	R25, 0025		
0025	LD	0026	START	0026	R26, 0026		
0026	LD	0027	START	0027	R27, 0027		
0027	LD	0028	START	0028	R28, 0028		
0028	LD	0029	START	0029	R29, 0029		
0029	LD	0030	START	0030	R30, 0030		
0030	LD	0031	START	0031	R31, 0031		
0031	LD	0032	START	0032	R32, 0032		
0032	LD	0033	START	0033	R33, 0033		
0033	LD	0034	START	0034	R34, 0034		
0034	LD	0035	START	0035	R35, 0035		
0035	LD	0036	START	0036	R36, 0036		
0036	LD	0037	START	0037	R37, 0037		
0037	LD	0038	START	0038	R38, 0038		
0038	LD	0039	START	0039	R39, 0039		
0039	LD	0040	START	0040	R40, 0040		
0040	LD	0041	START	0041	R41, 0041		
0041	LD	0042	START	0042	R42, 0042		
0042	LD	0043	START	0043	R43, 0043		
0043	LD	0044	START	0044	R44, 0044		
0044	LD	0045	START	0045	R45, 0045		
0045	LD	0046	START	0046	R46, 0046		
0046	LD	0047	START	0047	R47, 0047		
0047	LD	0048	START	0048	R48, 0048		
0048	LD	0049	START	0049	R49, 0049		
0049	LD	0050	START	0050	R50, 0050		
0050	LD	0051	START	0051	R51, 0051		
0051	LD	0052	START	0052	R52, 0052		
0052	LD	0053	START	0053	R53, 0053		
0053	LD	0054	START</				

0505	0472	0000	0532
0505	0472	0000	0532
0506	0472	0000	0532
0507	0472	0000	0532
0508	0472	0000	0532
0509	0472	0000	0532
0510	0472	0000	0532
0511	0472	0000	0532
0512	0472	0000	0532
0513	0472	0000	0532
0514	0472	0000	0532
0515	0472	0000	0532
0516	0472	0000	0532
0517	0472	0000	0532
0518	0472	0000	0532
0519	0472	0000	0532
0520	0472	0000	0532
0521	0472	0000	0532
0522	0472	0000	0532
0523	0472	0000	0532
0524	0472	0000	0532
0525	0472	0000	0532
0526	0472	0000	0532
0527	0472	0000	0532
0528	0472	0000	0532
0529	0472	0000	0532
0530	0472	0000	0532
0531	0472	0000	0532
0532	0472	0000	0532
0533	0472	0000	0532
0534	0472	0000	0532
0535	0472	0000	0532
0536	0472	0000	0532
0537	0472	0000	0532
0538	0472	0000	0532
0539	0472	0000	0532
0540	0472	0000	0532
0541	0472	0000	0532
0542	0472	0000	0532
0543	0472	0000	0532
0544	0472	0000	0532
0545	0472	0000	0532
0546	0472	0000	0532
0547	0472	0000	0532
0548	0472	0000	0532
0549	0472	0000	0532
0550	0472	0000	0532
0551	0472	0000	0532
0552	0472	0000	0532
0553	0472	0000	0532
0554	0472	0000	0532
0555	0472	0000	0532
0556	0472	0000	0532
0557	0472	0000	0532
0558	0472	0000	0532
0559	0472	0000	0532
0560	0472	0000	0532
0561	0472	0000	0532
0562	0472	0000	0532
0563	0472	0000	0532
0564	0472	0000	0532
0565	0472	0000	0532
0566	0472	0000	0532
0567	0472	0000	0532
0568	0472	0000	0532
0569	0472	0000	0532
0570	0472	0000	0532
0571	0472	0000	0532
0572	0472	0000	0532
0573	0472	0000	0532
0574	0472	0000	0532
0575	0472	0000	0532
0576	0472	0000	0532
0577	0472	0000	0532
0578	0472	0000	0532
0579	0472	0000	0532
0580	0472	0000	0532
0581	0472	0000	0532
0582	0472	0000	0532
0583	0472	0000	0532
0584	0472	0000	0532
0585	0472	0000	0532
0586	0472	0000	0532
0587	0472	0000	0532
0588	0472	0000	0532
0589	0472	0000	0532
0590	0472	0000	0532
0591	0472	0000	0532
0592	0472	0000	0532
0593	0472	0000	0532
0594	0472	0000	0532
0595	0472	0000	0532
0596	0472	0000	0532
0597	0472	0000	0532
0598	0472	0000	0532
0599	0472	0000	0532
0600	0472	0000	0532

LOCATION INSTRUCTION SEQUENCE LABEL INST OPERANDS C3043 CHANNEL 40, BLOCK 0 PAGE 0

```

0540 24 3003 10740 03
0541 64 3000 10745 A
0542 64 3573 10790 STG
0543 10 2746 10800 SGT
0544 12 0546 10805 RZT1
0545 10 0740 10810 /RAKDA
*** READ DATA INPUTS ***
*** MACH AND IMPACT TEMP. ***
*** LATERAL ACCELERATION (ASURY) , RUDDER PEDAL POS., TRIM, ***
0546 72 2045 10815 /RAKDA
0547 10 2755 10820 CORNTHETA) SIN(PHI) VSURI (FROM
0548 24 0007 10825 SUR 7
0549 64 3167 10830 AL 5/2**7
0550 40 3167 10835 SYN THETA
0551 40 3167 10840 COSINE THETA
0552 40 3167 10845 MPV
0553 40 3167 10850 STU
0554 40 3167 10855 CLA
0555 40 3167 10860 SUB
0556 40 3167 10865 TBR
0557 40 3167 10870 CLA
0558 40 3167 10875 CTHETA
0559 40 3167 10880 E21
0560 40 3167 10885 SUB
0561 40 3167 10890 AL
0562 40 3167 10895 SPHI
0563 40 3167 10900 E22
0564 40 3167 10905 SUB
0565 40 3167 10910 B1C
0566 40 3167 10915 CPHI
0567 40 3167 10920 LXA
0568 40 3167 10925 SYN
0569 40 3167 10930 LXA
0570 40 3167 10935 LXA
0571 40 3167 10940 LXA
0572 73 3056 10945 INPUT RDG*
0573 40 3167 10950 STG
0574 40 3167 10955 SUB
0575 40 3167 10960 ANA
0576 40 3167 10965 /RVK17
0577 40 3167 10970 /RVK5
0578 40 3167 10975 /RVK6
0579 40 3167 10980 /RVK6
0580 40 3167 10985 /RVK6
0581 40 3167 10990 /RVK6
0582 40 3167 10995 /RVK6
0583 40 3167 11000 /RVK6
0584 40 3167 11005 /RVK6
0585 40 3167 11010 /RVK6
0586 40 3167 11015 /RVK6
0587 40 3167 11020 /RVK6
0588 40 3167 11025 /RVK6
0589 40 3167 11030 /RVK6
0590 40 3167 11035 /RVK6
0591 40 3167 11040 /RVK6
0592 40 3167 11045 /RVK6
0593 40 3167 11050 /RVK6
0594 40 3167 11055 /RVK6
0595 40 3167 11060 /RVK6
0596 40 3167 11065 /RVK6
0597 40 3167 11070 /RVK6
0598 40 3167 11075 /RVK6
0599 40 3167 11080 /RVK6
0600 40 3167 11085 /RVK6
0601 40 3167 11090 /RVK6
0602 40 3167 11095 /RVK6
0603 40 3167 11100 /RVK6
0604 40 3167 11105 /RVK6
0605 40 3167 11110 /RVK6
0606 40 3167 11115 /RVK6
0607 40 3167 11120 /RVK6
0608 40 3167 11125 /RVK6
0609 40 3167 11130 /RVK6
0610 40 3167 11135 /RVK6
0611 40 3167 11140 /RVK6
0612 40 3167 11145 /RVK6
0613 40 3167 11150 /RVK6
0614 40 3167 11155 /RVK6
0615 40 3167 11160 /RVK6
0616 40 3167 11165 /RVK6
0617 40 3167 11170 /RVK6
0618 40 3167 11175 /RVK6
0619 40 3167 11180 /RVK6
0620 40 3167 11185 /RVK6
0621 40 3167 11190 /RVK6
0622 40 3167 11195 /RVK6
0623 40 3167 11200 /RVK6
0624 40 3167 11205 /RVK6
0625 40 3167 11210 /RVK6
0626 40 3167 11215 /RVK6
0627 40 3167 11220 /RVK6
0628 40 3167 11225 /RVK6
0629 40 3167 11230 /RVK6
0630 40 3167 11235 /RVK6
0631 40 3167 11240 /RVK6
0632 40 3167 11245 /RVK6
0633 40 3167 11250 /RVK6
0634 40 3167 11255 /RVK6
0635 40 3167 11260 /RVK6
0636 40 3167 11265 /RVK6
0637 40 3167 11270 /RVK6
0638 40 3167 11275 /RVK6
0639 40 3167 11280 /RVK6
0640 40 3167 11285 /RVK6
0641 40 3167 11290 /RVK6
0642 40 3167 11295 /RVK6
0643 40 3167 11300 /RVK6
0644 40 3167 11305 /RVK6
0645 40 3167 11310 /RVK6
0646 40 3167 11315 /RVK6
0647 40 3167 11320 /RVK6
0648 40 3167 11325 /RVK6
0649 40 3167 11330 /RVK6
0650 40 3167 11335 /RVK6
0651 40 3167 11340 /RVK6
0652 40 3167 11345 /RVK6
0653 40 3167 11350 /RVK6
0654 40 3167 11355 /RVK6
0655 40 3167 11360 /RVK6
0656 40 3167 11365 /RVK6
0657 40 3167 11370 /RVK6
0658 40 3167 11375 /RVK6
0659 40 3167 11380 /RVK6
0660 40 3167 11385 /RVK6
0661 40 3167 11390 /RVK6
0662 40 3167 11395 /RVK6
0663 40 3167 11400 /RVK6
0664 40 3167 11405 /RVK6
0665 40 3167 11410 /RVK6
0666 40 3167 11415 /RVK6
0667 40 3167 11420 /RVK6
0668 40 3167 11425 /RVK6
0669 40 3167 11430 /RVK6
0670 40 3167 11435 /RVK6
0671 40 3167 11440 /RVK6
0672 40 3167 11445 /RVK6
0673 40 3167 11450 /RVK6
0674 40 3167 11455 /RVK6
0675 40 3167 11460 /RVK6
0676 40 3167 11465 /RVK6
0677 40 3167 11470 /RVK6
0678 40 3167 11475 /RVK6
0679 40 3167 11480 /RVK6
0680 40 3167 11485 /RVK6
0681 40 3167 11490 /RVK6
0682 40 3167 11495 /RVK6
0683 40 3167 11500 /RVK6
0684 40 3167 11505 /RVK6
0685 40 3167 11510 /RVK6
0686 40 3167 11515 /RVK6
0687 40 3167 11520 /RVK6
0688 40 3167 11525 /RVK6
0689 40 3167 11530 /RVK6
0690 40 3167 11535 /RVK6
0691 40 3167 11540 /RVK6
0692 40 3167 11545 /RVK6
0693 40 3167 11550 /RVK6
0694 40 3167 11555 /RVK6
0695 40 3167 11560 /RVK6
0696 40 3167 11565 /RVK6
0697 40 3167 11570 /RVK6
0698 40 3167 11575 /RVK6
0699 40 3167 11580 /RVK6
0700 40 3167 11585 /RVK6
0701 40 3167 11590 /RVK6
0702 40 3167 11595 /RVK6
0703 40 3167 11600 /RVK6
0704 40 3167 11605 /RVK6
0705 40 3167 11610 /RVK6
0706 40 3167 11615 /RVK6
0707 40 3167 11620 /RVK6
0708 40 3167 11625 /RVK6
0709 40 3167 11630 /RVK6
0710 40 3167 11635 /RVK6
0711 40 3167 11640 /RVK6
0712 40 3167 11645 /RVK6
0713 40 3167 11650 /RVK6
0714 40 3167 11655 /RVK6
0715 40 3167 11660 /RVK6
0716 40 3167 11665 /RVK6
0717 40 3167 11670 /RVK6
0718 40 3167 11675 /RVK6
0719 40 3167 11680 /RVK6
0720 40 3167 11685 /RVK6
0721 40 3167 11690 /RVK6
0722 40 3167 11695 /RVK6
0723 40 3167 11700 /RVK6
0724 40 3167 11705 /RVK6
0725 40 3167 11710 /RVK6
0726 40 3167 11715 /RVK6
0727 40 3167 11720 /RVK6
0728 40 3167 11725 /RVK6
0729 40 3167 11730 /RVK6
0730 40 3167 11735 /RVK6
0731 40 3167 11740 /RVK6
0732 40 3167 11745 /RVK6
0733 40 3167 11750 /RVK6
0734 40 3167 11755 /RVK6
0735 40 3167 11760 /RVK6
0736 40 3167 11765 /RVK6
0737 40 3167 11770 /RVK6
0738 40 3167 11775 /RVK6
0739 40 3167 11780 /RVK6
0740 40 3167 11785 /RVK6
0741 40 3167 11790 /RVK6
0742 40 3167 11795 /RVK6
0743 40 3167 11800 /RVK6
0744 40 3167 11805 /RVK6
0745 40 3167 11810 /RVK6
0746 40 3167 11815 /RVK6
0747 40 3167 11820 /RVK6
0748 40 3167 11825 /RVK6
0749 40 3167 11830 /RVK6
0750 40 3167 11835 /RVK6
0751 40 3167 11840 /RVK6
0752 40 3167 11845 /RVK6
0753 40 3167 11850 /RVK6
0754 40 3167 11855 /RVK6
0755 40 3167 11860 /RVK6
0756 40 3167 11865 /RVK6
0757 40 3167 11870 /RVK6
0758 40 3167 11875 /RVK6
0759 40 3167 11880 /RVK6
0760 40 3167 11885 /RVK6
0761 40 3167 11890 /RVK6
0762 40 3167 11895 /RVK6
0763 40 3167 11900 /RVK6
0764 40 3167 11905 /RVK6
0765 40 3167 11910 /RVK6
0766 40 3167 11915 /RVK6
0767 40 3167 11920 /RVK6
0768 40 3167 11925 /RVK6
0769 40 3167 11930 /RVK6
0770 40 3167 11935 /RVK6
0771 40 3167 11940 /RVK6
0772 40 3167 11945 /RVK6
0773 40 3167 11950 /RVK6
0774 40 3167 11955 /RVK6
0775 40 3167 11960 /RVK6
0776 40 3167 11965 /RVK6
0777 40 3167 11970 /RVK6
0778 40 3167 11975 /RVK6
0779 40 3167 11980 /RVK6
0780 40 3167 11985 /RVK6
0781 40 3167 11990 /RVK6
0782 40 3167 11995 /RVK6
0783 40 3167 12000 /RVK6
0784 40 3167 12005 /RVK6
0785 40 3167 12010 /RVK6
0786 40 3167 12015 /RVK6
0787 40 3167 12020 /RVK6
0788 40 3167 12025 /RVK6
0789 40 3167 12030 /RVK6
0790 40 3167 12035 /RVK6
0791 40 3167 12040 /RVK6
0792 40 3167 12045 /RVK6
0793 40 3167 12050 /RVK6
0794 40 3167 12055 /RVK6
0795 40 3167 12060 /RVK6
0796 40 3167 12065 /RVK6
0797 40 3167 12070 /RVK6
0798 40 3167 12075 /RVK6
0799 40 3167 12080 /RVK6
0800 40 3167 12085 /RVK6
0801 40 3167 12090 /RVK6
0802 40 3167 12095 /RVK6
0803 40 3167 12100 /RVK6
0804 40 3167 12105 /RVK6
0805 40 3167 12110 /RVK6
0806 40 3167 12115 /RVK6
0807 40 3167 12120 /RVK6
0808 40 3167 12125 /RVK6
0809 40 3167 12130 /RVK6
0810 40 3167 12135 /RVK6
0811 40 3167 12140 /RVK6
0812 40 3167 12145 /RVK6
0813 40 3167 12150 /RVK6
0814 40 3167 12155 /RVK6
0815 40 3167 12160 /RVK6
0816 40 3167 12165 /RVK6
0817 40 3167 12170 /RVK6
0818 40 3167 12175 /RVK6
0819 40 3167 12180 /RVK6
0820 40 3167 12185 /RVK6
0821 40 3167 12190 /RVK6
0822 40 3167 12195 /RVK6
0823 40 3167 12200 /RVK6
0824 40 3167 12205 /RVK6
0825 40 3167 12210 /RVK6
0826 40 3167 12215 /RVK6
0827 40 3167 12220 /RVK6
0828 40 3167 12225 /RVK6
0829 40 3167 12230 /RVK6
0830 40 3167 12235 /RVK6
0831 40 3167 12240 /RVK6
0832 40 3167 12245 /RVK6
0833 40 3167 12250 /RVK6
0834 40 3167 12255 /RVK6
0835 40 3167 12260 /RVK6
0836 40 3167 12265 /RVK6
0837 40 3167 12270 /RVK6
0838 40 3167 12275 /RVK6
0839 40 3167 12280 /RVK6
0840 40 3167 12285 /RVK6
0841 40 3167 12290 /RVK6
0842 40 3167 12295 /RVK6
0843 40 3167 12300 /RVK6
0844 40 3167 12305 /RVK6
0845 40 3167 12310 /RVK6
0846 40 3167 12315 /RVK6
0847 40 3167 12320 /RVK6
0848 40 3167 12325 /RVK6
0849 40 3167 12330 /RVK6
0850 40 3167 12335 /RVK6
0851 40 3167 12340 /RVK6
0852 40 3167 12345 /RVK6
0853 40 3167 12350 /RVK6
0854 40 3167 12355 /RVK6
0855 40 3167 12360 /RVK6
0856 40 3167 12365 /RVK6
0857 40 3167 12370 /RVK6
0858 40 3167 12375 /RVK6
0859 40 3167 12380 /RVK6
0860 40 3167 12385 /RVK6
0861 40 3167 12390 /RVK6
0862 40 3167 12395 /RVK6
0863 40 3167 12400 /RVK6
0864 40 3167 12405 /RVK6
0865 40 3167 12410 /RVK6
0866 40 3167 12415 /RVK6
0867 40 3167 12420 /RVK6
0868 40 3167 12425 /RVK6
0869 40 3167 12430 /RVK6
0870 40 3167 12435 /RVK6
0871 40 3167 12440 /RVK6
0872 40 3167 12445 /RVK6
0873 40 3167 12450 /RVK6
0874 40 3167 12455 /RVK6
0875 40 3167 12460 /RVK6
0876 40 3167 12465 /RVK6
0877 40 3167 12470 /RVK6
0878 40 3167 12475 /RVK6
0879 40 3167 12480 /RVK6
0880 40 3167 12485 /RVK6
0881 40 3167 12490 /RVK6
0882 40 3167 12495 /RVK6
0883 40 3167 12500 /RVK6
0884 40 3167 12505 /RVK6
0885 40 3167 12510 /RVK6
0886 40 3167 12515 /RVK6
0887 40 3167 12520 /RVK6
0888 40 3167 12525 /RVK6
0889 40 3167 12530 /RVK6
0890 40 3167 12535 /RVK6
0891 40 3167 12540 /RVK6
0892 40 3167 12545 /RVK6
0893 40 3167 12550 /RVK6
0894 40 3167 12555 /RVK6
0895 40 3167 12560 /RVK6
0896 40 3167 12565 /RVK6
0897 40 3167 12570 /RVK6
0898 40 3167 12575 /RVK6
0899 40 3167 12580 /RVK6
0900 40 3167 12585 /RVK6
0901 40 3167 12590 /RVK6
0902 40 3167 12595 /RVK6
0903 40 3167 12600 /RVK6
0904 40 3167 12605 /RVK6
0905 40 3167 12610 /RVK6
0906 40 3167 12615 /RVK6
0907 40 3167 12620 /RVK6
0908 40 3167 12625 /RVK6
0909 40 3167 12630 /RVK6
0910 40 3167 12635 /RVK6
0911 40 3167 12640 /RVK6
0912 40 3167 12645 /RVK6
0913 40 3167 12650 /RVK6
0914 40 3167 12655 /RVK6
0915 40 3167 12660 /RVK6
0916 40 3167 12665 /RVK6
0917 40 3167 12670 /RVK6
0918 40 3167 12675 /RVK6
0919 40 3167 12680 /RVK6
0920 40 3167 12685 /RVK6
0921 40 3167 12690 /RVK6
0922 40 3167 12695 /RVK6
0923 40 3167 12700 /RVK6
0924 40 3167 12705 /RVK6
0925 40 3167 12710 /RVK6
0926 40 3167 12715 /RVK6
0927 40 3167 12720 /RVK6
0928 40 3167 12725 /RVK6
0929 40 3167 12730 /RVK6
0930 40 3167 12735 /RVK6
0931 40 3167 12740 /RVK6
0932 40 3167 12745 /RVK6
0933 40 3167 12750 /RVK6
0934 40 3167 12755 /RVK6
0935 40 3167 12760 /RVK6
0936 40 3167 12765 /RVK6
0937 40 3167 12770 /RVK6
0938 40 3167 12775 /RVK6
0939 40 3167 12780 /RVK6
0940 40 3167 12785 /RVK6
0941 40 3167 12790 /RVK6
0942 40 3167 12795 /RVK6
0943 40 3167 12800 /RVK6
0944 40 3167 12805 /RVK6
0945 40 3167 12810 /RVK6
0946 40 3167 12815 /RVK6
0947 40 3167 12820 /RVK6
0948 40 3167 12825 /RVK6
0949 40 3167 12830 /RVK6
0950 40 3167 12835 /RVK6
0951 40 3167 12840 /RVK6
0952 40 3167 12845 /RVK6
0953 40 3167 12850 /RVK6
0954 40 3167 12855 /RVK6
0955 40 3167 12860 /RVK6
0956 40 3167 12865 /RVK6
0957 40 3167 12870 /RVK6
0958 40 3167 12875 /RVK6
0959 40 3167 12880 /RVK6
0960 40 3167 12885 /RVK6
0961 40 3167 12890 /RVK6
0962 40 3167 12895 /RVK6
0963 40 3167 12900 /RVK6
0964 40 3167 12905 /RVK6
0965 40 3167 12910 /RVK6
0966 40 3167 12915 /RVK6
0967 40 3167 12920 /RVK6
0968 40 3167 12925 /RVK6
0969 40 3167 12930 /RVK6
0970 40 3167 12935 /RVK6
0971 40 3167 12940 /RVK6
0972 40 3167 12945 /RVK6
0973 40 3167 12950 /RVK6
0974 40 3167 12955 /RVK6
0975 40 3167 12960 /RVK6
0976 40 3167 12965 /RVK6
0977 40 3167 12970 /RVK6
0978 40 3167 12975 /RVK6
0979 40 3167 12980 /RVK6
0980 40 3167 12985 /RVK6
0981 40 3167 12990 /RVK6
0982 40 3167 12995 /RVK6
0983 40 3167 13000 /RVK6
0984 40 3167 13005 /RVK6
0985 40 3167 13010 /RVK6
0986 40 3167 13015 /RVK6
0987 40 3167 13020 /RVK6
0988 40 3167 13025 /RVK6
0989 40 3167 13030 /RVK6
0990 40 3167 13035 /RVK6
0991 40 3167 13040 /RVK6
0992 40 3167 13045 /RVK6
0993 40 3167 13050 /RVK6
0994 40 3167 13055 /RVK6
0995 40 3167 13060 /RVK6
0996 40 3167 13065 /RVK6
0997 40 3167 13070 /RVK6
0998 40 3167 13075 /RVK6
0999 40 3167 13080 /RVK6
1000 40 3167 13085 /RVK6

```



CHANNEL 40, BLOCK B PAGE 7

LOCATION	INSTRUCTION	SEQUENCE	LABEL	INST	OPERANDS	C3043	CHANNEL
000000	000000	000000	STO	02	A0	(1+2M**2)/4	
000001	000001	000001	ALB	04	A0	(2-35.4)/414(2**7)	
000002	000002	000002	ADD	04	/A02	414/2**9	
000003	000003	000003	ADD	04	/A03	35.2/2**12	
000004	000004	000004	STO	02	B	217/2**12	
000005	000005	000005	STO	01	D1	217/((1+.2M**2)*2**10	
000006	000006	000006	ALB	01	S0907		
000007	000007	000007	STO	04	/A04	49.01/2**6	
000008	000008	000008	STO	04	V0408	VEL OF SOUND /2**11 FT/SEC	
000009	000009	000009	STO	04	V0408	VEL OF SOUND /2**11	
000010	000010	000010	STO	04	V0408	VEL OF SOUND /2**11	
000011	000011	000011	STO	04	V0408	VEL OF SOUND /2**11	
000012	000012	000012	STO	04	V0408	VEL OF SOUND /2**11	
000013	000013	000013	STO	04	V0408	VEL OF SOUND /2**11	
000014	000014	000014	STO	04	V0408	VEL OF SOUND /2**11	
000015	000015	000015	STO	04	V0408	VEL OF SOUND /2**11	
000016	000016	000016	STO	04	V0408	VEL OF SOUND /2**11	
000017	000017	000017	STO	04	V0408	VEL OF SOUND /2**11	
000018	000018	000018	STO	04	V0408	VEL OF SOUND /2**11	
000019	000019	000019	STO	04	V0408	VEL OF SOUND /2**11	
000020	000020	000020	STO	04	V0408	VEL OF SOUND /2**11	
000021	000021	000021	STO	04	V0408	VEL OF SOUND /2**11	
000022	000022	000022	STO	04	V0408	VEL OF SOUND /2**11	
000023	000023	000023	STO	04	V0408	VEL OF SOUND /2**11	
000024	000024	000024	STO	04	V0408	VEL OF SOUND /2**11	
000025	000025	000025	STO	04	V0408	VEL OF SOUND /2**11	
000026	000026	000026	STO	04	V0408	VEL OF SOUND /2**11	
000027	000027	000027	STO	04	V0408	VEL OF SOUND /2**11	
000028	000028	000028	STO	04	V0408	VEL OF SOUND /2**11	
000029	000029	000029	STO	04	V0408	VEL OF SOUND /2**11	
000030	000030	000030	STO	04	V0408	VEL OF SOUND /2**11	
000031	000031	000031	STO	04	V0408	VEL OF SOUND /2**11	
000032	000032	000032	STO	04	V0408	VEL OF SOUND /2**11	
000033	000033	000033	STO	04	V0408	VEL OF SOUND /2**11	
000034	000034	000034	STO	04	V0408	VEL OF SOUND /2**11	
000035	000035	000035	STO	04	V0408	VEL OF SOUND /2**11	
000036	000036	000036	STO	04	V0408	VEL OF SOUND /2**11	
000037	000037	000037	STO	04	V0408	VEL OF SOUND /2**11	
000038	000038	000038	STO	04	V0408	VEL OF SOUND /2**11	
000039	000039	000039	STO	04	V0408	VEL OF SOUND /2**11	
000040	000040	000040	STO	04	V0408	VEL OF SOUND /2**11	
000041	000041	000041	STO	04	V0408	VEL OF SOUND /2**11	
000042	000042	000042	STO	04	V0408	VEL OF SOUND /2**11	
000043	000043	000043	STO	04	V0408	VEL OF SOUND /2**11	
000044	000044	000044	STO	04	V0408	VEL OF SOUND /2**11	
000045	000045	000045	STO	04	V0408	VEL OF SOUND /2**11	
000046	000046	000046	STO	04	V0408	VEL OF SOUND /2**11	
000047	000047	000047	STO	04	V0408	VEL OF SOUND /2**11	
000048	000048	000048	STO	04	V0408	VEL OF SOUND /2**11	
000049	000049	000049	STO	04	V0408	VEL OF SOUND /2**11	
000050	000050	000050	STO	04	V0408	VEL OF SOUND /2**11	



CHANNEL 40, BLOCK 8 PAGE 9

LOCATION	INSTRUCTION	SEQUENCE	LABEL	INST	OPERANDS	C3043	TRIM INPUT/160 LATERAL STICK POSITION TRIM/4 FOR USE IN DIFF ELEVON CALC
0761	00	1775	/TRIM	DATA	00		
0762	00	1776	/DELPS	DATA	00		
0763	00	1777	/ALTM	DATA	00		
0764	04	1778	/FANDA	DATA	00		
0765	04	1779		DATA	00		
0766	04	1780		DATA	00		
0767	04	1781		DATA	00		
0768	04	1782		DATA	00		
0769	04	1783		DATA	00		
0770	04	1784		DATA	00		
0771	04	1785		DATA	00		
0772	04	1786		DATA	00		
0773	04	1787		DATA	00		
0774	04	1788		DATA	00		
0775	04	1789		DATA	00		
0776	04	1790		DATA	00		
0777	04	1791		DATA	00		

**C3043**

## OPERANDS

**INST**

**SEQUENCE LABEL**

## LOCATION INSTRUCTION

[illegible]

**C3043**

## OPERANDS

**INGY**

**SEQUENCE LABEL**

**LOCATION INSTRUCTION**

Figure 1 displays four plots showing the distribution of alpha constants for the four nucleotides (A, C, G, T) in the 120000 bp region of the human genome. Each plot has 'INDEX' on the x-axis (0-10000) and 'SM POS' on the y-axis (0-10000). The plots are labeled 'CONSTANTS SCALED OVER 4' for each nucleotide. The distributions are highly skewed, with most values concentrated at the lower end of the index.

**C3043**

## OPERANDS

**INGY**

130V7 32N3N03S NO13CNU15N1 NO11AV30T

[illegible]

LOCATION	INSTRUCTION	SEQUENCE	LABEL	INST	OPERANDS	C3043	CHANNEL 40, BLOCK C PAGE 13
----------	-------------	----------	-------	------	----------	-------	-----------------------------

**C3043**

## OPERANDS

**SEQUENCE LABEL**

**LOCATION INS**

Line	Address	Hex	Assembly	Comments
1260	0070	0000	CALCULATE RUDDER COMMAND	
1261	0080	0000	BETA DOT EQUATION	
1262	0090	0000	BETA DOT EQUATION	
1263	00A0	0000	BETA DOT EQUATION	
1264	00B0	0000	BETA DOT EQUATION	
1265	00C0	0000	BETA DOT EQUATION	
1266	00D0	0000	BETA DOT EQUATION	
1267	00E0	0000	BETA DOT EQUATION	
1268	00F0	0000	BETA DOT EQUATION	
1269	0100	0000	BETA DOT EQUATION	
1270	0110	0000	BETA DOT EQUATION	
1271	0120	0000	BETA DOT EQUATION	
1272	0130	0000	BETA DOT EQUATION	
1273	0140	0000	BETA DOT EQUATION	
1274	0150	0000	BETA DOT EQUATION	
1275	0160	0000	BETA DOT EQUATION	
1276	0170	0000	BETA DOT EQUATION	
1277	0180	0000	BETA DOT EQUATION	
1278	0190	0000	BETA DOT EQUATION	
1279	01A0	0000	BETA DOT EQUATION	
1280	01B0	0000	BETA DOT EQUATION	
1281	01C0	0000	BETA DOT EQUATION	
1282	01D0	0000	BETA DOT EQUATION	
1283	01E0	0000	BETA DOT EQUATION	
1284	01F0	0000	BETA DOT EQUATION	
1285	0200	0000	BETA DOT EQUATION	
1286	0210	0000	BETA DOT EQUATION	
1287	0220	0000	BETA DOT EQUATION	
1288	0230	0000	BETA DOT EQUATION	
1289	0240	0000	BETA DOT EQUATION	
1290	0250	0000	BETA DOT EQUATION	
1291	0260	0000	BETA DOT EQUATION	
1292	0270	0000	BETA DOT EQUATION	
1293	0280	0000	BETA DOT EQUATION	
1294	0290	0000	BETA DOT EQUATION	
1295	02A0	0000	BETA DOT EQUATION	
1296	02B0	0000	BETA DOT EQUATION	
1297	02C0	0000	BETA DOT EQUATION	
1298	02D0	0000	BETA DOT EQUATION	
1299	02E0	0000	BETA DOT EQUATION	
1300	02F0	0000	BETA DOT EQUATION	
1301	0300	0000	BETA DOT EQUATION	
1302	0310	0000	BETA DOT EQUATION	
1303	0320	0000	BETA DOT EQUATION	
1304	0330	0000	BETA DOT EQUATION	
1305	0340	0000	BETA DOT EQUATION	
1306	0350	0000	BETA DOT EQUATION	
1307	0360	0000	BETA DOT EQUATION	
1308	0370	0000	BETA DOT EQUATION	
1309	0380	0000	BETA DOT EQUATION	
1310	0390	0000	BETA DOT EQUATION	
1311	03A0	0000	BETA DOT EQUATION	
1312	03B0	0000	BETA DOT EQUATION	
1313	03C0	0000	BETA DOT EQUATION	
1314	03D0	0000	BETA DOT EQUATION	
1315	03E0	0000	BETA DOT EQUATION	
1316	03F0	0000	BETA DOT EQUATION	
1317	0400	0000	BETA DOT EQUATION	
1318	0410	0000	BETA DOT EQUATION	
1319	0420	0000	BETA DOT EQUATION	
1320	0430	0000	BETA DOT EQUATION	
1321	0440	0000	BETA DOT EQUATION	
1322	0450	0000	BETA DOT EQUATION	
1323	0460	0000	BETA DOT EQUATION	
1324	0470	0000	BETA DOT EQUATION	
1325	0480	0000	BETA DOT EQUATION	
1326	0490	0000	BETA DOT EQUATION	
1327	04A0	0000	BETA DOT EQUATION	
1328	04B0	0000	BETA DOT EQUATION	
1329	04C0	0000	BETA DOT EQUATION	
1330	04D0	0000	BETA DOT EQUATION	
1331	04E0	0000	BETA DOT EQUATION	
1332	04F0	0000	BETA DOT EQUATION	
1333	0500	0000	BETA DOT EQUATION	
1334	0510	0000	BETA DOT EQUATION	
1335	0520	0000	BETA DOT EQUATION	
1336	0530	0000	BETA DOT EQUATION	
1337	0540	0000		

[illegible][illegible]



CHANNEL 40, BLOCK C PAGE 15

C3043

OPERANDS

INST

SEQUENCE LABEL

40

END

21490  
21490

39 4350  
39 7616

1374  
1377

529 DRUM LOCATIONS UTILIZED, 239 REMAIN AVAILABLE IN THIS CHANNEL  
TAPE SUM 0176776

\*\*\*CHANNEL 40\*\*\*

\*\*\*GLOBAL SYMBOLS DEFINED BY AND/OR REFERENCED IN THIS CHANNEL\*\*\*

DEF/REF

SYMBOL

410	411	412	413	414	415	416	417	418	419	420	421	422	423	424	425	426	427	428	429	430	431	432	433	434	435	436	437	438	439	440	441	442	443	444	445	446	447	448	449	450	451	452	453	454	455	456	457	458	459	460	461	462	463	464	465	466	467	468	469	470	471	472	473	474	475	476	477	478	479	480	481	482	483	484	485	486	487	488	489	490	491	492	493	494	495	496	497	498	499	500	501	502	503	504	505	506	507	508	509	510	511	512	513	514	515	516	517	518	519	520	521	522	523	524	525	526	527	528	529	530	531	532	533	534	535	536	537	538	539	540	541	542	543	544	545	546	547	548	549	550	551	552	553	554	555	556	557	558	559	560	561	562	563	564	565	566	567	568	569	570	571	572	573	574	575	576	577	578	579	580	581	582	583	584	585	586	587	588	589	590	591	592	593	594	595	596	597	598	599	600	601	602	603	604	605	606	607	608	609	610	611	612	613	614	615	616	617	618	619	620	621	622	623	624	625	626	627	628	629	630	631	632	633	634	635	636	637	638	639	640	641	642	643	644	645	646	647	648	649	650	651	652	653	654	655	656	657	658	659	660	661	662	663	664	665	666	667	668	669	670	671	672	673	674	675	676	677	678	679	680	681	682	683	684	685	686	687	688	689	690	691	692	693	694	695	696	697	698	699	700	701	702	703	704	705	706	707	708	709	710	711	712	713	714	715	716	717	718	719	720	721	722	723	724	725	726	727	728	729	730	731	732	733	734	735	736	737	738	739	740	741	742	743	744	745	746	747	748	749	750	751	752	753	754	755	756	757	758	759	760	761	762	763	764	765	766	767	768	769	770	771	772	773	774	775	776	777	778	779	780	781	782	783	784	785	786	787	788	789	790	791	792	793	794	795	796	797	798	799	800	801	802	803	804	805	806	807	808	809	810	811	812	813	814	815	816	817	818	819	820	821	822	823	824	825	826	827	828	829	830	831	832	833	834	835	836	837	838	839	840	841	842	843	844	845	846	847	848	849	850	851	852	853	854	855	856	857	858	859	860	861	862	863	864	865	866	867	868	869	870	871	872	873	874	875	876	877	878	879	880	881	882	883	884	885	886	887	888	889	890	891	892	893	894	895	896	897	898	899	900	901	902	903	904	905	906	907	908	909	910	911	912	913	914	915	916	917	918	919	920	921	922	923	924	925	926	927	928	929	930	931	932	933	934	935	936	937	938	939	940	941	942	943	944	945	946	947	948	949	950	951	952	953	954	955	956	957	958	959	960	961	962	963	964	965	966	967	968	969	970	971	972	973	974	975	976	977	978	979	980	981	982	983	984	985	986	987	988	989	990	991	992	993	994	995	996	997	998	999	1000
-----	-----	-----	-----	-----	-----	-----	-----	-----	-----	-----	-----	-----	-----	-----	-----	-----	-----	-----	-----	-----	-----	-----	-----	-----	-----	-----	-----	-----	-----	-----	-----	-----	-----	-----	-----	-----	-----	-----	-----	-----	-----	-----	-----	-----	-----	-----	-----	-----	-----	-----	-----	-----	-----	-----	-----	-----	-----	-----	-----	-----	-----	-----	-----	-----	-----	-----	-----	-----	-----	-----	-----	-----	-----	-----	-----	-----	-----	-----	-----	-----	-----	-----	-----	-----	-----	-----	-----	-----	-----	-----	-----	-----	-----	-----	-----	-----	-----	-----	-----	-----	-----	-----	-----	-----	-----	-----	-----	-----	-----	-----	-----	-----	-----	-----	-----	-----	-----	-----	-----	-----	-----	-----	-----	-----	-----	-----	-----	-----	-----	-----	-----	-----	-----	-----	-----	-----	-----	-----	-----	-----	-----	-----	-----	-----	-----	-----	-----	-----	-----	-----	-----	-----	-----	-----	-----	-----	-----	-----	-----	-----	-----	-----	-----	-----	-----	-----	-----	-----	-----	-----	-----	-----	-----	-----	-----	-----	-----	-----	-----	-----	-----	-----	-----	-----	-----	-----	-----	-----	-----	-----	-----	-----	-----	-----	-----	-----	-----	-----	-----	-----	-----	-----	-----	-----	-----	-----	-----	-----	-----	-----	-----	-----	-----	-----	-----	-----	-----	-----	-----	-----	-----	-----	-----	-----	-----	-----	-----	-----	-----	-----	-----	-----	-----	-----	-----	-----	-----	-----	-----	-----	-----	-----	-----	-----	-----	-----	-----	-----	-----	-----	-----	-----	-----	-----	-----	-----	-----	-----	-----	-----	-----	-----	-----	-----	-----	-----	-----	-----	-----	-----	-----	-----	-----	-----	-----	-----	-----	-----	-----	-----	-----	-----	-----	-----	-----	-----	-----	-----	-----	-----	-----	-----	-----	-----	-----	-----	-----	-----	-----	-----	-----	-----	-----	-----	-----	-----	-----	-----	-----	-----	-----	-----	-----	-----	-----	-----	-----	-----	-----	-----	-----	-----	-----	-----	-----	-----	-----	-----	-----	-----	-----	-----	-----	-----	-----	-----	-----	-----	-----	-----	-----	-----	-----	-----	-----	-----	-----	-----	-----	-----	-----	-----	-----	-----	-----	-----	-----	-----	-----	-----	-----	-----	-----	-----	-----	-----	-----	-----	-----	-----	-----	-----	-----	-----	-----	-----	-----	-----	-----	-----	-----	-----	-----	-----	-----	-----	-----	-----	-----	-----	-----	-----	-----	-----	-----	-----	-----	-----	-----	-----	-----	-----	-----	-----	-----	-----	-----	-----	-----	-----	-----	-----	-----	-----	-----	-----	-----	-----	-----	-----	-----	-----	-----	-----	-----	-----	-----	-----	-----	-----	-----	-----	-----	-----	-----	-----	-----	-----	-----	-----	-----	-----	-----	-----	-----	-----	-----	-----	-----	-----	-----	-----	-----	-----	-----	-----	-----	-----	-----	-----	-----	-----	-----	-----	-----	-----	-----	-----	-----	-----	-----	-----	-----	-----	-----	-----	-----	-----	-----	-----	-----	-----	-----	-----	-----	-----	-----	-----	-----	-----	-----	-----	-----	-----	-----	-----	-----	-----	-----	-----	-----	-----	-----	-----	-----	-----	-----	-----	-----	-----	-----	-----	-----	-----	-----	-----	-----	-----	-----	-----	-----	-----	-----	-----	-----	-----	-----	-----	-----	-----	-----	-----	-----	-----	-----	-----	-----	-----	-----	-----	-----	-----	-----	-----	-----	-----	-----	-----	-----	-----	-----	-----	-----	-----	-----	-----	-----	-----	-----	-----	-----	-----	-----	-----	-----	-----	-----	-----	-----	-----	-----	-----	-----	-----	-----	-----	-----	-----	-----	-----	-----	-----	-----	-----	-----	-----	-----	-----	-----	------



IRAM ASSEMBLY SUMMARY INFORMATION:

CHANNEL	STATUS
-----	-----
40	ASSEMBLED WITHOUT ERROR
---	-----
1	CHANNELS ASSEMBLED

CHANNELS WITH ASSEMBLY ERRORS (IF ANY) HAVE BEEN WRITTEN TO C3043.PRINTER.DATA

REFERENCES

1. Blakelock, J.H., Automatic Control of Aircraft and Missiles, John Wiley and Sons, New York, 1965.
2. Burroughs, J.D., and A.W. Warren, Application of the EASY Dynamic Analysis Program to Aircraft Modeling Users Manual, Boeing Computer Services, Inc., Seattle, Washington, November 1976.
3. Campbell, A., and M. Abramovitz, Lateral-Directional Stability Augmentation Methods for the STOL Flight Regime, Douglas Paper 6373, McDonnell Douglas Corporation, August 1975.
4. D'Azzo, J.J., and C.H. Houpis, Linear Control System Analysis and Design Conventional and Modern, McGraw-Hill, Inc., New York, 1975.
5. Etkin, B., Dynamics of Atmospheric Flight, John Wiley and Sons, Inc., New York, 1972.
6. Holt, R.L., F-102/F-106 Five Degree-of-Freedom Flight Response Program (P5474), GDCA-DFM-72-001, April 1972.
7. McRuer, D., I. Ashkenas, and D. Graham, Aircraft Dynamics and Automatic Control, Princeton University Press, Princeton, New Jersey, 1973.
8. McRuer, D.T., C.L. Bates, and I.L. Ashkenas, Dynamics of the Airframe, Bureau of Aeronautics Navy Department Report AE-61-411, Sept 1952.
9. Roskam, Jan, Flight Dynamics of Rigid and Elastic Airplanes, Roskam Aviation and Engineering Corporation, Lawrence, Kansas, 1975.